



Das Freiburger Zentrum für interaktive Werkstoffe und bioinspirierte Technologien  
Freiburg Center for Interactive Materials and Bioinspired Technologies



# Report 2021

REPORT

2021

FIT

FREIBURG CENTER FOR  
INTERACTIVE MATERIALS AND  
BIOINSPIRED TECHNOLOGIES



FIT

FIT

# FREIBURG CENTER FOR INTERACTIVE MATERIALS AND BIOINSPIRED TECHNOLOGIES

Georges-Köhler-Allee 105

79110 Freiburg

Germany

P: (+49) 761 203 67879

F: (+49) 761 203 4709

E: [mail@fit.uni-freiburg.de](mailto:mail@fit.uni-freiburg.de)

I: <http://www.fit.uni-freiburg.de>

Secretariat: Christian Neumann

Info Management: Manuel Birk, Dr. Matthias Ebert

Managing Director: Prof. Dr. Jürgen Rühle

Administrative Management: Dr. Stefanie Meisen

Scientific Coordination: Dr. Olga Speck

Cover photo: Seminar room of FIT during an event, © Olga Speck, FIT, 2018

ISBN: 987-3-946018-07-0

# Table of Contents

FIT .....	2
Table of Contents .....	3
Foreword.....	6
FIT – Materials and Advanced Systems for a More Sustainable Future.....	6
The Center.....	7
Structure .....	7
Future Fields.....	8
Adaptive and Active Polymer Materials.....	8
Biomimetic, Biobased and Bioactive Materials Systems.....	10
(Micro)Systems for Energy Conversion, Storage and Energy-autonomy .....	12
Core Facilities .....	14
Imaging of Materials Systems .....	14
Functional Processing .....	15
Modelling and Simulation of Materials Systems.....	16
Management.....	17
Directorate .....	17
Members.....	17
Scientific Advisory Board.....	18
Integrative Board .....	19
Figures and Finances .....	19
Highlights .....	22
Future Field “Adaptive and Active Polymer Materials” .....	22
Evaluation of photoswitchable stiffness and wetting properties of soft and hard spiropyran-containing surfaces.....	22
Exploring the performance of bimetallic MIL-100(Fe, M) MOFs toward removal of antibiotics from wastewater .....	23
Dynamic Chemical Networks: Steps Towards Living Materials .....	24
Responsive Dendritic Networks in Soft Elastic Material Systems.....	25
Flow-Induced Instabilities of Soft Walls in Microfluidics .....	27
Facile fabrication of micro-/nanostructured, superhydrophobic membranes with adjustable porosity by 3D printing .....	29
Heterogeneous mechanical metamaterials: towards adaptivity and learning .....	31
Demonstrator for soft autonomous machines – soft robotic low energy gripper systems based on livMatS materials with sensing capabilities.....	32
[2+2]-Photocycloadditions of Heterocoumarins as Effective Tool for the Reversible Formation of Covalent Bonds – Towards the Design of Sustainable Materials .....	33
Future Field “Biomimetic, Biobased and Bioactive Materials Systems” .....	34
Multi-material 3D-printer for rapid prototyping of bio-inspired demonstrators.....	34
Development of a baseline bioinspired macroscopic gripper system within <i>livMatS</i> .....	36
Functional morphology of citrus fruit peels via high-resolution X-ray computed tomography (HRXCT) as inspiration for highly damping materials systems.....	38

## Table of Contents

Simulation of cactus junctions based on geometric and biomechanical analyses of the biological role models.....	40
The petiole-lamina transition zone of foliage leaves: model for a damage-resistant connection.....	42
Biomechanics of climbing plant attachment: The tendrils and adhesive pads of the passionflower <i>Passiflora discophora</i> .....	44
Artificial Venus flytraps demonstrators outperforming the biological model .....	46
Biosensor-enabled multiplexed on-site therapeutic drug monitoring of antibiotics.....	48
DINAMIK - Digital detection of interactome biomarkers for cancer diagnostics using HER2/HER3 interaction as an example.....	50
Fused Deposition Modeling of Microfluidic Chips in Transparent Polystyrene.....	52
Future Field “(Micro)Systems for Energy Conversion, Storage and Energy-autonomy” .....	54
CO <sub>2</sub> electrolysis.....	54
Quantitative STEM Tomography for Proton Exchange Membrane Fuel Cell Applications.....	56
Theoretical studies of hybrid perovskites at room temperature .....	58
Pan-European Network of Fundamental pH Research: UnipHied.....	59
Development of integrated and flexible manufacturing processes for micro-Thermoelectric generators – MiTEG.....	61
Realistic Aging Modelling in Fuel Cells .....	62
Integrated Photosupercapacitors based of Perovskite Solar Cells and Electrochemical Double Layer Supercapacitors.....	64
Understanding Electrocatalyst Dynamics under electrochemical conditions by In-Situ Electrochemical (Scanning) Transmission Electron Microscopy "In-Situ EC-(S)TEM" .....	67
Simulation of S-based Li-ion batteries .....	69
PGM-free Anode Catalysts and Improved Water Management in Anion Exchange Membrane Fuel Cell.....	71
ThermoBatS – Thermoelectric Battery Systems.....	74
Future Field “New materials: Societal Challenges“ .....	75
Multimethod approach to assess Cognitive-Affective Maps for changing attitudes – A quantitative validation study.....	75
Tiered Approach for Prospective Assessment of Benefits and Challenges (TAPAS) .....	76
Core Facility "Functional Processing" .....	78
A Soft Biomimetic Actuator Inspired by the Self-Sealing Motion of Succulent Plants .....	78
Core Facility "Modelling and Simulation of Materials Systems".....	79
Force dependence activation energy for C-S and S-S bond .....	79
Development of polarizability calculators in the Atomic Simulation Environment and GPAW .....	82
Projects .....	85
<i>liv</i> MatS—Living, adaptive and energy-autonomous materials systems .....	85
GrowBot—Towards a new generation of plant-inspired growing artefacts.....	89
IPROM—Interactive and programmable materials .....	91
Publications .....	92
Peer-reviewed Publications.....	92
Conference Proceedings.....	97

Book Chapters .....	97
Editorial Work .....	97
Theses .....	98
Habilitation .....	98
PhD theses .....	98
Diploma, Master, Bachelor and State Examination Theses .....	98
Awards .....	100
FIT Colloquium 2021 .....	101
Impressum .....	103

## FOREWORD

### FIT – MATERIALS AND ADVANCED SYSTEMS FOR A MORE SUSTAINABLE FUTURE

The year 2021 kept FIT, like every other place in Germany inside and outside of universities, firmly in the grip of the pandemic. At the beginning of the year, with the development of effective vaccines, we thought the worst was almost over. But with the exception of a somewhat quieter summer, the COVID pandemic kept us on our toes again for the rest of the year. Great efforts had to be made to ensure the health and safety of our employees and to prevent the further spread of viral infections. While at least a few hybrid meetings and some P2P discussions were possible during the summer, most of the events in spring, fall and winter had to be converted to virtual formats. We all hope sincerely that that the situation will improve somewhat next year.

The year 2021 also brought important contributions to infrastructure, such as the continued development of the Writers Studio and the introduction of a Data Steward who will help implement data management plans for *livMatS* and then continue to maintain the data infrastructure at FIT. To enhance technology transfer opportunities, a Technology Transfer Manager has been hired who is deeply embedded in FIT's scientific work and will promote intellectual property generation.

New instrumentation was added to FIT's shared laboratories, further enhancing our unique infrastructure. In addition, a joint effort between FIT, FMF and *livMatS* won funding for a new film processing facility. The funding comes from the European Union and is intended for the purchase of large-scale equipment at universities to support the transition to a more sustainable society and post-Covid economy. In addition, the next rounds of the Master Lab have been implemented to enhance the research-based education of our graduate students.

I would like to take this opportunity to thank the entire FIT team, all our members, all students, visitors, and all other FIT users who have contributed to the success of FIT. Only with an excellent infrastructure is it possible to conduct excellent science. A special thanks goes to our administrative and technical staff, as well as to the many supporters inside and outside the university.

We hope that the Corona pandemic subsides and does not affect our FIT team too much, and despite all the challenges, we look forward to an exciting scientific year in 2022. But we should keep in mind the words of Winston Churchill: "A pessimist sees the difficulty in every opportunity; an optimist sees the opportunity in every difficulty." Stay healthy and optimistic, and please enjoy reading our annual report.

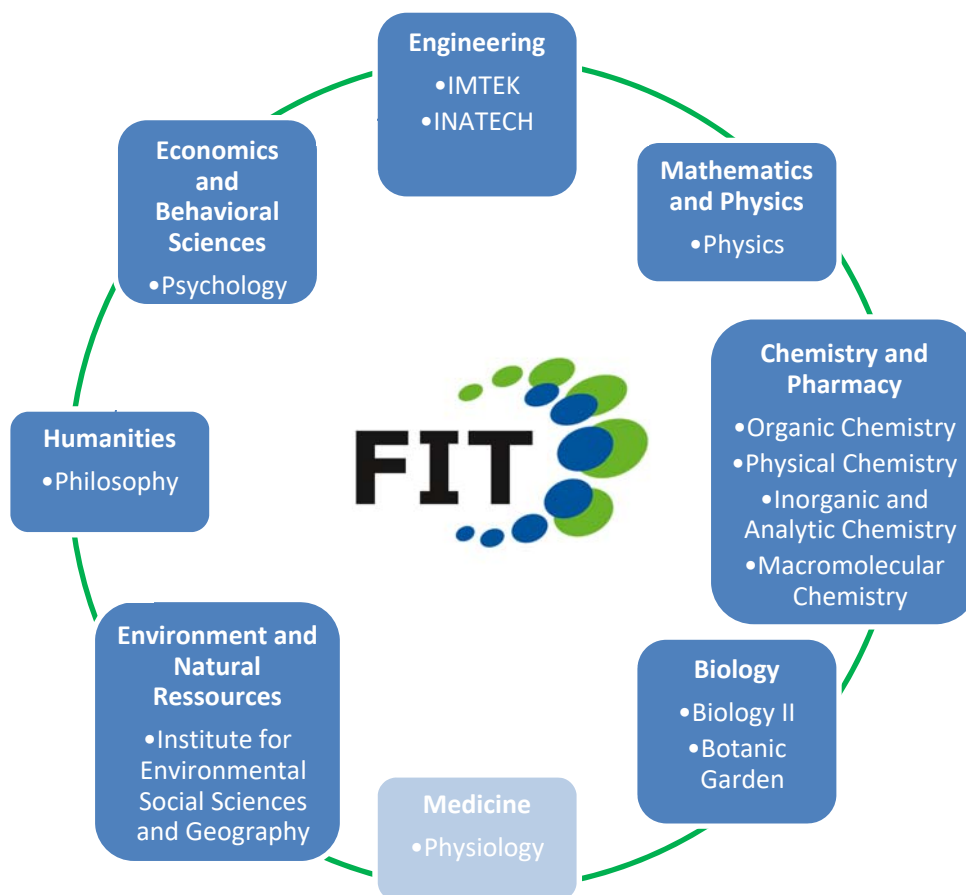


*Jürgen Rühle*

(Executive Director FIT)

# THE CENTER

## STRUCTURE



Overview of the various faculties and institutes that carry out disciplinary and interdisciplinary projects within the framework of basic research at FIT. A list of current and completed projects is available on the FIT website.

The FIT is a research institution of national and international importance for the development of future-oriented, innovative materials and materials systems. Special focus is placed on materials systems that react to changes in the environment and thus, inspired by plants and animals, have life-like functions.

Following the model of living nature, these "vital" materials systems are interactive, adaptive, energy-autonomous, self-repairing, self-improving or even learning. These extraordinary properties and functions make them a decisive advance in the sustainable development of technology and society.

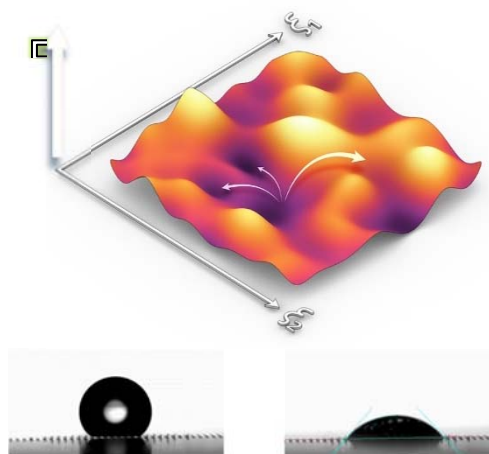
## FUTURE FIELDS

## Adaptive and Active Polymer Materials

Today's technical materials and materials systems are designed in such a way that they have more or less constant properties. These properties are given to them during the manufacturing process and should (apart from a little aging) not change in the course of time in the desired application. This immutability of material properties constitutes accordingly one of the core concepts of modern engineering and a rational systems design. In nature, on the other side, all living beings are designed to adapt as good as possible to their environment and to react to changes in environmental conditions with an appropriate response. A (young) sunflower, for example, moves its head according to the position of the sun in order to capture as much sunlight as possible, while a pine cone opens and closes depending on the ambient humidity to release its seeds under favorable conditions. Indeed one might rephrase Darwin's description of evolution by "Survival of the most adaptive".

The aim of the research program in the Future Field "Adaptive and Active Polymer Materials" is to develop new types of technical materials and advanced systems that do not have unchanging properties, but react to changing environmental conditions by adapting their shape and structure. This requires the generation of complex responsive systems, where the system can end up in different states depending on the nature of the stimulus, so that it can adapt to changes in the environment in a similar way as it is the case for living things. Fig. 1 gives an artist's impression for an energy landscape of such a multi-stimulus responsive system. Depending on the strength or type of the stimulus the system can end up in very different states represented by valleys in the energy landscape. This simplest case is observed, when the system responds to the stimulus only while the stimulus is still present. Such a behavior of the system is commonly called responsive. A simple example for responsive behavior is thermal expansion of a material. Switching, on the other side, occurs

when the stimulus leads to reversible movement of the system between two states (example: photoisomerization of azo compounds). Here the system remains (at least for a while) in the second state and can return back to the original one through application of a different stimulus. Truly adaptive materials, however, can store these structural changes and retain the properties changed this way for further, later use. Taking the picture described above true adaptivity is only achieved when the stimulus leads to a reshaping of the energy landscape and thus keeps a memory of the conditions to which it had been exposed to. This way it resembles in a way a simple form of training / learning.



Artists impression of an energy landscape describing the effect of several stimuli acting on a materials system b) Wetting of a water drop on a mechanically actuated sample © Rajak, Rühle; unpublished results

Examples for such adaptive changes of materials, in which the outer appearance of the system is altered, are an origami-like folding of structures or the actuation of hair-like surface structures. But also the inner structure of a material can adapt to external stimuli as it is the case for auxetic materials which stiffen as a reaction to the application of a certain force. This adaptability of materials can be used to adjust properties of materials such as adhesion, wettability (see Fig. 1b) or mechanical properties, to environmental changes and thus opens up novel design spaces for the generation of complex objects. Materials systems with adaptive properties will allow breakthrough innovations in many different fields such as soft robotics, smart optical devices,

self-adaptive medical prostheses and orthoses, adaptive safety equipment, adaptive light guiding systems or interactive architectural components such as façade elements, which open and close with changes in the weather conditions.

In more complex systems not only one stimulus directs the behavior of a materials system, but usually several different stimuli act together, either subsequently or simultaneously. In this case the different signals need to be processed (and eventually weighed against each other). This weighing of different system responses leads to a gated behavior, not unlike logic gates in computer science (AND, OR, NOT). For example, systems can be designed which actuate in a certain fashion when either sufficient heat or humidity are present (OR condition). In another case bilayers systems can be generated where for example high humidity is required to “unlock” the system. An example could be here a lowering the glass transition temperature of a hydrogel layer rendering the layer much softer. This softening effect could then allow thermal or magnetic actuation of the bilayer system, where the movement is otherwise “frozen in”. Such a system requires for a successful actuation the presence of both stimuli, a typical AND condition. From a more general point of view, pathways to reach such complex adaptive behavior, which show features of an embodied intelligence, are the generation of reaction networks or the creation of complex metamaterials.

In nature, which serves as a great source of inspiration for the envisioned interactive and adaptive materials, the creation of such systems involves the integration of structures across many size scales, e.g., from the chemical structure of a cellulose molecule to the overall structure of a many meters high bamboo. Only when the components on the various length scales for cell to tissue and whole

organism interact with each other in an appropriate way, adaptive behavior is observed. This is in a similar way true for artificial systems, where molecular changes e.g. by photoisomerization or swelling lead to macroscopic changes of an actuator.

However, the spatial domain is not the only one which needs to be addressed, but also timing can be crucial. In cases when the response to the signal relaxes with time (i.e. the system returns spontaneously, without the presence of an external stimulus back to the original state) also the time difference between the receptions of two separate stimuli will play an important role on the systems behavior. An example is a situation, where the first stimulus is needed to unlock the system and allow a response of the system to the second one. When relaxation after the first is faster than the application of the second stimulus, the “memory” of the occurrence of the first stimulus will be erased, the system remains locked and the presence of the second stimulus yields no systems response. However, when the arrival of the second stimulus, is faster than relaxation, the system is unlocked and can respond to this stimulus. Accordingly, complex adaptive systems might also require the consideration of different time scales ranging from rapid molecular changes, such as the closing or breaking of chemical bonds occurring within nano- to microseconds, to very slow processes such as thermal relaxation or creeping of materials that might take minutes or days. Successful development of interactive and adaptive materials thus requires a scale-bridging approach both from a theoretical and experimental point of view that extends all the way from a molecular oriented scale in time and space to that of a macroscopic object.

*Jürgen Rühle*

## Biomimetic, Biobased and Bioactive Materials Systems

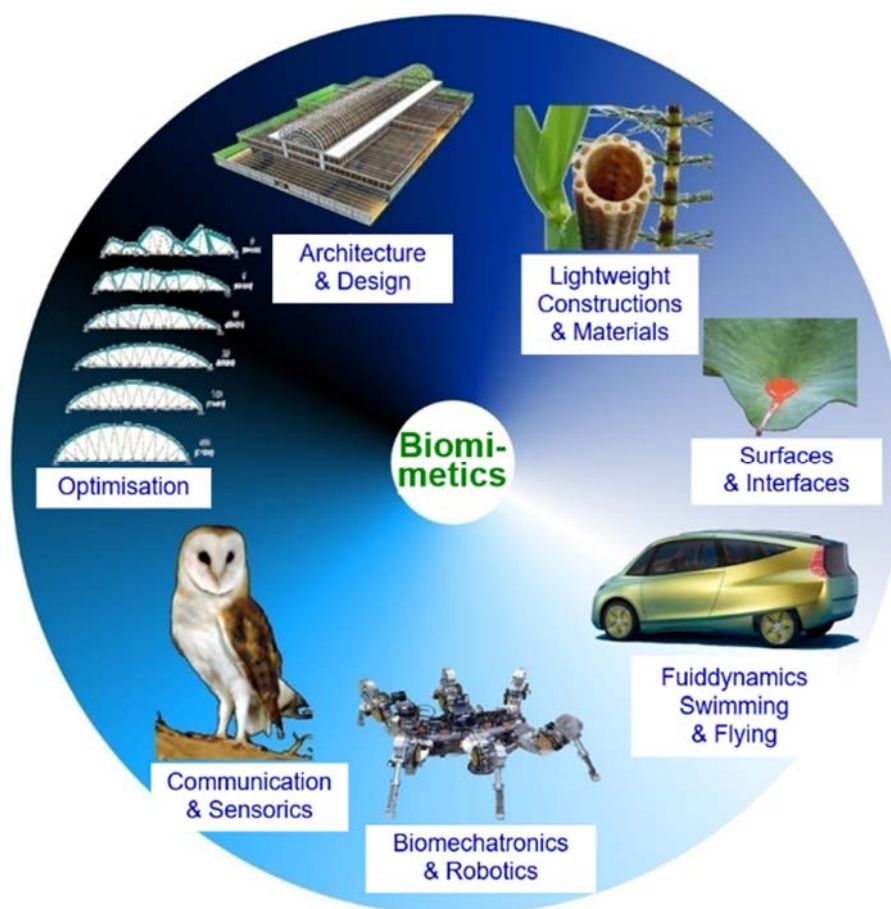


Fig. 1: Varioust fields of biomimetic research. © Plant Biomechanics Group Freiburg

The research focuses in this future field deal with the development and construction of bio-inspired, biomimetic, biobased and bioactive material systems. In addition to the transfer of functional principles from living nature to technical systems, this also includes the development of new active hybrids by the integration of synthetic and biological components, and the bioactive functionalization of materials and (micro)systems to enable them to interact with proteins, cells and tissues.

### Biomimetic materials systems @ FIT

During the last decades biomimetics has attracted increasing attention as well from basic and applied research as from various fields of industry and building construction. Biomimetics has a high innovation potential and offers the possibility for the development of sustainable technical products and production chains.

The huge number of organisms with the specific structures and functions they have developed during evolution in adaptation to differing environments represents the basis for all biomimetic R&D-projects. Novel sophisticated methods for quantitatively analyzing and simulating the form-structure-function-relation on various hierarchical levels allow new fascination insights in multi-scale mechanics and other functions of biological materials and surfaces. Additionally, new production methods enable for the first time the transfer of many outstanding properties of the biological role models into innovative biomimetic products for reasonable costs (Fig. 1). In the FIT we concentrate on the development of biomimetic materials systems with various self-x-properties including self-repair, self-adaptation, self-cleaning and self-organization. Other research topics deal with bioinspired materials systems

with pronounced energy dissipation, trainable materials systems, and the usage and development of 4D-printing technologies for the production of novel bioinspired materials systems.

### Biobased materials @ FIT

In the biobased materials research @ FIT, we try to use biomimetic approaches to design novel materials from renewable resources. Our efforts particularly focus on the utilization of lignocellulosic biopolymers towards the design of advanced materials and materials systems. One such project has attempted to develop novel processing approaches of lignin, the second most abundant biopolymer on

earth, by utilizing a liquid crystalline cellulosic polymer as processing aid and lubricant. This processing approach is inspired by the biosynthesis and the morphogenesis of the plant cell wall. During the plant cell wall morphogenesis, a liquid crystalline cellulose / hemicellulose network serves as a host structure for the in-situ polymerization of monolignols. The monolignols polymerize into a 3D highly branched lignin biopolymer, which consolidates the composite structure to finally deliver a high-strength, high toughness composite lignocellulosic material. The resulting lignocellulosic blends can be processed in solution by direct ink writing. This research paves the way to new processing avenues for lignocellulosic polymers and thus novel applications.



Fig. 2: Winter view of the cactus wood inspired sustainable “livMatS Pavilion” in the Botanic Garden Freiburg and details of the reticulated supporting structure. © Plant Biomechanics Group Freiburg. Detailed information may be found at the following link.

In the framework of the Cluster of Excellence Living, Adaptive and Energy-autonomous Materials Systems (*livMatS*), which is located at the FIT, the “*livMatS Pavilion*” was built in the Botanic Garden of the University of Freiburg as a model for a bioinspired sustainable construction (Fig. 2). The “*livMatS Pavilion*” is inspired by the saguaro cactus (*Carnegia gigantea*) and the prickly pear cactus (*Opuntia* sp.), which are characterized by their special reticulated light-weight wood structure. The saguaro cactus has a cylindrical wooden core that is hollow inside and thus particularly light. It consists of a net-like wood structure, which

gives the wood additional stability. Based on this bioinspiration civil engineers and architects of Cluster of Excellence “Integrative Computational Design and Construction for Architecture” (IntCDC) at the University of Stuttgart realized the “*livMatS Pavilion*” by using computer-aided design methods and robot-controlled production. The “*livMatS Pavilion*” is a prime example for a bioinspired sustainable construction in which the light-weight biobased supporting structure was produced by coreless winding of flax fiber-bundles and sisal cords, an ancient crop used by humankind since thousands of years.

### Lignin-based ink

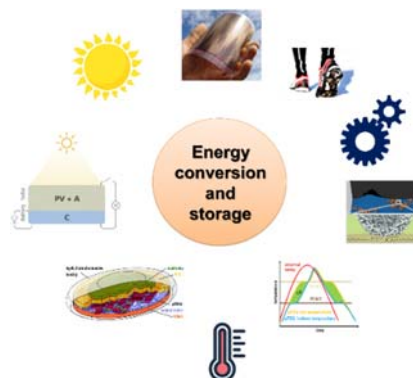
Inspired from the morphogenesis of the wood cell wall, the FIT project *Lignosit* aimed at developing high-value materials from organosolv lignin through its mixing and processing within a liquid crystalline cellulosic mesophase. *Lignosit* resulted in new fundamental knowledge on the liquid crystalline phase behavior of lignin/ liquid crystalline celluloses. Building on this fundamental understanding, new lignin-based inks for 3D printing have been recently developed within the *Pilot Project Lignin* at the Sustainability Center Freiburg and Freiburg Materials Research Center (FMF) by blending organosolv lignin with a liquid crystalline cellulose derivative. This fully bio-based and bioinspired ink for direct ink writing (DIW) has been recently highlighted by the Leichtbau BW in the “Thinking November 2020”.

*Thomas Speck & Marie-Pierre Laborie*

### (Micro)Systems for Energy Conversion, Storage and Energy-autonomy

In this future field, the research focuses on the development and construction of material systems for energy conversion and storage. As such, inspired by nature, materials and systems are developed for the conversion of solar energy (solar cells and photoelectrochemical cells for artificial photosynthesis), chemical energy (fuel cells), thermal energy (thermoelectric generators) and vibrational energy (triboelectric generators). One aspect thereby aims to realize material systems with an embedded energy autonomy, i.e. materials systems which are ideally able to harvest the required energy from the ambient. In that sense, the materials and systems developed in this future field range from macro to highly embedded micro systems. As most ambient energy forms are intermittent, systems for energy storage must also be developed, so that the required energy is available on demand. Breaking with classical modular approaches, one vision is hereby to develop multifunctional conversion and storage systems at the highest level of integration, realizing a seamless inte-

gration of both functions. In this context, advanced multifunctional material processing techniques are of highest importance to realize this integration challenge.



Different forms of energy conversion and storage and associated materials and systems. © Area A of the *livMatS* Cluster.

### Material systems for energy conversion and storage @ FIT

The largest activities in the future field are presently associated with the research activities in research area A of the *livMatS* Cluster in which novel concepts and systems for energy autonomous materials systems are developed.

#### Solar energy conversion and storage

Solar energy is converted and stored as electrical charges in *SolStore* devices; devices, which fuse the function of light-induced charge carrier generation/separation and charge carrier storage at different levels of integrations, ranging from 3 electrode systems, in which a solar cell shares an electrode with an electrochemical energy storing system (supercapacitor or battery) to 2 electrode systems, in which the light-induced charge carrier generation/separation and charge carrier storage are truly embedded in one multifunctional material system.

This central *livMatS* research is complemented by other FIT research projects in the future field related amongst others to a) solar energy conversion with novel tandem solar cells or photoanodes for photoelectrochemical water splitting, b) electrochemical energy conversion with bioinspired materials for Pt-free

fuel cells as well as c) improved electrochemical energy storage with novel battery concepts and materials and interfaces.

### **Thermal energy conversion and storage**

This area is anticipated by the development of highly efficient thermoelectric generators (TEGs) with integrated phase shift materials to be used as a storage unit for thermal energy. The corresponding project ThermoBatS is therefore again aiming at an intricate fusion of energy conversion and storage. The thermoelectric materials chosen are fabricated as highly nano-micro scale powders and formulated as thermoelectric inks or pastes. Fabrication of TEGs happens via dispensing or printing into flexible substrate materials, thus creating a versatile multi-material system suitable for the ambient temperature range. Other projects outside of livMatS will tackle the area of high-temperature energy harvesting using powder-pressed and sintered or electroplated thermoelectric materials. A third direction to be followed in all projects is the characterization of thermoelectric materials and systems.

### **Mechanical energy conversion**

In *livMatS*, triboelectric generators are the actual main topic of research in the project Tribo-Gen. Here, we will do an extensive study on the fundamental physical effects of triboelectric charge generation, to gain more insight into this phenomenon, which is known for thousands of years but still a matter of scientific debate. As a result, optimized materials and suitable surface topologies will be developed for highly efficient triboelectric generators. Charge extraction will happen through innovative concepts and automatic frequency tuning will be performed through the mechanical design of self-adaptive triboelectric vibration harvesters.

These named projects are exemplary for the trend of energy research followed in FIT. Aside of the mentioned activities additional related projects are planned to widen the research platform with additional and highly innovative concepts for energy conversion, storage and transfer.

*Anna Fischer & Peter Woias*

## CORE FACILITIES

### Imaging of Materials Systems

- Scientific head: Prof. Dr. Anna Fischer<sup>1</sup>
- Responsible manager and scientist:  
Drs. Yi Thomann<sup>1</sup> and Ralf Thomann<sup>2</sup>

<sup>1</sup> Freiburg Center for Interactive Materials and Bio-inspired Technologies (FIT)

<sup>2</sup> Institute of Macromolecular Chemistry

The core facility “Imaging of Materials System” (CF1) represents a specialized laboratory with electron microscopes (200 kV HR-TEM/STEM, 120 kV TEM, SEM, FIB/SEM), a  $\mu$ -CT, two atomic force microscopes (AFM) and a variety of peripheral devices.

For an overview of the instruments, methods, expertise in CF1 etc. please refer to:

<https://miap.eu/miap-unit/core-facility-imaging-of-materials-systems/>

The facility is accessible to all research groups within the university, as long as the projects are financed on a non-profit basis. Users can do measurements themselves or under supervision of the CF1 staff. We also provide service measurements, image processing methods and data analysis for various microscopic and tomographic applications.

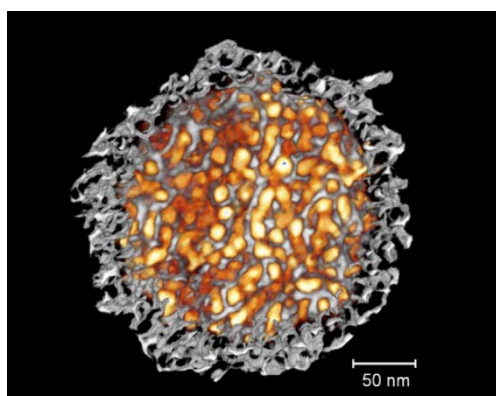


Fig. 1: Cryo TEM-Tomography of a sulfur (orange) filled mpnc (gray, mesoporous N-doped carbon particle [1]). Sample: Group Anna Fischer. Picture: © Yi & Ralf Thomann

One focus of the CF1 is the 3D-tomography on multiple length scales. The following Figures show a few results accomplished in the CF1 in the last year.

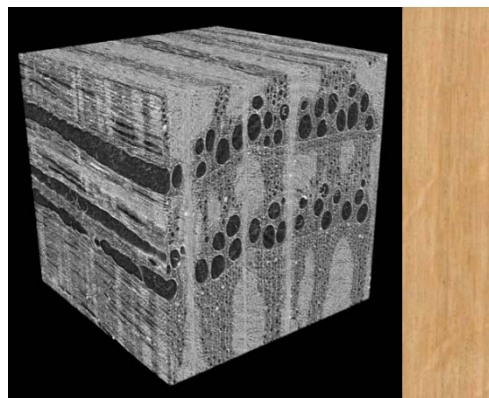


Fig. 2: Robinia wood.  $\mu$ -CT image / cube size 2.5 mm and photograph. © R. Thomann

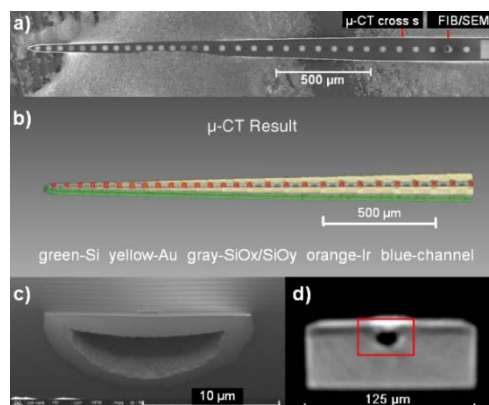


Fig. 3: Internal structural investigation of a microfluidic probe [2] in multiple length scales. a) SEM image, b)  $\mu$ -CT tomographic image, c) FIB-SEM cross section of the micro channel and d)  $\mu$ -CT cross section [3]. Sample: Group P. Ruther. Pictures: © Yi Thomann

### References

- [1] Melke et.al. 2019, “Electrochemical Stability of Silica Templated Polyaniline Derived Mesoporous N-Doped Carbons for the Design of ...”, doi.org/10.1016/J.CARBON.2019.01.057
- [2] Sharma et.al. 2021, “Multifunctional optrode for opsin delivery, optical stimulation, and electrophysiological recordings in ...”, doi.org/10.1088/1741-2552/ac3206
- [3] Thomann et.al. 2021, “3D visualization of micrometer sized structures in technical materials via Micro-CT and FIB/SEM - tomographic datasets and video files of a microfluidic probe –”, doi.org/10.5281/zenodo.5082095

## Functional Processing

**Manufacturing technique for bioinspired materials with focus on nanolithography, film technology, and generative processes**

- Scientific head: Prof. Dr. Claas Müller<sup>1,2</sup>
- Responsible manager: Dr. Jing Becker<sup>1</sup>

<sup>1</sup>FIT Core Facility "Functional Processing",  
<sup>2</sup>IMTEK Department of Microsystem Engineering,  
 Laboratory for Process Technology



Fig. 1: Arrangement of the process modules in the technology platform 2 (from left): roll laminator, PVD & PECVD system, screen printer, electrophoretic deposition system and aerosol jet printer. © Core Facility 2, FIT, Freiburg

**Short description of research goals:** Manufacturing technique for bioinspired materials with focus on nanolithography, macromolecular foil technology, and 3D-printing technology

In order to support the research projects running in FIT, a powerful technology department, Core Facility "Functional Processing", is established for functional design and efficient manufacturing of (micro-) systems and adaptive bioinspired materials.

The Core Facility "Functional Processing" concentrates particularly on the fabrication of nano- and micro-structures on macromolecular foils. Besides UV-NIL (UV-nanoimprint-lithography) as well as HE-NIL (hot-embossing-nanoimprint-lithography) technologies, various novel manufacturing technologies, such as roll lamination, thin film deposition, surface modification, aerosol jet printing technology, electrophoretic deposition, as well as screen printing technology are developed for special applications on polymer foils.

The equipment installed in the Core Facility "Functional Processing" is divided into two different categories according to the operation complexity. The category 1 includes the Cryomill system for material grinding with its integrated liquid nitrogen cooling system, the Stork roll laminator and the electrophoretic

deposition system (EPD) from Permatecs. For this equipment category, after the application from the users and the evaluation by Core Facility "Functional Processing" group, the applicants would receive a clearly defined training course offered by the CF 2 staffs. Following the training activities, the applicants will be issued a permit to work on the system. For the other system in CF 2, due to the operation complexity and the maintenance requirements, the users outside the CF 2 group are not allowed to perform alone on the systems. The equipment in this category could only be operated by the CF 2 staffs.

In year 2021, Core Facility "Functional Processing" has cooperated with research group Speck in FIT on the topic of "A Soft Biomimetic Actuator Inspired by the Self-Sealing Motion of Succulent Plants" (for detailed information see highlights).

## Modelling and Simulation of Materials Systems

- Scientific head: Prof. Dr. Michael Moseler
- Responsible manager: PD Dr. Michael Walter

<sup>1</sup>Institute of Physics, University of Freiburg, <sup>2</sup>Freiburg Center for Interactive Materials and Bioinspired Technologies (FIT)

FIT supports materials development and system integration through modelling and simulation. The funding granted by the Landesstiftung and the German Research Foundation for this purpose was used in 2017 for an extension of the NEMO-cluster located at the University of Freiburg, where FIT participates in a “shareholder” principle. Due to synergy-effects additional 1000 cores (therefore approx. 20% more than were granted) were included to the cluster corresponding to a 5.6% of the full extended cluster. The “shareholder”-status allowed to use the computational resources already before this extension, a possibility that was used extensively by the simulation group of FIT. As shown in fig. 1, the actual use of the computational resources summed up to 6.3% of the full NEMO-Cluster.

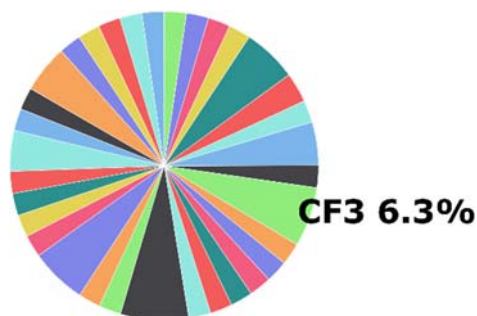


Fig. 1: Partition of computational time used on the full NEMO-cluster in the year 2019. The fraction used by CF3 is highlighted. © RZ University of Freiburg

These calculations performed and models developed allowed addressing current problems in tribology, polymer chemistry, organic photo-voltaics and catalysis in simulation as well as modelling of materials based on natural resources. This work resulted in 10 peer-reviewed publications during the year 2019. These studies are possible due to the co-development of the internationally developed software packages ASE and GPAW.

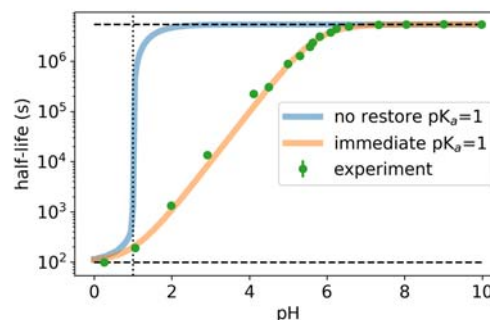


Fig. 2: Comparison of the modeled and measured half-lives for the thermal spontaneous transition back-transition of AAP (see text) from the Z-form to the E-form. The model uses the experimental half-lives  $\tau_{1/2}$  (pH > 7) =  $5.40 \cdot 10^6$  s (upper dashed line) and  $\tau_{1/2}$  (pH 0.3) = 98.5 s (lower dashed line) as well as a numerically optimized  $pK_a$  (Z) of 1 (dotted line). Experimental data from S. Ludwanowski, group Andreas Walther (© core facility 3).

The outcome of one of our activities in direct collaboration at FIT is depicted in Figure 2 as an example. We have investigated the thermal transition of arylazopyrazole (AAP) from the Z-form to the energetically lower E-form. AAP is similar to azobenzene, the prime example of a photoswitch molecule that changes conformation under irradiation, a property that allow its use as molecular machine. Experimental results of the group of Andreas Walther showed a strong pH dependence in the thermal back-reaction in AAP. The half-lives cover the range from ~100 seconds to more than 60 days at room temperature. Our modeling activities not only helped to reveal a pH-dependent change in the transition path from density functional theory calculations of the corresponding barriers, but also helped to understand the exact dependence of the half-life with pH. An effective rate model developed by us furthermore reveals that the protonation is practically immediate at the timescale of these transitions in AAP. The figure shows the excellent agreement between model and measurements.

## MANAGEMENT

Prof. Dr. Jürgen Rühle  
(Managing Director)  
IMTEK  
Department of Microsystems Engineering  
Chemistry and Physics of Interfaces

Prof. Dr. Thomas Speck  
(Deputy Managing Director)  
Plant Biomechanics Group  
Botanic Garden  
Faculty of Biology

Dr. Stefanie Meisen  
(Administrative Director), FIT

Dr. Olga Speck  
(Scientific Coordinator), FIT

## DIRECTORATE

The Board of Directors of the FIT consists of five full-time professors from the participating faculties of the University of Freiburg that must also be members of the FIT. These professors are appointed by the Rectorate for a term of three years on the recommendation of the general meeting. The Directorate elects the Managing Director and the Rectorate appoints him for a term of three years. The Board of Directors is responsible for managing the business and decides on all matters that are not assigned to another body of the university. It coordinates the tasks to be performed within the FIT and draws up an annual research and financial plan. The members of the Directorate also include the respective Managing Director of the FMF and a representative of the young scientists. In 2020, members of the Directorate were:

Prof. Dr. Jürgen Rühle  
(Managing director)  
Faculty of Engineering

Prof. Dr. Thomas Speck  
(Deputy managing director)  
Faculty of Biology

Prof. Dr. Anna Fischer  
Faculty of Chemistry and Pharmacy

Prof. Dr. Peter Woias  
Faculty of Engineering

Prof. Dr. Bastian E. Rapp  
(Managing director of the FMF)  
Faculty of Engineering

Dr. Severin Vierrath / Dr. Can Dincer  
(Representative of young scientists)  
Faculty of Engineering

## MEMBERS

Laboratories with the corresponding infrastructure and office space are made available to members for a limited period of time. The members have access to the three Core Facilities. In 2021, the members included (in alphabetical order):

Dr. Maria Asplund (Faculty of Engineering)

Prof. Dr. Frank Balle (Faculty of Engineering)

Dr. Céline Calvino (*livMatS*)

Dr. Can Dincer (Faculty of Engineering)

Prof. Dr. Christoph Eberl (Faculty of Engineering)

apl. Prof. Dr. Christian Elsässer (Faculty of Mathematics and Physics)

Prof. Dr. Birgit Esser (Faculty of Chemistry and Pharmacy)

Prof. Dr. Anna Fischer (Faculty of Chemistry and Pharmacy)

Prof. Dr. Stefan Glunz (Faculty of Engineering)

Dr. Frank Goldschmidtböing (Faculty of Engineering)

Prof. Dr. Rainer Grießhammer (Faculty of Environment and Natural Resources)

Dr. Dorothea Helmer (Faculty of Engineering)

Prof. Dr. Lore Hühn (Faculty of Humanities)

Prof. Dr. Thorsten Hugel (Faculty of Chemistry and Pharmacy)

Prof. Dr. Henning Jacob Jessen (Faculty of Chemistry and Pharmacy)

Prof. Dr. Andrea Kiesel (Faculty of Economics and Behavioral Sciences)

Dr. Peter Koltay (Faculty of Engineering)

## Scientific Advisory Board

Prof. Dr. Ingo Krossing (Faculty of Chemistry and Pharmacy)

Prof. Dr. Karen Lienkamp (Faculty of Engineering, until 31.03.2021)

Dr. Tom Masselter (Faculty of Biology)

Prof. Dr. Michael Moseler (Faculty of Mathematics and Physics)

Prof. Dr. Claas Müller (Faculty of Engineering)

Dr. Anayancy Osorio (Faculty of Engineering)

Dr. Charalampos Pappas (*livMatS*)

Prof. Dr. Lars Pastewka (Faculty of Engineering)

Dr. Uwe Pelz (Faculty of Engineering)

Dr. Thomas Pfohl (Faculty of Mathematics and Physics)

Prof. Dr. Bastian E. Rapp (Faculty of Engineering)

Prof. Dr. Günter Reiter (Faculty of Mathematics and Physics)

Prof. Dr. Ralf Reski (Faculty of Biology)

Prof. Dr. Winfried Römer (Faculty of Biology)

Prof. Dr. Jürgen Rühle (Faculty of Engineering)

Dr. Viacheslav Slesarenko (*livMatS*)

Dr. Olga Speck (Faculty of Biology)

Prof. Dr. Thomas Speck (Faculty of Biology)

Dr. Severin Vierrath (Faculty of Engineering)

PD Dr. Michael Walter (Faculty of Mathematics and Physics)

Prof. Dr. Peter Woias (Faculty of Engineering)

Dr. Uli Würfel (Faculty of Mathematics and Physics)

Prof. Dr. Roland Zengerle (Faculty of Engineering)

## SCIENTIFIC ADVISORY BOARD

The Scientific Advisory Board accompanies the scientific work of the FIT and shall provide the directorate with suggestions for its further development. Members of the Scientific Advisory Board are external university professors whose research focus lies in the field of activity of the FIT. They are appointed by the rectorate for a period of five years. The following professors belonged to the Scientific Advisory Board:

Spokesperson: Dr. Karine Anselme (Institut de Science des Matériaux de Mulhouse (IS2M), France)

Deputy spokesperson: Prof. Dr. Christoph Weder (Adolphe Merkle Institute, Fribourg, Switzerland)

Prof. Dr. Eduard Arzt (Saarland University and Leibniz Institute for New Materials, Germany)

Prof. Dr. Clothilde Boulanger (Université de Lorraine, France)

Prof. Dr. Ingo Burgert (ETH Zurich, Switzerland)

Prof. Dr. Peter Fratzl (Max Planck Institute of Colloids and Interfaces, Potsdam, Germany)

Prof. Dr. Oskar Paris (University of Leoben, Austria)

Prof. Dr. Eric Yeatman, Imperial College London, UK)

## INTEGRATIVE BOARD

The Integrative Board is set up as a university-internal advisory body and monitors the development of the FIT. It works towards the reconciliation of interests of the faculties and institutions involved in FIT. In 2021 the following persons were members of the Integrative Board, with the deans always changing to the winter semester.

Prof. Dr. Jürgen Rühle (Managing Director of FIT)

Prof. Dr. Thomas Speck (Deputy Managing Director of FIT)

Prof. Dr. Heiner Schanz (Dean of the Faculty of Environmental and Natural Resources)

Prof. Dr. Sonja-Verena Albers (Dean of the Faculty of Biology)

Prof. Dr. Michael Thoss (Dean of the Faculty of Mathematics and Physics)

Prof. Dr. Andreas Bechthold (Dean of the Faculty of Chemistry and Pharmacy)

Prof. Dr. Roland Zengerle (Dean of the Faculty of Engineering)

Prof. Dr. Lutz Hein (Dean of the Faculty of Medicine)

Prof. Dr. Bastian Rapp (Management Director of the Freiburg Materials Center)

Dr. Frank Krüger (Head of Freiburg Research Services)

Dr. Karine Anselme (Spokesperson of the Scientific Advisory Board)

Dr. Stefanie Meisen (Administrative Management of FIT)

## FIGURES AND FINANCES

Although we are reaching our limits in terms of space, we were again able to increase both the number of projects and the amount of spending available from 2020 to 2021. A total of 3.7 million € was available for research. In this context, 72% of the funds were spent on personnel. A total of 350 staff were active, of which 38 were postdocs, 130 were doctoral students, 79 were master's students and 21 were bachelor's students.

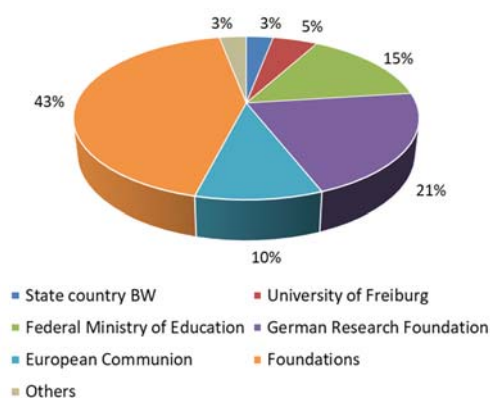


Fig. 1: Percentage participation of funding providers in the FIT budget 2021 (without *livMatS*)

The successful further development is to be particularly highly credited in view of the current critical situation. In addition to spending on personnel, 8% of the budget was spent on material resources and 20% on new investments. In order to be able to follow the figures accordingly, please refer to the following graphs and tables for further details.

Our associated Cluster of Excellence *livMatS*, which is funded under the Excellence Strategy, started its third funding year in 2021.

The cluster's 23 long-term projects were continued in 2021. In addition, 16 booster projects and 14 short projects were completed in 2021. In total, more than 120 scientists of all career stages were involved in *livMatS* projects in 2021.

A total of 4,383 k€ was spent on personnel and material costs in the cluster projects. 4,354 k€ were spent on strategic measures, investments in the Shared Labs, and administration.

Tab. 1: FIT budget by funding sources from 2018 until today in € (without *livMatS*)

	2018	2019	2020	2021
German Research Foundation	1.055.197	1.062.597	828.882	792.305
State country BW	928.292	0	98.857	112.471
Federal Ministry of Education	409.381	407.970	243.345	552.549
European Communion	355.219	518.315	576.875	360.206
University of Freiburg	75.200	82.000	183.964	182.300
Others	189.235	270.947	777.965	1.714.111
<b>Total (€)</b>	<b>5.529.693</b>	<b>3.012.525</b>	<b>2.341.829</b>	<b>3.713.942</b>

Tab. 2: Projects in 2021 (including *livMatS*)

Leader of the project	Project	Total budget without overhead (€)	Expenditure in 2021 (€)
Dincer	DFG miPAT	366.549	85.326
	DFG miRNAs	369.904	77.414
	MERGE	710.520	123.402
Fischer	Vectorstiftung AlkaCell	201.644	64.083
	VW-Stiftung	952.500	51.984
Fischer, Rhe, T. Speck and Pls	Cluster of Excellence <i>livMatS</i>	37.497.200	8.737.000
Glunz	PrEsto	498.030	118.617
Goldschmidtboing	DFG Adaptive Linsen	157.400	50.332
Helmer	DFG Schaltbare Oberflchen	234.200	50.680
Koltay	MWK DINAMIK	299.987	112.471
	DFG 4D-Bioprinting	204.000	53.547
Krossing	EU ERC UnipHied	270.000	14.821
Lienkamp	BMBF ANTIBUG	1.408.848	282.543
	BMBF BioMAMPs	379.680	54.136
Mller	DFG Polymerbasierte	181.830	1.167
Osorio	Emmy-Noether-Overhead	7.500	1.919
Pelz	DFG MiTEG	321.649	77.258
Rapp	EU ERC CaLa	1.999.750	222.606
Rhe	DFG Modifizierte Papiere	211.400	43.770
	DFG PAK	165.800	55.386
	DFG Dynamisches	202.500	37.332

Leader of the project	Project	Total budget with-out overhead (€)	Expenditure in 2021 (€)
	DFG KOMMA	246.250	38.294
	Carl-Zeiss IPROM	4.500.000	1.242.970
Speck, T.	EU ERC GrowBot	696.166	78.254
Vierrath	Vectorstiftung AlkaCell	259.778	87.690
	Vectorstiftung CO2-to-X	1.000.000	145.599
	Alexander von Humbold	63.600	3.168
	BMBF FC CAT	330.000	57.562
	BMBF FC RAT	467.864	34.907
Walter	DFG Donor Akzepter	162.950	45.934
	DFG HYBRIDS	159.850	14.261
	DFG Synthese , X-ray	169.550	48.963
Woiias	DFG NiLax	150.500	38.486

Tab. 3: Expenditure of project groups from 2018 until 2021 in €

Project group	2018	2019	2020	2021
Dincer	30.727	93.407	153.439	286.141
Fischer	71.540	65.373	151.342	116.067
Glunz	69.746	54.468	0	118.617
Goldschmidtböing	0	19.138	75.581	50.332
Helmer	0	0	30.104	50.680
Koltay	0	0	138.692	166.018
Krossing	0	47.578	50.562	14.821
Lienkamp	665.109	507.898	285.240	381.203
Müller	0	82.220	89.065	1.167
Osorio	0	0	0	1.919
Pelz	0	0	61.853	77.258
Rapp	0	39.077	100.530	222.606
Rühe	174.286	234.350	550.142	1.417.754
Speck, T.	186.637	126.483	98.011	78.254
Vierrath	0	31.703	339.089	328.926
Walter	56.464	84.064	66.759	109.159
Woiias	0	51.887	39.552	38.486

## HIGHLIGHTS

### FUTURE FIELD “ADAPTIVE AND ACTIVE POLYMER MATERIALS”

#### Evaluation of photoswitchable stiffness and wetting properties of soft and hard spiropyran-containing surfaces

Niloofar Nekoonam<sup>1,2,3</sup>, Dorothea Helmer<sup>1,2,3</sup>

<sup>1</sup>Freiburg Materials Research Center (FMF), Albert-Ludwigs-University Freiburg; <sup>2</sup>Laboratory of Process Technology, HelmerLab, Department of Microsystem Engineering (IMTEK); <sup>3</sup>Freiburg Centre for Interactive Materials and Bioinspired Technologies (FIT)

Project funding: German Research Foundation (DFG)

This project focuses on photoswitchable wetting properties of soft and hard materials containing spiropyran either as a spiropyran molecule or as a spiropyran-methacrylate monomer. Reversible switch between spiropyran (SP) and merocyanine (MC) that have different dipole moments, color and molecular size by various triggers including heat, pH, metal ions, and light<sup>1</sup> make it stand out among the other molecular switches.

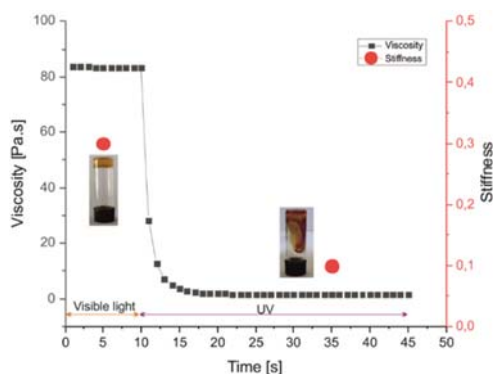


Fig. 1: Viscosity and stiffness decrease of the SP-containing photorheological soft samples upon UV exposure. Inset: real image of the samples in an inverted vial (©HelmerLab, IMTEK)

In the first part of the project, photorheological fluids<sup>[2]</sup> containing lecithin, a bile salt, organic

solvent and SP were engineered and improved to be used as switchable soft substrate for droplet movement studies. Photo-switching of SP to MC under UV irradiation induced structural changes in the entangled wormlike micelles of the gel-like material causing a decrease in viscoelastic properties including viscosity (Fig. 1) and stiffness. This photo-induced stiffness-gradient was employed to move a 2  $\mu$ l oil droplet towards softer region as a negative durotaxis effect (Fig. 2).

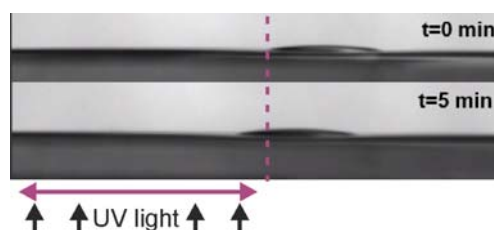


Fig. 2: Durotaxis: Droplet movement towards softer regions caused by UV-induced stiffness-gradient (©HelmerLab, IMTEK)

As the switch is accompanied by a color change from yellowish to magenta, a micrometer switching resolution could be achieved using our maskless projection lithography system<sup>3</sup> (Fig. 3). High resolution and reversibility of the change in material properties will be used for patterning a stiffness-gradient on the soft substrate to move the droplets on-demand.



Fig. 3: High resolution switching patterns of the photo-rheological fluids: Magenta MC Patterns created by introducing UV-light using maskless lithography. Masks are shown in black and white (©HelmerLab, IMTEK)

In the second part of the project, two different SP-methacrylate monomers (SPM-A and SPM-B) were synthesized<sup>[4,5]</sup> and copolymerized with various acrylate and methacrylate monomers such as methyl methacrylate (MMA) to fabricate SP bulk functionalized polymers (Fig. 5). So that the photoswitching properties of the surface would not be lost even when the top layer is damaged or removed.

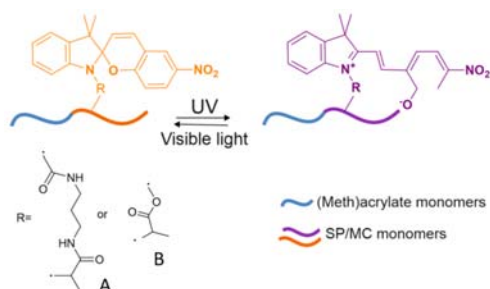


Fig. 4: Switching dynamics of our fabricated copolymers (©HelmerLab, IMTEK)

The surface energy of the SP containing polymer decreased upon UV exposure due to the higher dipole moment of MC compared to SP. Hence, the static contact angle (SCA) change of up to  $10^\circ$  was measured on non-porous poly (MMA-co-SPM-A). Enhanced SCA change was achieved by introducing roughness to the SP-containing polymers by creating porous structures. An adaptive surface could be created by immersion of samples in  $\text{Cu}^{2+}$  solution, which stabilizes the MC form and increases the change in SCA (Fig. 5).<sup>6</sup>

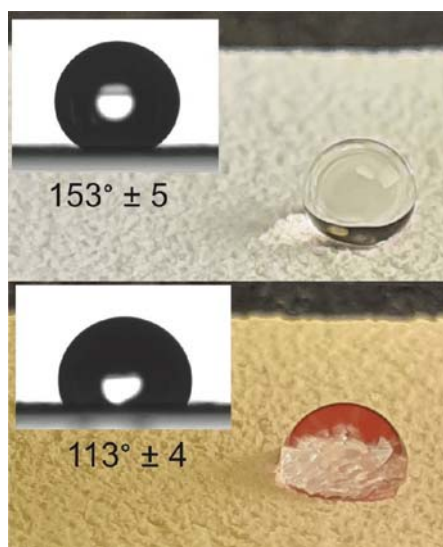


Fig. 5: High SCA change on porous surfaces:  $5 \mu\text{l}$  water droplet on porous poly(MMA-co-SPM-A) surface after stabilization of the MC form by  $\text{Cu}(\text{II})$ . (©HelmerLab, IMTEK)

The concept will be employed to achieve higher SCA and later dynamic contact angle change for SP smooth and porous copolymers. Results will be included in numerical models created by cooperation partners within

Schwerpunktprogramm SPP2171 – this will allow for the tuning of surfaces in terms of softness and switchability towards functional surfaces for material transport and selective wetting.

#### References

1. Klajn, R. *Chem Soc Rev* 43, 148–184 (2014).
2. Lee, H.-Y., Diehn, K. K., Sun, K., Chen, T. & Raghavan, S. R. *J. Am. Chem. Soc.* 133, 8461–8463 (2011).
3. Waldbaur, A., Waterkotte, B., Schmitz, K. & Rapp, B. E. *Small* 8, 1570–1578 (2012).
4. Schenderlein, H., Voss, A., Stark, R. W. & Bialski, M. *Langmuir* 29, 4525–4534 (2013).
5. Gossweiler, G. R., Kouznetsova, T. B. & Craig, S. L. *J. Am. Chem. Soc.* 137, 6148–6151 (2015).
6. Wojtyk, J. T. C., Buncel, E. & Kazmaier, P. M. *Chem. Commun.* 1703–1704 (1998).

### Exploring the performance of bimetallic MIL-100(Fe, M) MOFs toward removal of antibiotics from wastewater

<sup>1,2</sup>Naghmeh Sadat Mirbagheri, <sup>1,2</sup>Matthias Breitwieser, <sup>1,2</sup>Severin Vierrath

<sup>1</sup>Freiburg Center for Interactive Materials and Bio-inspired Technologies (FIT), University of Freiburg; <sup>2</sup>Electrochemical Energy Systems Group, IMTEK - Department of Microsystems Engineering, University of Freiburg

Project funding: Alexander von Humboldt-Stiftung / Foundation

Nowadays the amount of antibiotics consumption in various sectors, such as agriculture, livestock and human medicine, is growing rapidly. Residual antibiotic, unfortunately, can persist in water after they have been disposed of, posing a clear threat to ecosystems and raising the possibility of antibiotic resistance [1]. As reported in 2016 [2], antibiotic resistance claimed the lives of approximately 700,000 individuals and this number is expected to rise to ten million people by 2050 if it is not addressed. Therefore, numerous efforts have been made over the last decades to resolve this environmental issue. In this context, heterogeneous photocatalysis, particularly advanced oxidation processes, have

been regarded as an efficient and environmental-friendly approach for the treatment of antibiotic-contaminated water with the help of solar energy and highly reactive hydroxyl radicals (Fig. 1).

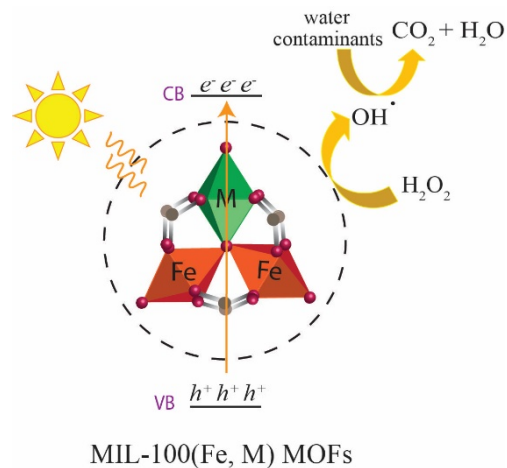


Fig. 1: Photo-Fenton degradation of water contaminants by bimetallic MIL-100(Fe,M) MOFs. M: doping metals. (© Electrochemical Energy System Group)

MIL-100(Fe) is one of the well-known metal organic frameworks (MOFs) photocatalysts that not only possess highly porous channels and numerous active sites suitable for the heterogeneous photocatalytic applications, but also are chemically active in the advanced oxidation processes. In the MIL-100(Fe) photocatalyst, the  $\mu$ 3-oxo clusters act as antennas for harvesting solar energy, creating charge separation, and producing highly reactive hydroxyl radicals via a photo-Fenton process for degradation of released pollutants in water. However, the efficiency of the MIL-100(Fe) MOFs toward the removal of water contaminants is still low due to the poor catalytic activity of this photocatalyst [3].

To address this issue, different strategies have been investigated. Among them, incorporation of elements into the MIL-100(Fe) framework, which results in the formation of bimetallic MOFs, is a unique and promising approach to improve the performance of this photocatalyst while overcoming the challenges associated with the previously reported strategies.

Recently, a scalable, facile and green methodology has been reported by Steenhaut

et al.[4] for synthesizing a wide range of bimetallic MIL-100(Fe,M) MOFs with suitable physicochemical properties. This approach not only allows the doping of MIL-100(Fe) with different cationic metals but also facilitates the large-scale and low cost production of the bimetallic MIL-100(Fe,M) MOFs. On the basis of this inspiration, the focus of the current project is on the incorporation of cationic elements with different oxidation state into the MIL-100(Fe) frameworks. The adsorptive and photo-Fenton degradation properties of the bimetallic MOFs are then investigated towards the removal of antibiotics from aqueous solutions. Furthermore, a number of characterisation techniques are utilized to fully examine the chemical, physical, and electrical properties of the bimetallic MIL-100(Fe,M) in order to elucidate the role of each element on the performance of these MOFs.

#### References

- [1] S. A. Kraemer, A. Ramachandran, and G. G. Perron, *Microorganisms*, 7, 180, (2019)
- [2] T. P. Robinson, D. P. Bu, J. Carrique-Mas et al., *Trans. R. Soc. Trop. Med. Hyg.*, 110, 377, (2016)
- [3] J. Guo, H. Jia, A. Zhang et al., *Sep. Purif. Technol.*, 118334, (2021)
- [4] T. Steenhaut, S. Hermans, and Y. Filinchuk, *New J. Chem.*, 44, 3847, (2020)

## Dynamic Chemical Networks: Steps Towards Living Materials

Charalampos G. Pappas

Freiburg Center for Interactive Materials and Bioinspired Technologies (FIT)

Project funding: Funded by the Deutsche Forschungsgemeinschaft (DFG, German Research Foundation) under Germany's Excellence Strategy – EXC-2193/1 – 390951807

Living systems possess overwhelming molecular complexity that largely results from combinations of just twenty amino acids that are found across all life forms.<sup>1</sup> It is increasingly clear that structure and functionality may be observed in single amino acids and in much simpler combinations of these building blocks in short peptides. However, the majority of peptide assemblies have mostly been designed such that the (closed) system goes

thermodynamically downhill; i.e. the product state is of lower Gibbs energy, yielding stable molecules that can be isolated and stored. Yet the chemistry of life operates in a very different way: most molecules from which living systems are constituted are turned over continuously and are not necessarily thermodynamically stable. Nevertheless, living systems can be stable, but in a homeostatic sense: molecules are being formed at approximately the same rate as they are being degraded.<sup>2</sup> Inspired by such dynamics, where molecular assemblies perform tasks that exceed the functionality of their basic constituents, systems chemistry<sup>3</sup> focuses on connectedness, interactivity and patterns. This network concept contrasts with the more traditional reductionist approach and has empowered soft matter systems with the abilities to replicate, compartmentalize and adapt in response to chemical and physical signals from the environment. In this project, we follow a systems chemistry pathway towards adaptivity in peptide libraries. We demonstrate the spontaneous formation of peptide oligomers emerging from single monomers, which are capable of forming supramolecular structures in water. The autonomous construction of chemically activated peptide libraries is achieved through modification of single amino acids with phosphate esters. Upon reactivating the libraries with phosphate “food”, the system is capable of achieving selectivity, as a result of self-assembly. Moreover, pathway-dependent complexity is triggered upon offering into the system competing nucleophiles, such as thiols, where thioesters can give rise to transient supramolecular reconfigurations leading to increased peptide coupling (Fig. 1). Competition between nucleophiles for the phosphate sources (“food molecule”) enables the peptide network to access different supramolecular structures and ultimately to assemble into hydrogels with enhanced mechanical properties. We are currently investigating the effect of the environment on the oligomerisation process and whether catalysis can switch off the pathway, by activating a secondary response. The chemically activated approach enables access to materials that respond to the presence of chemical energy and displaying mnemonic effects.



Fig. 1: *Pathway-dependent complexity in peptide libraries*: Formation of supramolecular structures in water using aminoacyl phosphate esters as energy sources, which can trigger spontaneous peptide oligomerisation through the transient assembly of phosphate anhydrides or thioesters. © Pappas Research Group

## References

- Hendricks, M. P.; Sato, K.; Palmer, L. C.; Stupp, S. I., Supramolecular Assembly of Peptide Amphiphiles. *Acc. Chem. Res.* 2017, 50 (10), 2440-2448.
- Boekhoven, J.; Hendriksen, W. E.; Koper, G. J.; Eelkema, R.; van Esch, J. H., Transient assembly of active materials fueled by a chemical reaction. *Science* 2015, 349 (6252), 1075-9.
- Mattia, E.; Otto, S., Supramolecular systems chemistry. *Nat. Nanotechnol.* 2015, 10 (2), 111-119.

## Responsive Dendritic Networks in Soft Elastic Material Systems

Efstathios Mitropoulos<sup>1</sup>, Claas-Hendrik Stamp<sup>1,2</sup>, Thomas Pfohl<sup>1,2</sup>

<sup>1</sup>Cluster of Excellence *livMatS*, University of Freiburg; <sup>2</sup>Department of Physics, University of Freiburg

Project funding: Funded by the Deutsche Forschungsgemeinschaft (DFG, German Research Foundation) under Germany's Excellence Strategy – EXC-2193/1 – 390951807

To achieve longevity regarding vital adaptive material systems, the common consensus indicates that mechanisms are needed to detect reduced functionality due to damage, to seal damage and to repair that damage. More rarely addressed is the necessity for a properly designed communication network that would allow those systems to exchange information

as well as materials to fulfil their expected functions.

The goal of this project is to design bio-inspired, responsive microfluidic dendritic networks that in their initial state are designed to facilitate flow from a starting point to multiple end points with the lowest possible required pumping power [1,2]. Moreover, in case of an error in the system, the network should be able to respond and change the network properties in order to address and correct the error. To emulate this error-induced behaviour, the response of the system to different stimuli, such as varying applied pressures or flow rates, local blockages, etc., can be studied.

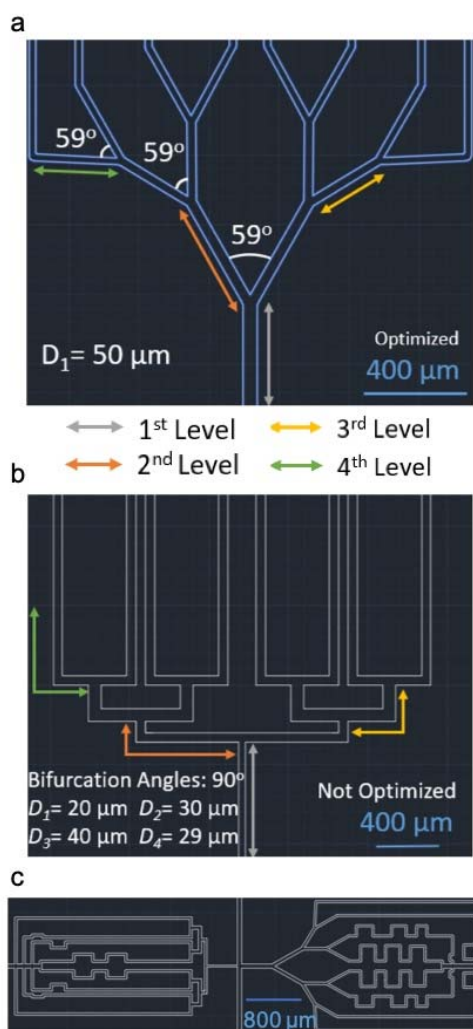


Fig. 1: Sketch of an optimized dendritic microfluidic system (a), non-optimized system of the same total volume (b) and a comparator design (c). © Pfohl Group

Dendritic structures are prominent in nature [3]. From river basins to vascular systems and tree-branching, very similar patterns can be observed. Behind this choice of nature is a common rule: The attempt of finite-sized systems to gain better access to surrounding flows. In the case of fluid flow, this choice results in a special constant volume design that minimizes the pumping power required for a steady flow rate [2,4]. Microfluidic network systems composed of polydimethylsiloxane (PDMS) offer a number of advantages, including a high surface-to-volume ratio for reactions (e.g. for sealing), small amounts of required working fluids, easy reproducibility and an adjustable Young's modulus between 0.5 and 3.7 MPa [5]. Moreover, channels in such systems can occupy only a small portion of the total bulk material, resulting in reduced risk in regard to the structural integrity of the system [6]. One of the disadvantages of microfluidic channel networks is the fact that the pressure difference, required to generate flow in them, scales inversely with the fourth power of their diameter. The combination of microfluidic channels and dendritic structures seems able to limit the effects of this drawback.

Our first realized iteration of the dendritic microfluidic network of four levels (generations) connects a single starting point with eight distributed end points (Fig. 1). The diameter  $D_i$  of the channels of the  $i^{\text{th}}$  level varies following the constructal law  $D_{i+1}/D_i = 1/\sqrt[3]{2}$  [1]. The occupied volume of the channels is kept constant by keeping the channel length for each level and height of the channels constant. Additionally, a bifurcation angle of  $59^\circ$  is used to further reduce of required pumping power [4]. In order to compare and characterize the improvements of this optimized system, a second microfluidic system with the same channel volume but without the diameter and bifurcation angle optimizations is designed in parallel with the first. The two parallelly linked systems connect the same starting point to eight end points each (Fig. 1c). The flow velocity distribution within the microfluidic comparator platform can be qualitatively analysed by means of particle image velocimetry (PIV). These comparator experiments can be carried out in two dif-

ferent modes, either at constant applied pressure or at constant flow rate. However, the obtained overall flow velocities as well as the velocities at the different levels are always larger for the optimized system as expected from the theory of optimization [2,3,4].

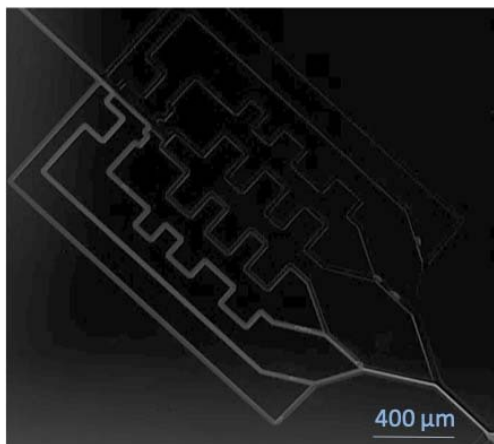


Fig. 2: Fluorescently stained isopropanol directed at specific regions of the dendritic structure. Iso-propanol flows in parallel with ethanol and the flow paths within the dendritic system are controlled by the flow ratio of isopropanol to ethanol. © Pfohl Group

For the spatiotemporal manipulation of the hydraulic resistance within the dendritic structure, we are using the co-flow of isopropanol, which is swelling PDMS, and ethanol, which shows a less pronounced tendency to swell PDMS. Channels, through which isopropanol flows, show reduced cross-sectional diameters and therefore increased hydraulic resistances, which lead to a redistribution of the flow velocities within the dendritic microfluidic system. Here, the flow paths or specific regions within the dendritic system, which have an increased hydraulic resistance, can be directly adjusted by the relative flow ratio of the co-flowing isopropanol and ethanol (Fig. 2).

This experimental setup can be used to topically change and test the response of the system to different internal and external stimuli, such as pressure drops or solvents with different swelling behavior. Moreover, due to smart design and right choice of fluids, we have a responsive microfluidic system with information transmission and feedback control at hand.

#### References

[1] Bejan, A., Rocha, L. & Lorente, S. (2000). Thermodynamic optimization of geometry: T- and Y-

shaped constructs of fluid streams. *International Journal of Thermal Sciences. Int. J. Therm. Sci.* **39**, 949-960.

[2] Bejan, A. & Errera, M. (1997). Deterministic tree networks for fluid flow: Geometry for minimal flow resistance between a volume and one Point. *Fractals* **5**, 685-695.

[3] Bejan, A. & Lorente, S. (2010). The constructal law of design and evolution in nature. *Phil. Trans. R. Soc. B* **365**, 1335–1347.

[4] Murray, C.D. (1926). The physiological principle of minimum work applied to the angle of branching arteries. *J. Gen. Physiol.* **9**, 835-841.

[5] Saliterman, S.S. (2006). *Fundamentals of BioMEMS and medical microdevices*. Wiley-Interscience, Bellingham, Wash., SPIE Press.

[6] Beaumont, P.W.R. (2020). The structural integrity of composite materials and long-life implementation of composite structures. *Applied Composite Materials* **27**, 449-478.

## Flow-Induced Instabilities of Soft Walls in Microfluidics

Claas-Hendrik Stamp<sup>1,2</sup> and Thomas Pfohl<sup>1,2</sup>

<sup>1</sup>Experimentelle Polymerphysik, Albert-Ludwigs-Universität Freiburg; <sup>2</sup>Freiburg Center for Interactive Materials and Bioinspired Technologies (FIT)

Project funding: German Research Foundation (DFG) – Priority Programme 2171

The field of microfluidic applications in technology as well as in research has developed rapidly in the last decades. The ever-growing application areas require new mechanisms and modes of operation from microfluidic systems. One promising approach is to introduce elastic elements into microfluidic devices, which can be used e.g. as pneumatically driven valves and pumps in highly integrated microfluidic networks [1,2] or surface charge-sensitive nano-trapping and sorting [3,4]. In addition, microfluidic flows can be controlled by pressure-induced elastic deformations, since the flow velocity depends strongly on the geometric properties of the channel.

To study the coupling of flows through thin, soft, and elastic walls and to exploit their potential to control material and information transport in fluid networks, we have developed a straightforward microfluidic device to characterize elasto-fluid dynamics interactions in

## Highlights

these systems. The microfluidic device consists of two closed channels which are separated by a thin elastic wall (Fig. 1) and was made of polydimethylsiloxane (PDMS) by a regular monolithic soft lithography process [5].

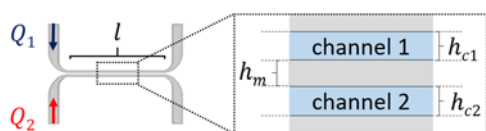


Fig. 1: Schematic representation of the used microfluidic device. Side view on the thin wall (length  $l$ , width  $h_m$ ) separating two channels realized (width  $h_{c1} = h_{c2}$ ) in the microfluidic device. The volume flow rates  $Q_1, Q_2$  in the channels can be independently controlled. © Pfohl Group

The thin wall has a length  $l = 1000 \mu\text{m}$ , a height  $w = 200 \mu\text{m}$  and a width  $h_m = 20 \mu\text{m}$ . The width of the channels are  $h_{c1} = h_{c2} = h_m = 20 \mu\text{m}$ . To optimize the elasto-fluid dynamics interactions, the aspect ratio of the thin wall is as close as possible to the fabrication limits,  $w/h_m = 10$ . The (volume) flow rates of the fluids in the channels  $Q_1$  and  $Q_2$  can be controlled by syringe pumps.

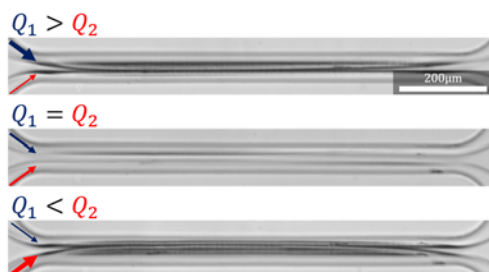


Fig. 2: Deformation of the thin wall depending on the flow rates in the adjacent channels. For  $Q_1 > Q_2$  the wall is bent towards channel 2, for  $Q_1 = Q_2$  no deflection can be observed and for  $Q_1 < Q_2$  the wall is bent towards channel 1. The flow rates are symbolized by blue (channel 1) and red (channel 2) arrows. © Pfohl Group

In initial experiments, we studied the impact of two parallel flows of water on the shape of the thin wall as shown in Fig. 2. For imaging the wall separating the two channels from the side, we focused the microscope at half of the channel height. Due to the parallel flow, a pressure gradient along the flow direction forms. In case  $Q_1 = Q_2$ , the pressure difference between both sides of the thin wall is 0. Therefore, no deformation of the thin wall can

be observed in the micrograph for  $Q_1 = Q_2$  in Fig. 2. For  $Q_1 > Q_2$ , due to the higher flow rate and therefore higher pressure in channel 1, the thin wall is deflected and bent towards channel 2. The bending and deflection of the wall causes reflections of light away from the imaging paths of the microscope, which can be recognized by the darker areas close to the bent wall in the micrographs. For  $Q_1 < Q_2$ , now the wall is consequently bent and deflected towards channel 2.

This observed behavior is consistent with lamellar conditions in microfluidics, where friction forces are predominant. In order to test the impact of additional inertial forces on the deformation of the thin wall, we increased the flow rate  $Q_1$ , while leaving the ratio  $Q_1/Q_2 = 4$ . The ratio of the inertial forces to the friction forces in fluidic systems is commonly described by the Reynolds number  $Re = \rho \cdot v \cdot w / \eta$ , with density  $\rho$ , viscosity  $\eta$  and the velocity  $v = Q / (w \cdot h)$ . For a flow rate of  $Q_1 = 1.6 \mu\text{L/s}$  with  $Re_1 \approx 8$ , which means that the inertial forces are 8 times larger than the friction forces, a deformed wall bent towards channel 2 can be observed (Fig. 3), as also seen in the experiments in Fig. 2.

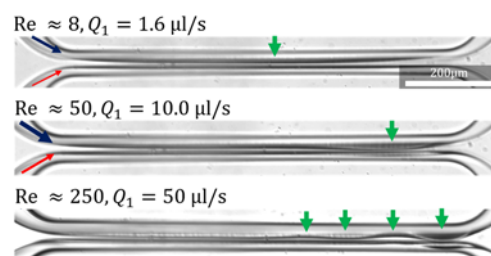


Fig. 3: Emergence of a flow-induced instability. Micrographs showing the deflection of the thin wall as a function  $Q_1$  or  $Re_1$ . The ratio of  $Q_1/Q_2 = 4$  is fixed in the experiments. The positions of the (local) maximum deflections are marked with a green arrow. © Pfohl Group

Increasing the flow rate to  $Q_1 = 10.0 \mu\text{L/s}$  and thus  $Re_1 \approx 50$ , meaning that the inertial forces becoming more dominant, a more localized bending of the wall towards channel 2, which moved further downstream and closer to the end of the wall, can be observed (green arrow, Fig. 3). Increasing the flow rate even further to  $Q_1 = 50.0 \mu\text{L/s}$  or  $Re_1 \approx 250$ , which means that the friction forces can be neglected, an in-

stability (buckling) can be seen with alternating bending of the wall towards channel 2 (green arrows, Fig. 3) and inwards to channel 1. The maximum deflection of the instability is increasing in downstream direction. We observed an instability, caused by two parallel flows with different flow velocities separated by a thin wall, which has some analogies to Kelvin-Helmholtz instabilities.

Using the coupling of elastic walls with fluid dynamics within a microfluidic device, we are able to induce an instability and therefore introducing a non-linear behavior into our system. This setup has great potential for integrating feedback and adaptability into fluid networks and for development of logic gates in microfluidics.

#### References

- [1] Unger, M.A., Chou, H.P., Thorsen, T., Scherer, A., & Quake, S.R. (2000). Monolithic microfabricated valves and pumps by multilayer soft lithography. *Science* **288**, 113-116.
- [2] Thorsen, T., Maerkl, S.J., & Quake, S.R. (2002). Microfluidic large-scale integration. *Science* **298**, 580-584.
- [3] Gerspach, M.A., Mojarad, N., Sharma, D., Pfohl, T., & Ekinici V. (2017). Soft electrostatic trapping in nanofluidics. *Microsystems & Nanoengineering* **3**, 17051.
- [4] Gerspach, M.A., Mojarad, N., Sharma, D., Ekinici, Y., & Pfohl, T. (2018). Pneumatically controlled nanofluidic devices for contact-free trapping and manipulation of nanoparticles. *Part. Part. Syst. Charact.* **35**, 1800161.
- [5] Xia, Y. & Whitesides, G.M. (1998). Soft lithography. *Annual Review of Materials Science* **28**, 153-184.

## Facile fabrication of micro-/nanostructured, superhydrophobic membranes with adjustable porosity by 3D printing

Fadoua Mayoussi<sup>1</sup>, Frederik Kotz-Helmer<sup>1</sup>, Dorothea Helmer<sup>1,2</sup>, Bastian E. Rapp<sup>1,2</sup>

<sup>1</sup>Laboratory of Process Technology (NeptunLab), Department of Microsystems Engineering; <sup>2</sup>Freiburg Center for Interactive Materials and Bioinspired Technologies (FIT)

Project funding: Funded by the Federal Ministry of Education and Research 03X5527, the German Research Foundation (Deutsche Forschungsgemeinschaft, DFG) under Germany's Excellence Strategy – EXC-2193/1 – 390951807

Porous membranes with special wetting properties have attracted significant attentions in many application such as water purification <sup>[1]</sup>, water-oil separation <sup>[2]</sup> and oil skimming <sup>[3]</sup> due to their high separation efficiency. Special wetting properties, such as superhydrophobicity are obtained by controlling both the surface topography and the surface chemistry.

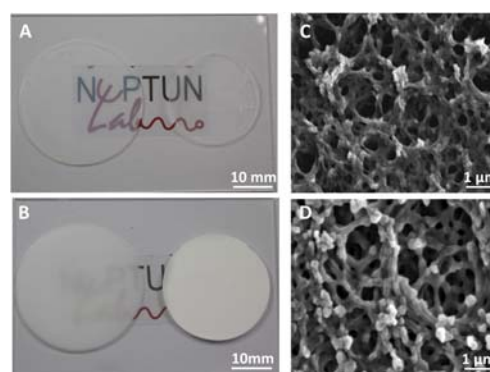


Fig. 1: 3D printed disc shaped membranes with 500  $\mu\text{m}$  thickness. (A) 3D printed translucent membrane with smaller pores; (left) after printing and (right) shrunken dried membrane stack after porogen removal. (B) 3D printed white membrane with larger pores; (left) after printing and (right) shrunken dried membrane stack after porogen removal. (C) cross-sectional SEM image of membrane from image (A), (D) cross-sectional SEM image of membrane from image (B). (© NeptunLab, IMTEK)

Three-dimensional (3D) printing has recently emerged as a promising method to fabricate porous membranes due to its great flexibility to generate objects with complex structures. <sup>[4-6]</sup> Most common reported methods rely on a

two-steps procedure; 3D printing of a pre-defined geometry followed by a chemical post-processing, e.g. spray coating or dip coating, using materials with low surface energy. However, these methods showed limitations in terms of the durability and stability of the coating layer as the layers are not mechanically stable. Furthermore, the reported post-modifications can only be applied onto the surfaces and not into the bulk. Thus, mechanical abrasion leads to the loss of the (super-) hydrophobicity in these materials.

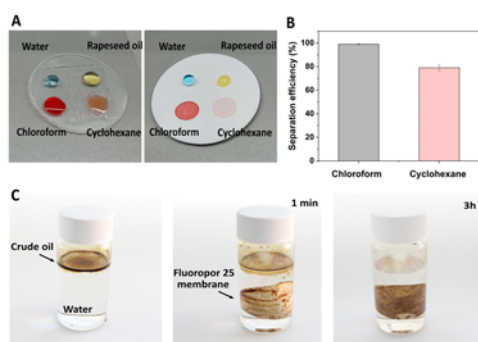


Fig. 2: (A) Photograph of water droplet and different liquid droplets on translucent Fluoropor membrane (left) and on white Fluoropor membrane (right), (B) the separation efficiency of the white Fluoropor membrane for mixtures of water–chloroform and water–cyclohexane. (C) absorption of crude oil drop in water using the white membrane. (© NeptunLab, IMTEK)

In this work, a facile fabrication method to produce porous membranes via stereolithography printing process and by combining both the required topography and surface chemistry is reported.<sup>[7]</sup> This was achieved by mixing a highly fluorinated photocurable resin with a porogen mixture, which consists of a non-solvent and an emulsifier. This creates a micro-/nanostructure throughout the bulk by phase separation during polymerization. This material, which we termed “Fluoropor”<sup>[8]</sup> possesses a bulk porosity which makes it insensitive to abrasion. The printed membrane showed a porosity in the submicron range, which could be easily adjusted from 30 nm to 300 nm by only varying the porogen ratio in the mixture, resulting in translucent or white materials depending on pore sizes after porogen removal and drying (see Fig. 1).

Due to their bulk porosity and hydrophobicity, the printed porous membranes were tested in terms of their liquid absorption and separation capability. The membranes with an average pore size around 300 nm achieved an excellent water-oil separation efficiency of 99% for chloroform/water. Moreover, they showed excellent capacity to absorb crude oil, which enables their potential use in oily wastewater treatments. (see Fig. 2).

With this printing technology the fabrication of thin superhydrophobic membranes was also shown. The resin was printed into a “staircase” design, which with help of the layer-by-layer nature of the SLA printing process, enables the peeling off of thin layers from the bulk. The thin membranes (100 μm – 400 μm) showed superhydrophobic wetting properties and achieved a static contact angle of 164 ° with water.

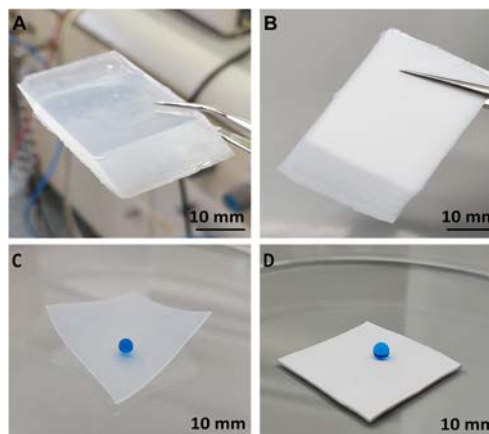


Fig. 3: Fabrication of thin superhydrophobic membranes by 3D printing peelable layers. Printed blocks of (A) translucent Fluoropor with smaller pores, (B) white Fluoropor with larger pores. (C) and (D) Peeled-off thin layers of the Fluoropor blocks shown in (A) and (B). (© NeptunLab, IMTEK)

The thin superhydrophobic Fluoropor 15 membranes were successfully used for the generation and detection of *Salvinia* layers. When submerged under water, an air film was trapped in the micro-/nanostructure of the membrane forming the *Salvinia* layer. This air retention capability is of great interest for drag reduction in maritime transportation and fouling prevention.

## References

- [1] J. Park, P. Bazylewski, G. Fanchini, *Nanoscale*. 8, 9563 (2016).
- [2] E.-C. Cho, C.-W. Chang-Jian, H.-C. Chen, K.-S. Chuang, J.-H. Zheng, Y.-S. Hsiao, K.-C. Lee, J.-H. Huang, *Chem. Eng. J.* 314, 347 (2017).
- [3] X. Zhao, L. Li, B. Li, J. Zhang, A. Wang, *J. Mater. Chem. A*. 2, 18281 (2014).
- [4] S. Yuan, J. Zhu, Y. Li, Y. Zhao, J. Li, P. V. Puyvelde, B. V. der Bruggen, *J. Mater. Chem. A*. 7, 2723 (2019).
- [5] R. K. Kankala, X.-M. Xu, C.-G. Liu, A.-Z. Chen, S.-B. Wang, *Polymers*. 10, 807 (2018).
- [6] R. Karyappa, A. Ohno, M. Hashimoto, *Mater. Horiz.* 6, 1834 (2019).
- [7] F. Mayoussi, E. H. Doeven, A. Kick, A. Goralczyk, Y. Thomann, P. Risch, R. M. Guijt, F. Kotz, D. Helmer, B. E. Rapp, *J. Mater. Chem. A*. 9, 21379 (2021).
- [8] D. Helmer, N. Keller, F. Kotz, F. Stolz, C. Greiner, T. M. Nargang, K. Sachsenheimer, B. E. Rapp, *Sci Rep.* 7, 15078 (2017).

## Heterogeneous mechanical metamaterials: towards adaptivity and learning

Viacheslav Slesarenko<sup>1,2</sup>, Gerrit Felsch<sup>1,2</sup>

<sup>1</sup>Cluster of Excellence livMatS; <sup>2</sup>Freiburg Center for Interactive Materials and Bioinspired Technologies (FIT)

Project funding: Funded by the Deutsche Forschungsgemeinschaft (DFG, German Research Foundation) under Germany's Excellence Strategy – EXC-2193/1 – 390951807

This project focuses on the development of adaptive heterogeneous mechanical metamaterials. While exploring natural materials and structures, it is easy to notice that their architecture is neither random nor strictly periodic. The heterogeneous architecture enables variance of the mechanical properties throughout different regions of material as well as introduces structural hierarchy beneficial, for instance, against damage. However, immense design space associated with heterogeneity amplifies the problem of predicting the resulting properties, therefore, compromising the implementation of such systems in real-life applications. While with an increase in the number of design variables forward problem of property prediction becomes gradually more

challenging, the inverse problem of designing materials with desired properties gets almost impossible in the framework of the classical approaches.

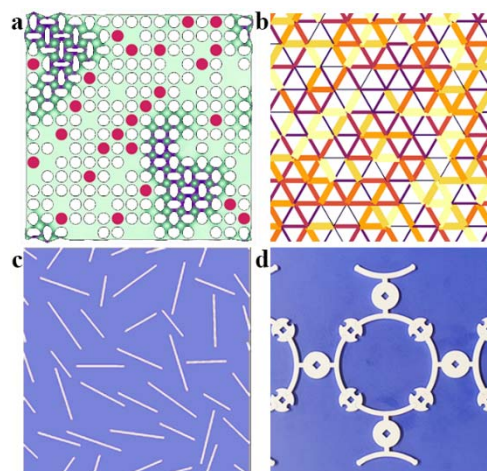


Fig. 1: (a) – instability-driven pixel metamaterials. (b) – defected architected lattice with trusses of variable thickness. (c) – elastic sheet with randomly oriented cuts. (d) – the concept of tillable elastic metamaterial. © Viacheslav Slesarenko

Therefore, in this subproject, we explored the potential of modern machine learning approaches to predict properties of heterogeneous mechanical/elastic metamaterials and generate structures with requested properties. We devoted our attention to three systems, in particular: instability-driven pixel metamaterials (Fig. 1a), defected architected lattices (Fig. 1b), and elastic sheets with randomly positioned cuts (Fig. 1c). By employing classical convolutional neural networks (CNNs), we demonstrated how the effective critical buckling strain depends on the arrangement of holes and stiff inclusions embedded into a soft matrix in the pixel metamaterials. The prediction capacity of the neural networks was also employed to reveal how manufacturing defects might lead to the degradation of the mechanical properties in architected materials. By processing many thousands of the architectures, we were able to select the most robust configurations. Finally, with the help of modern generative adversarial networks (GANs), we sped up the simulation of the elastic sheets with cuts by replacing finite element analysis with the predictions via GAN. While it was relatively straightforward to predict the mechanical behaviour of such materials, it

was very challenging to generate materials with the desired combination of mechanical properties. Exploring different training techniques, we showed that after learning from the training dataset, GAN started to prefer avoiding cuts intersections during generation without any explicit instruction to do that. Combining the loss functions responsible for geometric and material factors, GAN demonstrated relatively high accuracy of predictions.

A specific subclass of heterogeneous metamaterial – so-called tillable metamaterials – was employed to change and control the elastic properties of the system shown in Fig. 1d. Tillable systems can be assembled from the limited set of unit cells of different geometries. In our case, we considered tiles of two types only, however enabling 90-degree rotations. Preliminary experimental data demonstrated that by arranging the initial and rotated pieces in various order, it is possible to control the propagation of elastic waves through the metamaterial and open acoustic bandgaps that might be useful for adaptivity.

### Demonstrator for soft autonomous machines – soft robotic low energy gripper systems based on livMatS materials with sensing capabilities

Armin Jamali<sup>1,2</sup>, Robert Knörlein<sup>1</sup>, Dr. Frank Goldschmidtböing<sup>1,2</sup>, Prof. Dr. Peter Woias<sup>1,2</sup>

<sup>1</sup>Laboratory for the Design of Microsystems, Dept. of Microsystems Engineering (IMTEK); <sup>2</sup>Cluster of Excellence livMatS @ FIT – Freiburg Center for Interactive Materials and Bioinspired Technologies Bioinspired Technologies (FIT)

Project funding: Funded by the Deutsche Forschungsgemeinschaft (DFG, German Research Foundation) under Germany's Excellence Strategy – EXC-2193/1 – 390951807

Dielectric Elastomer Actuators (DEAs), known as artificial muscles, are a subset of electroactive polymers made of a thin layer of elastomer sandwiched between two compliant layers of electrodes and driven by electrostatic force. To fabricate the gripper (Fig. 4), we deposited

the mixture of ECOFLEX™ 00-10 and SILICONE THINNER™ (*KauPo Plankenhorn e.K.*) with a spin-coating machine. Then, the carbon powder (*P250, Ensaco*) was directly dry-brushed onto the cured elastomer **Fehler! Verweisquelle konnte nicht gefunden werden.**

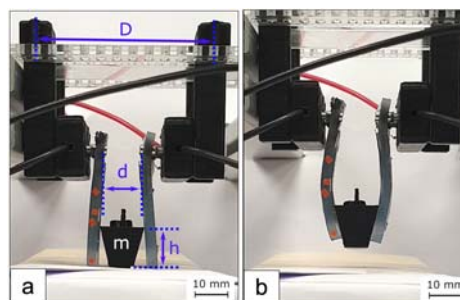


Fig. 4: (a) The soft gripper ready for actuation,  $m_{\max} = 10.29$  g,  $D = 55$  mm,  $d = 11$  mm,  $h = 14$  mm (b) the soft gripper lifting and holding the weight under 8 kV. (© Laboratory for Design of Microsystems)

This method turned out to be repeatable and reproducible. The key point for having bending actuators is the PMMA back-bones embedded in the last elastomer layer (Fig. 5). The back-bones increase the mechanical resistance on one side, making the actuator bend (Fig. 6). Eventually, the finger structure is made of two bending actuators facing each other (Fig. 4).

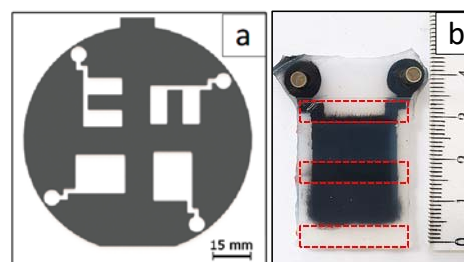


Fig. 5: (a) The PMMA mask with lasered pattern (b) The bending actuator. The red dashed lines indicate the position of the PMMA back-bone structure. (© Laboratory for Design of Microsystems)

The thickness of elastomer layers was tunable between 40  $\mu\text{m}$  and 800  $\mu\text{m}$  (Fig. 7), and the electrode layer was between 5  $\mu\text{m}$  to 10  $\mu\text{m}$  thick. We also characterized the elastomer electrically and mechanically (Young's modulus = 0.058 MPa, relative dielectric constant =  $4.39 \pm 0.01$  @ 20 Hz, electrical breakdown strength = 21.87  $\text{V} \cdot \mu\text{m}^{-1}$ ). The soft gripper was

able to bend up to  $67.9^\circ$  under no-load condition and successfully lift, hold, and release the objects up to 100.9 mN.



Fig. 6: Schematic of the cross-section of the bending actuator. (a) the passivation layer (b) PMMA backbones (c) elastomer layer (d) electrode layer (e) active elastomer layer for actuation (© Laboratory for Design of Microsystems)

The advantage of this work is the independence from any external frame, scalability, and ease of thickness control. This research paves the way for future works for the scientific community to miniaturize the gripper and optimize the back-bone structure to realize more complex motions like twisting grippers.

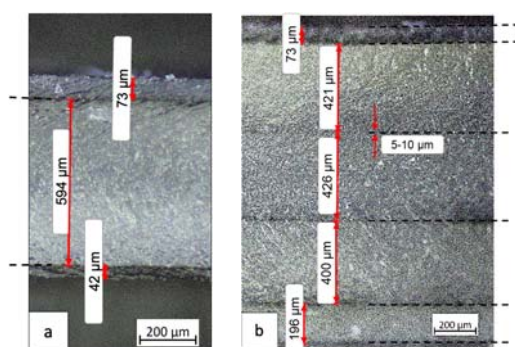


Fig. 7: Cross-section view of the actuators under the microscope. Dashed lines are the carbon layers. (a) a single-layer actuator (b) a multi-layer actuator (© Laboratory for Design of Microsystems)

## References

- [1] H. Shigemune et al., "Dielectric Elastomer Actuators with Carbon Nanotube Electrodes Painted with a Soft Brush," *Actuators*, vol.7, no. 3, p. 51, 2018, doi: 10.3390/act7030051.

## [2+2]-Photocycloadditions of Heterocoumarins as Effective Tool for the Reversible Formation of Covalent Bonds – Towards the Design of Sustainable Materials

Moritz Streicher<sup>1</sup>, Céline Calvino<sup>1</sup>

<sup>1</sup>Center of Excellence *livMatS*, Freiburg Center for Interactive Materials and Bioinspired Technologies (FIT)

Project funding: Funded by the Deutsche Forschungsgemeinschaft (DFG, German Research Foundation) under Germany's Excellence Strategy – EXC-2193/1 – 390951807

This research investigates new routes towards the design of renewable polymer materials and in this context, proposes the preparation of a new class of responsive materials that can be polymerized and depolymerized on demand upon photo-stimulation. To achieve such responsive materials, photo-switchable motifs - capable to break and reform covalent bonds upon dissimilar irradiations- will be incorporated into polymer backbones to form responsive building blocks. Hence, a first irradiation will trigger photo-chemical reactions between these motifs and enable the propagation of the polymer chains to produce high molecular weight polymers. Conversely, a second and dissimilar irradiation will trigger the disruption of these motifs and break down the polymer backbones to their original building blocks (Figure 1A). Combined these two orthogonal photo-processes will allow reshaping, repairing, or reprocessing of polymer materials.

To achieve these envisioned reversible polymerizations, this work focuses on the use of photoswitchable motifs that rely on reversible [2+2]-cycloaddition reaction mechanisms. This chemistry typically involves the photo-reaction of two alkene motifs to form a cyclobutane moiety (covalent bond formation) and that can be reversed into the original alkenes upon dissimilar irradiation (breaking bond). While some useful photo-switches have been already reported in the literature, these motifs usually lack in their overall photo-efficiency and present either low reaction rates, conversions or orthogonality. Most importantly, the produced cyclobutanes usually require high

energetic UV irradiation to undergo the cycloreversion that could potentially lead, in this framework, to photodamages of the polymer backbones.

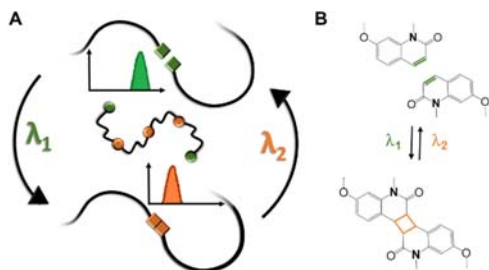


Fig. 1: A) scheme of the reversible photoligation of photo-responsive building blocks B) Reversible [2+2]-cycloaddition mechanism of quinolinone coumarin derivatives upon dissimilar irradiation. © Copyright Dr. Céline Calvino

To ensure a high efficiency of these photo-processes and thus the preparation of mechanically robust materials as well as their renewability, this research started investigating the enhancement of the photoswitches' properties through a rational modification of their molecular structures. These improved properties target the development of specific UV-vis triggered photo-processes, the minimization of the photoprocesses overlap (orthogonality) and the optimization of the reaction rates and conversions. In this context, a series of heterocoumarins carrying different heteroatoms (C, N, O, S, Se) in 1-position and their respective photo-dimers have been synthesized and characterized. The photo-efficiencies of the prepared photo-switches were investigated by means of UV-Vis and  $^1\text{H-NMR}$  spectroscopy. On the basis of these characterizations, the motifs were then tuned to achieve optimized photo-systems. So far, nitrogen substituted coumarin derivative (quinolinone derivative, Figure 1B) have shown a significant increase of the photocycloaddition rates in solution and conversions above 90%, compared to 70% obtained for standard coumarin derivatives. Furthermore, the higher extinction coefficient provided by the quinolinone dimers resulted in higher cycloreversion rates and enhanced orthogonal photo-processes. Additional optimizations are currently on going to further maximize these photo-switches' properties.

## FUTURE FIELD "BIOMIMETIC, BIOBASED AND BIOACTIVE MATERIALS SYSTEMS"

### Multi-material 3D-printer for rapid prototyping of bio-inspired demonstrators

Stefan Conrad<sup>1,2</sup>, Falk Tauber<sup>1,2</sup>, Thomas Speck<sup>1,2</sup>

<sup>1</sup>Plant Biomechanics Group (PBG) Freiburg, Botanic Garden of the University of Freiburg, <sup>2</sup>Cluster of Excellence *livMatS* @ FIT – Freiburg Center for Interactive Materials and Bioinspired Technologies

Project funding: Funded by the Deutsche Forschungsgemeinschaft (DFG, German Research Foundation) under Germany's Excellence Strategy – EXC-2193/1 – 390951807

Stefan Conrad is recipient of a Hermann-Staudinger-Fellowship.

A central goal within the *livMatS* research area "Demonstrators" are technical demonstrators like an artificial Venus flytrap [1-5], which will demonstrate the feasibility of the developed materials systems. Like their biological role models, these bio-inspired constructs will show complex behaviour in reaction to changing environmental conditions, whereby these reactions in form of motion or shape changes will not be initiated via a central control unit but in a plant-like manner through decentralized stimulus-response systems using embedded intelligence and embedded energy. Depending on the nature of the stimulus and the intended response, this requires the integration of diverse materials and mechanisms. Especially the material composition in complex systems requires special manufacturing methods that offer rapid prototyping and a high degree of automation.

For this purpose, a novel multi-material 3D-printer with on demand tool changing properties (Fig. 1A), has been developed. Unlike classic FDM printers, the filament extruders are not directly mounted to the motion system of the new device but kept in a standby position. Using a carriage with a specifically developed adaptive coupling mechanism the printer picks up the required tool, initializes it and

prints the specified part of the current layer. After use, the print head is returned to its docking station and the device switches to the next tool. In contrast to other printers with multiple extruders, this setup avoids any kind of unwanted interaction between nozzles, filaments or printheads, since the docking stations are located outside the build volume [6].

Currently, the printer is equipped with one filament print head and one syringe extruder, which can handle pastes and high viscous fluids. The directly driven FDM-head is optimized for extremely flexible materials, and the applied print parameters are under ongoing tuning to improve its reliability and to minimize the required maintenance. The tested “TPU A70” filament turned out to have a high potential for the fabrication of airtight channels and expandable membranes. The introduction of an adapted flow rate enabled the creation of resilient structures with high surface quality. Through this, we were able to gain experience in developing and printing different kinds of novel pneumatic actuators and other stretchable elements.

We tested and characterized fully flexible pneumatic fingers (see report “Development of a baseline bioinspired macroscopic gripper system within *livMatS* for” for more details), multi-material elements and generic, multiuse actuators, which can be easily and quickly modified after production to fit the specific application (Fig. 1). By cutting specific restrictions of the customizable actuator (Fig. 1A), it can be configured for bending (Fig. 1A-B) and linear (Fig. 1C-D) expansion or contraction behaviour with individual pressure control for separate segments.

Based on the gained experience we have gone beyond basic pneumatic actuators, and utilize 3D printed pneumatic systems to research and develop complex pneumatic elements that work as binary logic gates. Combining actuators and compressible channels, these structures mimic the work principle of electric transistors and are able to form logic elements and bigger pneumatic circuits. Since they are 3D printed in one piece and do not contain any support material, the gates are functional and ready-to-use directly after fabrication.

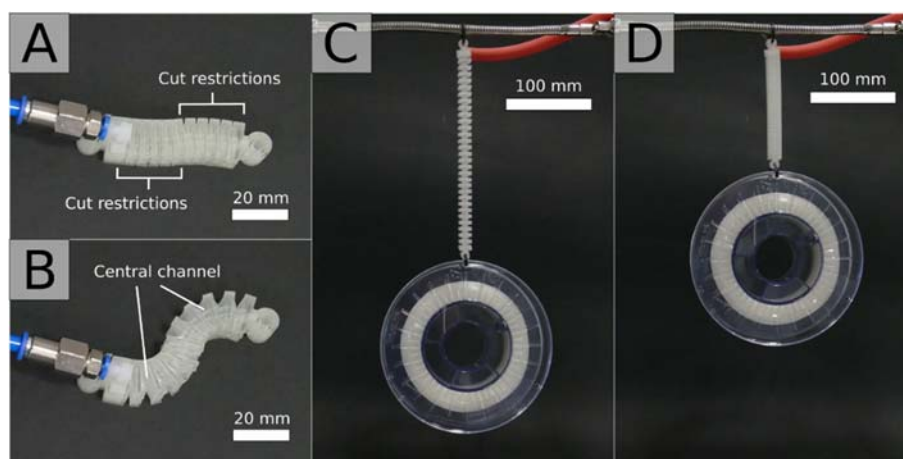


Fig. 1: Three configurations of the customizable pneumatic actuator (CPA) at pressure test. **A:** Relaxed CPA (10 segments). **B:** Pressurized (100 kPa) CPA (10 segments) expanding on sides with cut connections. **C:** Relaxed CPA (30 segments) stretched by 350 g weight. **D:** Evacuated (-99 kPa) CPA (30 segments) lifting 350 g weight [from 7, modified under Creative Commons Attribution 4.0 licence].

Basic elements are already designed, successfully tested and their application in more advanced dynamic circuits has been demonstrated. The current focus lies on the miniaturization and optimization of the existing models before it will shift towards new gates and demonstrator applications in the future.

The described progress in design and rapid prototyping of pneumatic actuators and logic circuits highlights the potential of our new multi-material printer. Combined with the innovative finger actuators developed in the PhD of Peter Kappel, the binary gates have the potential to realize an innovative pneumatic gripper, which is entirely controlled by a logic system powered by the same pressure source as the gripper itself. Such a demonstrator could be completely independent from any kind of electric power and were an important step towards the autonomous, quasi-living systems *livMatS* is aiming for.

### References

- [1] Poppinga, S. & Joyeux, M. (2011). Different mechanics of snap-trapping in the two closely related carnivorous plants *Dionaea muscipula* and *Aldrovanda vesiculosa*. *Phys. Rev. E*, 84(4), 041928, doi: 10.1103/PhysRevE.84.041928
- [2] Poppinga, S., Bauer, U., Speck, T. & Volkov, A.G. (2017) Motile traps. In: Ellison, A.M., Adamec, L. (eds.), *Carnivorous plants: physiology, ecology, and evolution*, 180-193. Oxford University Press, Oxford
- [3] Esser, F., Scherag, F.D., Poppinga, S., Westermeier, A., Mylo, M.D., Kampowski, T., Bold, G., R  he, J. & Speck, T. (2019) Adaptive Biomimetic Actuator Systems Reacting to Various Stimuli by and Combining Two Biological Snap-Trap Mechanics. In: Martinez-Hernandez U. et al. (eds.) *Biomimetic and Biohybrid Systems. Living Machines 2019. Lecture Notes in Computer Science*, vol. 11556, 114-121. Springer, Cham, doi: 10.1007/978-3-030-24741-6\_10
- [4] Westermeier, A., Sachse, R., Poppinga, S., V  gele, P., Adamec, L., Speck, T. & Bischoff M. (2018). How the carnivorous waterwheel plant (*Aldrovanda vesiculosa*) snaps. *P. Roy. Soc. B-Biol. Sc.*, 285. 20180012, doi: 10.1098/rspb.2018.0012
- [5] Sachse, R., Westermeier, A., Mylo, M., Nadasdi, J., Bischoff, M., Speck, T. & Poppinga, S. (2020). Snapping mechanics of the Venus flytrap (*Dionaea muscipula*). *PNAS*, 117(27), 16035-16042, doi: 10.1073/pnas.2002707117
- [6] Conrad, S., Speck, T. & Tauber, F. (2020). Multi-material 3D-printer for rapid prototyping of bioinspired soft robotic elements. In: V. Vouloutsis, A. Mura, F. Tauber, T. Speck, T.J. Prescott & P.F. Verschure (eds.), *Biomimetic and Biohybrid Systems. Living Machines 2020*, 46 – 54. Lecture Notes in Computer Science LNAI 12413. Springer International Publishing, Cham, doi: 10.1007/978-3-030-64313-3\_6
- [7] Conrad, S., Speck, T., & Tauber, F. (2021). Tool changing 3D printer for rapid prototyping of advanced soft robotic elements. *Bioinspiration & Biomimetics*, doi: 10.1088/1748-3190/ac095a

## Development of a baseline bioinspired macroscopic gripper system within *livMatS*

Peter Kappel<sup>1,2</sup>, C. Kramp<sup>1,2</sup>, A. Ladhad<sup>2</sup>, Thomas Speck<sup>1,2</sup>, Falk Tauber<sup>1,2</sup>

<sup>1</sup>Plant Biomechanics Group (PBG) Freiburg, Botanic Garden of the University of Freiburg;  
<sup>2</sup>Cluster of Excellence *livMatS* @ FIT – Freiburg Center for Interactive Materials and Bioinspired Technologies

Project funding: Funded by the Deutsche Forschungsgemeinschaft (DFG, German Research Foundation) under Germany's Excellence Strategy – EXC-2193/1 – 390951807

Within the "Demonstrator" research area, devices are developed, suitable for envisaging the feasibility of novel materials systems as aimed for in *livMatS*. As an example of such a device, a macroscopic gripper system is presented inspired by principles of elastic movements found in many soft motile plant and animal organs.

During evolution, various adaptive gripping systems emerged in living nature based on relatively simple functional processes. We use these biological examples as sources of inspiration to develop a gripping system with the ability to adapt the grasping movement and force to the qualities of a grasped object, such as shape, size, weight, and fragility. A centimeter-scaled macroscopic gripper is developed, representing an innovative device for future industrial and medical applications where robots grasp variable, often delicate objects or come in direct contact with humans. Such a device has a high potential as a showcase for the public outreach and science communication of novel bioinspired materials systems developed in the *livMatS* cluster. To achieve this,

we choose the approach of a soft, autonomous machine, with its suitable characteristics like softness, flexibility, and adaptability for human-machine interaction. The construction of a modular gripper platform will enable the integration of various materials and sensors of other *livMatS* projects in the future.

Pneumatic actuators induce the motion of our system by directly moving the fingers in response to changes in applied air pressure. While the pressure comes from an external pressure source, the material and design of the fingers determine the grasping characteristics. As our modular gripper platform approach allows easy exchange of main components for newer versions, we currently concentrate on design and fabrication processes to optimize the actuators. With the advent of flexible 3D printing materials, actuator designs that were previously difficult or impossible to produce can now be implemented. We use state-of-the-art additive manufacturing such as multi-material FDM and PolyJet 3D printing to rapidly prototype our novel designs.

The PolyJet method provides a broad range of flexible materials and is suitable for multi-material printing with complex and large overhanging structures. However, the print materials show a low ultraviolet light resistance and require a specific design that allows removing the supporting material from the inside of hollow structures, as e.g. the pneumatic chambers. In comparison, the FDM printer uses no supporting material that needs to be removed but limits, on the other hand, the extent of feasible overhangs. Furthermore, the nozzle size of the printer restricts currently small-scale actuator designs. To obtain airtight pressure chambers, pneumatic actuators are manufactured typically with a wall thickness that is a multiple of the nozzle diameter [1]. With the within *livMatS* developed multi-material printer [2], we are able to FDM print airtight pneumatic bending actuators from one of the softest available flexible filaments (Recreus, Filaflex, shore hardness A70) with a wall thickness of 0.5 mm [3]. Reducing the wall thickness of the expanding pressure membranes also reduces the necessary air pressure and overall power consumption for actuation. To determine

which actuator concepts can be best implemented with which of the aforementioned 3D printers, we have developed a test actuator that can be printed with both types of printers (Fig. 1). We achieved this through a design with air chambers and access openings large enough to remove the PolyJet supporting material. However, the test actuator's sidewall was an overhanging structure that was too large to be FDM printed conventionally. Therefore, we established a method, which uses a separately printed support inlay that we manually inserted during the printing process and removed afterward.

Characterization of the test actuators by bending angle and torque revealed distinct differences in their response to applied air pressure. On average, the test actuators printed with PolyJet material bent at 1.0 bar and below with a four times higher bending angle than the FDM printed actuators. The generated torque of both actuator types was up to 1.0 bar without a significant difference. However, beyond 1.0 bar, the PolyJet printed actuators failed while the FDM printed ones withstand applied air pressures up to 4 bar and above, indicating lower sensitivity but much higher robustness and performance. Currently, we establish FEA simulations to validate the results and deepen our understanding of the suitability of each method for specific applications. These results will form the basis to translate new inspirations from biological elastic movements into future designs of bioinspired low energy actuators and gripper systems by fully exploiting the advantages of each additive manufacturing method.

A further concept that will be integrated into our system soon is the posture of the relaxed human hand, whose underlying structural and functional principles we want to implement for an adaptive low-energy gripper. With the evolution of thumbs, grasping became a fundamental movement and a cornerstone of the development of the great apes (Hominidae), and opposable thumbs with their complex musculature are often discussed as contributing to the dominance of humans (genus *Homo*) and their direct precursors. However, the unconscious movement during grasping, an everyday occurrence for humans, requires

immense computing power in technical systems, especially in implementing grippers for fine and adaptive movements. Therefore, our approach is to relocate and reduce this computation by decentralized material-immanent processing, so to speak, material-based embodied intelligence.

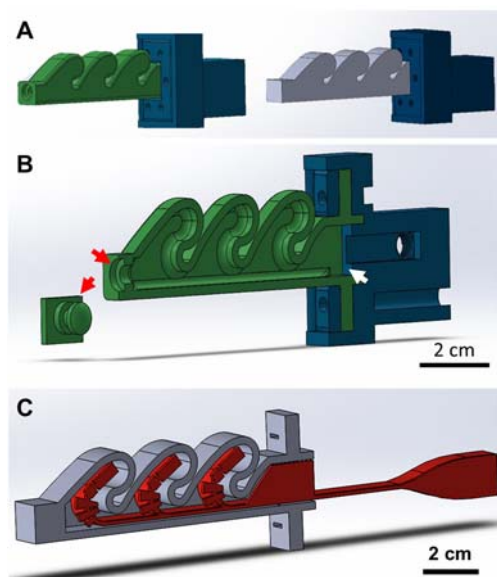


Fig. 1: CAD design of the pneumatic test actuator used to evaluate the suitability of FDM and PolyJet 3D printing for actuator fabrication. The design was suited to the needs of both printing methods by slight differences: (A) Exterior view of both test actuator design versions, which shared a common rigid adapter (blue) for fixation and pneumatic air supply. (B) The PolyJet printed design (green) had added to the large main opening (white arrow) a second closable opening at the tip (red arrows) to remove supporting material. (C) A separately printed inlay was used for the FDM print to support the sidewall as a large overhang lying on the side during printing, which was also removable by pulling out through the main opening. (© Plant Biomechanics Group)

## References

- [1] Yap, H.K., Ng, H.Y. & Yeow, C.-H. (2016). High-Force Soft Printable Pneumatics for Soft Robotic Applications. *Soft robotics*, 3(3), 144-158.
- [2] Conrad, S., Speck, T. & Tauber, F. (2020). Multi-material 3D-printer for rapid prototyping of bioinspired soft robotic elements. In: V. Vouloutsi, A. Mura, F. Tauber, T. Speck, T.J. Prescott & P.F. Verschure (eds.), *Biomimetic and Biohybrid Systems. Living Machines 2020*, 46 – 54. Lecture Notes in Computer Science LNAI 12413. Springer International Publishing, Cham.
- [3] Conrad, S., Speck, T. & Tauber, F. (2021). Tool changing 3D printer for rapid prototyping of advanced soft robotic elements. *Bioinspiration & Biomimetics*, 16, 055010

## Functional morphology of citrus fruit peels via high-resolution X-ray computed tomography (HRXCT) as inspiration for highly damping materials systems

Maximilian Jentzsch<sup>1,2</sup>, Thalia C. Kardamakis<sup>1,2</sup>, Thomas Speck<sup>1-3</sup>

<sup>1</sup>Plant Biomechanics Group (PBG) Freiburg, Botanic Garden of the University of Freiburg; <sup>2</sup>Cluster of Excellence *livMatS @ FIT* – Freiburg Center for Interactive Materials and Bioinspired Technologies; <sup>3</sup>Freiburg Center for Interactive Materials and Bioinspired Technologies (FIT)

Project funding: Funded by the Deutsche Forschungsgemeinschaft (DFG, German Research Foundation) under Germany's Excellence Strategy – EXC-2193/1 – 390951807

The focus of this project in Research Area B within the *livMatS* Excellence Cluster is to take inspiration from ontogenetic variations, adaptivity and the structural basis of plant tissues for bioinspired technical materials systems. The specific aim of this project is to analyze citrus peels as an inspiration for innovative engineering material systems with high energy dissipation and pronounced damping properties. In this study we compare two visualization methods for vascular bundles and cellular tissues comprising the citrus peels. These methods are also applicable for in-situ testing in a micro-computed tomography ( $\mu$ CT), which will be utilized in future investigations.

There exists a huge variety of citrus fruits in the different species and breeds markedly differing in size and shape, but all consisting of the same basic arrangement of seeds, pulp and peel [1]. The fruit peel protects the inner fruit parts and the seeds mechanically and dissipates most of the kinetic energy when the fruits drop from a tree. The fruits can be subdivided histologically into epidermis, flavedo (exocarp), albedo (mesocarp) and endocarp [2,3]. The parenchymatous flavedo includes oil glands and the whole peel is interspersed with vascular bundles. In order to understand the functional morphology of cells and tissues, the fruit peel's anatomy and structural components are studied in detail. Therefore, the peel has to be characterized on a macroscopic level with regard to its tissues, but also on a

microscopic level down to its cellular components.  $\mu$ CT scans of the peels of *Citrus x latifolia* and *Citrus x limon* were performed to gain a better understanding of the overall structure of the fruit at micrometer resolution. The  $\mu$ CT imaging technique allows 3D visualization and segmentation of individual components (e.g. vascular bundles) and tissues of the samples in a microscale without destroying the samples.

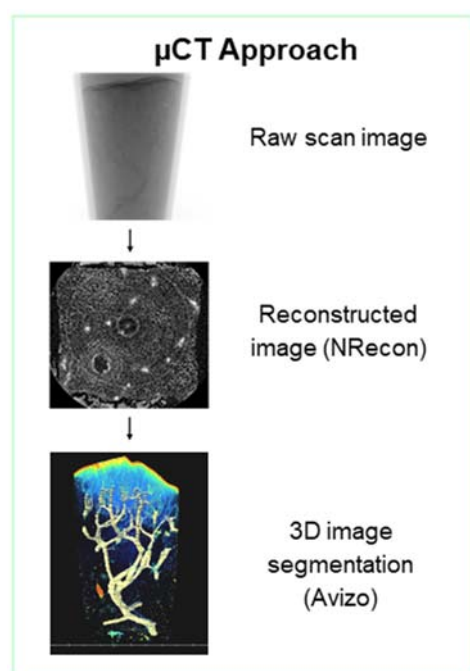


Fig. 1: Representation of the  $\mu$ CT approach: By using the raw scan images of the sample, individual slices were reconstructed via the NRecon software and were then visualized and segmented into 3D images using the Avizo software. Displayed is a sample of the fruit peel of *Citrus x limon* stained with 1% PTA (image pixel size = 2.5  $\mu$ m). (© Plant Biomechanics Group)

$\mu$ CT scans were conducted using a  $\mu$ CT scanner (Bruker Skyscan 1272, Belgium) and its corresponding software SkyScan 1272  $\mu$ CT (Version 1.1.10) (Figure 1) available in the FIT. Reconstructions of the scanned images were made using NRecon software (Version 1.6.10.1). The software, CTVox (Version 3.0.0 r1122), was used to obtain radial-section images and 3D videos. Volume renderings of the citrus peel samples were obtained by doing 3D image segmentation with the Avizo software (Version 2020.2).

During the visualization of the cellular structures and vascular bundles by scanning the fresh citrus peels, the samples would collapse due to moisture loss. Therefore, the samples had to be prepared by either being dried before the scan or stored in a preparation solution during the scan. To determine which preparation method was optimal, two different sample preparations were performed and compared: 1) Critical point dried samples; and 2) Samples stained with 1% phosphotungstic acid (PTA) in a liquid fixation medium (FM) (60% ethanol, 17% glycerin, 23% aqua dest; v/v) [4]. During scanning, the samples were placed into pipette tips filled with fixation medium.

Scanning of critical point dried samples gave best results with a pixel size of 1.68  $\mu$ m for *Citrus x limon* and 1.60  $\mu$ m for *Citrus x latifolia* allowing segmentation of cellular structures and vascular bundles. Our results of a PTA-stained sample of *Citrus x limon* (pixel size = 2.5  $\mu$ m) show that 3D visualization and segmentation of vascular bundles was achieved (Figure 2). In addition, the PTA-stained sample also showed the distribution of vascular bundles within the peel even without segmentation when visualizing an opaque reconstruction of the scan with the Avizo software (Figure 2).

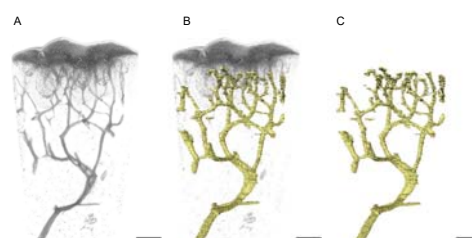


Fig. 2: 3D rendering of the fruit peel of *Citrus x limon* (A) of the reconstructed scan, (B) of the reconstructed scan with segmented vascular bundle network, and (C) of only the segmented vascular bundle network. All scale bars equal 1 mm. (© Plant Biomechanics Group)

The results of our comparisons show that visualization of vascular bundles in peels of both species is possible using  $\mu$ CT imaging with both preparation methods. However, depending on the focus of what should be visualized, different  $\mu$ CT settings, preparation methods, and sample heights should be applied. For *Cit-*

*rus x latifolia* segmentation of vascular bundles with the Avizo software, PTA staining showed the best enhancement of the relevant structures and is the fastest way of segmentation with an image pixel size of 1.6  $\mu\text{m}$  and an average sample height of 2.29 mm. In *Citrus x limon* peels PTA staining showed the best possible segmentation of vascular bundles with an image pixel size of 2.5  $\mu\text{m}$  and an average sample height of 7.06 mm. These values can be used as guidelines for future  $\mu\text{CT}$  scanning of citrus fruit peels. The use of critical point dried samples is also useful even if the segmentation takes longer due to the lower contrast. Even though critical point drying creates artifacts in the tissue due to the shrinking of the samples, it represents the only method to conduct in-situ mechanical tests in the  $\mu\text{CT}$ . For further characterization and visualization of citrus fruit peels, in-situ tests using  $\mu\text{CT}$  can give insight as to how the tissue responds to applied strain. A link between the morphology of cells, distribution of vascular bundles, and the peel's mechanical behavior could be investigated more precisely.

#### References

1. Klock, P.; Klock, M.; Klock, T.A. *Das große Ulmer-Buch der Zitruspflanzen*; Ulmer: Stuttgart, 2007, ISBN 9783800146932.
2. Ford, E.S. Anatomy and Histology of the Eureka Lemon. *Botanical Gazette* **1942**, 288–305, doi: 10.1086/335133.
3. Scott, F.M.; Baker, K.C. Anatomy of Washington Navel Orange Rind in Relation to Water Spot. *Botanical Gazette* **1947**, 459–475, doi: 10.1086/335434.
4. Westermeier, A.S.; Hiss, N.; Speck, T.; Popinga, S. Functional-morphological analyses of the delicate snap-traps of the aquatic carnivorous waterwheel plant (*Aldrovanda vesiculosa*) with 2D and 3D imaging techniques. *Annals of Botany* **2020**, 126, 1099–1107, doi: 10.1093/aob/mcaa135

## Simulation of cactus junctions based on geometric and biomechanical analyses of the biological role models

Max D. Mylo<sup>1,2</sup>, Anna Hoppe<sup>2,3</sup>, Lars Pastewka<sup>2,3</sup>, Thomas Speck<sup>1,2</sup>, Olga Speck<sup>1,2</sup>

<sup>1</sup>Plant Biomechanics Group (PBG) Freiburg, Botanic Garden of the University of Freiburg, Germany; <sup>2</sup>Cluster of Excellence *livMatS* @ FIT – Freiburg Center for Interactive Materials and Bioinspired Technologies, University of Freiburg, Georges-Köhler-Allee 105, D-79110 Freiburg, Germany; <sup>3</sup>Department of Microsystems Engineering, University of Freiburg, Freiburg, Germany

Project funding: Funded by the Deutsche Forschungsgemeinschaft (DFG, German Research Foundation) under Germany's Excellence Strategy – EXC-2193/1 – 390951807

This interdisciplinary cooperation within the project 'Abscission and self-repair in biological and artificial materials systems' of Area C of the Cluster of Excellence 'Living, Adaptive and Energy-autonomous Materials Systems' (*livMatS*) combines biological research with the approach of computer-based simulations. The aim of this sub-project is to gain a better understanding of the different mechanical behaviors of the lateral branch-branch connections of selected species of the Opuntioideae (a subfamily of cacti) and to characterize the most influencing factors. For this purpose the knowledge and data on morphology, anatomy and biomechanics of cacti collected over recent years are abstracted and imported into geometric models and finite element analysis (FEA) tensile tests.

The biological background of the research is the phenomenon that the mechanical behaviors of branch-branch junctions differ greatly within closely related species of the Opuntioideae, all of which have a growth habit of chains of multiple joined branches. *Opuntia ficus-indica*, for example, has rather stable connections, which enable its tree-like growth form. In *Cylindropuntia bigelovii*, on the other hand, the lateral branches break off under the slightest mechanical influence and can subsequently grow into new individuals as vegetative offshoots [1].

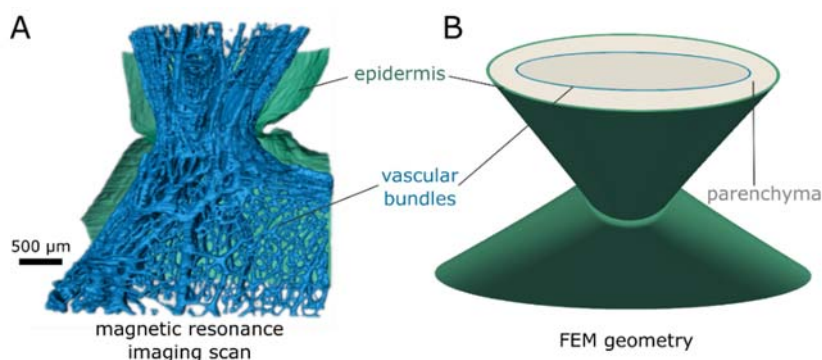


Fig. 1: Comparison of the junction geometry of *Opuntia ficus-indica* consisting of epidermis (green), vascular bundles (blue) and parenchyma (gray; shown only in B). A: Segmented tissue of a magnetic resonance scan (adapted from [2]). B: Constructed finite element modelling shell geometry. © Plant Biomechanics Group Freiburg & Department of Microsystems Engineering Freiburg.

Functional morphological data show that these differences can be attributed to a combination of the different tissues present in and around the junction (analyzed by light microscopy), their spatial arrangement (analyzed by magnetic resonance scans) and their mechanical properties (analyzed by tensile tests on dissected tissues) [2]. *C. bigelovii* exhibited a significantly larger taper of the branch cross-sectional area towards the junction compared to *O. ficus-indica*. A stiffening layer that accumulates on top of the dermal tissue, the so-called periderm, was only found in lateral branch junctions of *O. ficus-indica*, especially with increasing plant age. Periderm was also found in wound healing experiments [3] and increases the stiffness of the dermal tissue by a factor of about 10. Marked differences were additionally found in the mechanical properties of the vascular bundles that run net-like through the branches. Here, strength is about a factor of 25 and stiffness even about a factor of 150 larger for the samples of *O. ficus-indica* compared to those of *C. bigelovii*.

Within the cooperation project, a standardized finite element method (FEM) geometry, which serves as the basis of the simulations, was created based on these data (Figure 1). It is composed of shells representing the epidermis, the vascular bundles and the sponge-like parenchyma that lies in between; whereby the mechanical properties of the overall system are predominantly determined by the first two. Assigning the measured mechanical properties of the tissues of the two studied species to

the corresponding shells allows for a comparison between the simulated tensile experiments (using continuum elasticity) and the experimental data from biomechanical tensile tests across the junctions [4].

In addition to this comparison with the biological samples, the simulation approach also provides the possibility of ‘going beyond biology’, which enables the application and testing of combinations of mechanical properties and geometries that do not occur in nature. This will provide deeper insights into the bonding/debonding behavior of materials systems, which could be implemented in future *livMatS* projects, such as the application of the extracted mechanisms in demonstrators.

#### References

- [1] Gibson, A. C. & Nobel, P. S. (1986). *The cactus primer*. Harvard University Press.
- [2] Mylo, M. D., Hesse, L., Masselter, T., Leupold, J., Drozella, K., Speck, T. & Speck, O. (2021). Morphology and Anatomy of Branch–Branch Junctions in *Opuntia ficus-indica* and *Cylindropuntia bigelovii*: A Comparative Study Supported by Mechanical Tissue Quantification. *Plants*, 10(11), 2313.
- [3] Mylo, M. D., Krüger, F., Speck, T. & Speck, O. (2020). Self-Repair in Cacti Branches: Comparative Analyses of Their Morphology, Anatomy, and Biomechanics. *International Journal of Molecular Sciences*, 21(13), 4630.
- [4] Mylo, M. D., Hoppe, A., Pastewka, L., Speck, T. & Speck, O. (2022). Elastic properties and fracture mechanics of branch-branch junctions in cacti: a case study on *Opuntia ficus-indica* and *Cylindropuntia bigelovii* (in preparation).

## The petiole-lamina transition zone of foliage leaves: model for a damage-resistant connection

Max Langer<sup>1,2</sup>, Elena Hegge<sup>1,2</sup>, Mark Cedrik Kelbel<sup>1,3</sup>, Claas Müller<sup>2,3</sup>, Thomas Speck<sup>1,2</sup>, Olga Speck<sup>1,2</sup>

<sup>1</sup>Plant Biomechanics Group @ Botanic Garden, University of Freiburg; <sup>2</sup>Cluster of Excellence livMatS @ FIT – Freiburg Center for Interactive Materials and Bioinspired Technologies, University of Freiburg; <sup>3</sup>Department of Microsystems Engineering – IMTEK, University of Freiburg

Project funding: (1) State Ministry of Baden-Wuerttemberg for Sciences, Research and Arts in the framework of the collaborative project “Bio-inspirierte elastische Materialsysteme und Verbundkomponenten für nachhaltiges Bauen im 21ten Jahrhundert” (BioElast) within the “Zukunftsoffensive IV Innovation und Exzellenz-Aufbau und Stärkung der Forschungsinfrastruktur im Bereich der Mikro- und Nanotechnologie sowie der neuen Materialien”, and (2) the Deutsche Forschungsgemeinschaft (DFG, German Research Foundation) under Germany’s Excellence Strategy – EXC-2193/1 – 390951807

Connecting different structures with varying geometries is a challenge both in nature and in engineering. Especially the connection of rod-shaped and planar structures is particular demanding, as the geometry changes drastically over a short distance. Existing engineering approaches often rely on a large number of individual components, in between which areas of high stress and strain can occur, making them prone to failure. Foliage leaves offer successful implementations of such connections, which are free of the named issues [1].

These leaves consist of a rod-shaped stalk (= petiole) and a planar blade (= lamina) connected by a smooth and damage-resistant transition zone. Depending on the spatial arrangement of petiole and lamina (2D- or 3D-configured) and the body plan of the plant (mono- and dicotyledonous), there are different types of transition zones [2]. In 2D-configured leaves, the petiole is connected to the basal region of the lamina, as in *Hosta x tardiana* ‘El Niño’ and *Hemigraphis alternata*, while 3D-configured leaves are peltate, such as those of *Caladium bicolor* and *Pilea peperomioides*

(Fig. 1). The body plan affects the 3D-arrangement of the strengthening tissues in the leaves.

We quantitatively investigated the internal tissue arrangement and geometry, size and shape of the petiole-lamina transition zone of the four leaves described above using  $\mu$ CT scans and serial thin-sections. As a result, we found *H. tardiana* and *C. bicolor* having a scattered arrangement of the individual vascular bundles embedded in the parenchyma, typically for monocotyledonous plants. In contrast, bundles of *H. alternata* and *P. peperomioides* are more merged and centrally arranged, typically for dicotyledonous plants. In addition, we found gradients for the variables of geometry, size and shape that overlap and are interwoven in the transition zone, leading to the overall damage-resistant structure [2].

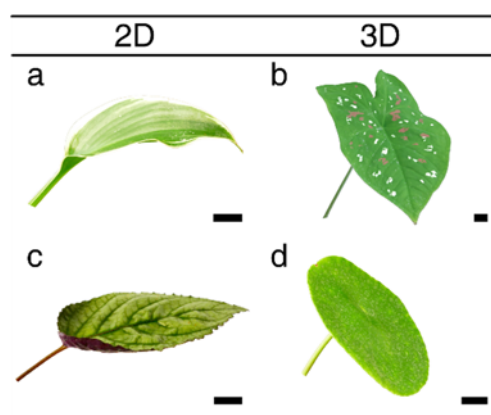


Fig. 1: Morphology of four foliage leaves, two with a 2D- and two with a 3D-configuration of petiole and lamina. *Hosta x tardiana* ‘El Niño’ (a) and *Caladium bicolor* (b) are monocotyledonous species, while *Hemigraphis alternata* (c) and *Pilea peperomioides* (d) are dicotyledonous species. Scale bars are 2 cm. (© Plant Biomechanics Group)

Since damage prevention is a crucial concept both in technical and biological materials systems, we also carried out mechanical tests (bending and torsional tests) on the petioles of the four species, focusing on their twist-to-bend ratios and their safety factors. The safety factors of all species were each around two in their median, indicating that all investigated leaves can carry at least twice their static weight without damage. Consequently, there is room for additional loads, such as those caused by wind or by mechanical touch [3].

However, leaves are also protected from damage by the immediate response by means of twisting and bending under wind loads and mechanical stress. A suitable measure for this mechanical trade-off between flexural rigidity and torsional rigidity is the twist-to-bend ratio. We found median twist-to-bend ratios of at least 10 for the petioles of the two dicotyledonous species (*H. alternata* and *P. peperomioides*), meaning that these petioles could be twisted 10 times more easily than they could be bent. This torsional flexibility allows the petioles to be easily twisted enabling the large leaf blades to streamline under wind loads, ultimately preventing damage to the leaf. Compared to the dicotyledons, the median twist-to-bend ratios of the petioles of the monocotyledonous species *H. tardiana* and *C. bicolor* were significantly higher with values greater than 20 (Fig. 2). In the case of *H. tardiana*, high ratios can be explained by the U-profiled geometry of the petiole, which can be easily twisted and thus reveal low values of torsional rigidity. Conversely, in *C. bicolor*, the additional peripherally arranged strengthening tissue in the form of stiff collenchyma strands increase the bending (flexural) rigidity and thus the twist-to-bend ratio [3].

In contrast to the petioles of *P. peperomioides*, the transition zone had a median twist-to-bend ratio of below one (Fig. 2) [4]. This is unique, as most biological structures, for which a twist-to-bend ratio has been calculated, have ratios higher than one. The significant difference in the twist-to-bend ratio of petiole and petiole-lamina transition zone indicates that bending loads are accommodated by the petiole, whereas torsional loads are shared between the petiole and transition zone. After six weeks of treatment with wind and/or mechanical stimulation, we could not detect any acclimatisation changes in petioles and transition zones of *P. peperomioides* leaves [4]. In summary, the damage resistance of the petiole-lamina transition zone in foliage leaves is based on (i) the superimposed gradients in geometry, size and shape, (ii) the mechanical trade-off between flexural rigidity and torsional rigidity and (iii) the mechanical interplay between petiole and transition zone.

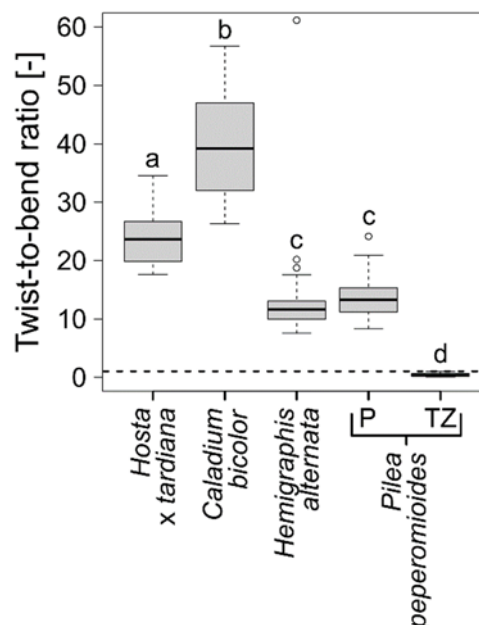


Fig. 2: Boxplots of the twist-to-bend ratios of the petioles of *Hosta x tardiana* 'El Niño', *Caladium bicolor*, *Hemigraphis alternata* and of the petiole (P) and the petiole-lamina transition zone (TZ) of *Pilea peperomioides*. The dotted line marks a twist-to-bend ratio of one. Significant differences ( $p$ -value < 0.05) are indicated by lower case letters. Sample size:  $n = 25$  for the petioles and  $n = 20$  for the transition zone. (© Plant Biomechanics Group)

Altogether, these results show that plant leaves are promising models for solving the challenge of connecting structures with different geometries (rod-shaped and planar) in technical applications.

#### References

- [1] O. Speck, M. Langer, M.D. Mylo (2021): Plant-inspired damage control – an inspiration for sustainable solutions in the Anthropocene. *The Anthropocene Review* 20530196211018489
- [2] M. Langer, T. Speck, O. Speck (2021): Petiole-lamina transition zone: a functionally crucial but often overlooked leaf trait. *Plants* 10(4): 774.
- [3] M. Langer, M.C. Kelbel, T. Speck, C. Müller, O. Speck (2021): Twist-to-bend ratios and safety factors of petioles having various geometries, sizes and shapes. *Frontiers in Plant Science* 12: 765605.
- [4] M. Langer, E. Hegge, T. Speck, O. Speck (2021): Acclimations to wind loads and/or contact stimuli? A biomechanical study of peltate leaves of *Pilea peperomioides*. *Journal of Experimental Botany*: erab541.

## Biomechanics of climbing plant attachment: The tendrils and adhesive pads of the passionflower *Passiflora discophora*

Frederike Klimm<sup>1,3</sup>, Thomas Speck<sup>1,3</sup>,  
Marc Thielen<sup>1,2</sup>

<sup>1</sup>Plant Biomechanics Group Freiburg, Botanic Garden, University of Freiburg; <sup>2</sup>Freiburg Materials Research Center (FMF); <sup>3</sup>Cluster of Excellence *IMatS @ FIT* – Freiburg Center for Interactive Materials and Bioinspired Technologies, University of Freiburg, Georges-Köhler-Allee 105, D-79110 Freiburg, Germany

www.growbot.eu

**Project funding:** This project has received funding within the European Union's Horizon 2020 research and innovation programme under the grant agreement No 824074.

Instead of building a solid, self-supporting trunk, climbing plants rely on external structures as supports to grow upwards [e.g. 1-4]. The passionflower *Passiflora discophora*, for example, climbs using branched tendrils (Fig. 1).



Fig. 1: Turgescent tendril of *Passiflora discophora*. The branched tendril attaches to the substrate via adhesive pads. Its main axis coils and forms a spring-like structure. Scale bar 5 mm. Figure adapted from [6].

On the tendril tips, adhesive pads develop that securely anchor the plant to a variety of substrates, including flat vertical surfaces. The tendril coils and thereby forms a spring-like structure linking the shoot to the adhesive pads. The spring consists of a minimum of two helices of opposite handedness. After ~2-6 weeks the fresh green turgescent tendrils dry out and die back [5]. They are now described as senescent, but still remain attached and functional.

We investigated the mechanics of *P. discophora*'s attachment system, by carrying out pull-off tests on the whole tendrils (Fig. 2.1) and on individual pads [6]. In order to assess the quality of the anchoring on different surfaces, we offered the tendrils a variety of substrates to grow on, and found that they reach maximum median failure forces up to 1.44 N (IQR 0.23 N) on a plywood surface (turgescent tendrils). Due to their particular spring-like structure, tendrils unwind with increasing tension (Fig. 2.2 & 2.3), leading to a considerable increase in tendril length, with a mean ratio of straightened length to coiled length of  $1.4 \pm 0.2$  (turgescent tendrils). This behaviour contributes to the ability of the tendrils to dissipate considerable amounts of energy before they eventually fail, which in case of turgescent tendrils can be as high as 14.7 mJ (median). Failure usually occurred at the tendril main axis (74% of failures), which is thus the tendrils' weakest point. Failure of the adhesive pads themselves was rare. We found that the large central pads tested individually withstood higher loads than the entire tendril. Nevertheless the tendril morphology was well balanced (total pad area per tendril and tendril cross-sectional area correlated), which leads us to conclude that the slight oversizing of the pads is of evolutionary advantage as it allows the plant to cope better with the part of the attachment process that it cannot control: The substrate.

Overall, we interpret the attachment as a fail-safe system, which is optimized towards high displacements and energy dissipation rather than high failure forces. A comparable system has been described for Boston ivy (*Parthenocissus tricuspidata*) [7]. *P. tricuspidata* too climbs using branched tendrils with adhesive pads, but they are organized differently than in *P. discophora* (Fig. 3): The tendrils of *P. tricuspidata* comprise a series of 5-10 secondary axes terminating in adhesive pads. As in *P. discophora*, the adhesive system of *P. tricuspidata* is not force-optimized, as individual adhesive pads withstand similar forces than the entire adhesive system with several pads. However the energy dissipation of the entire adhesive system is considerably increased by the structure. This is in this species mainly

achieved by sequential failure of one or several pads at a time, thus in a different way than in *P. discophora*.

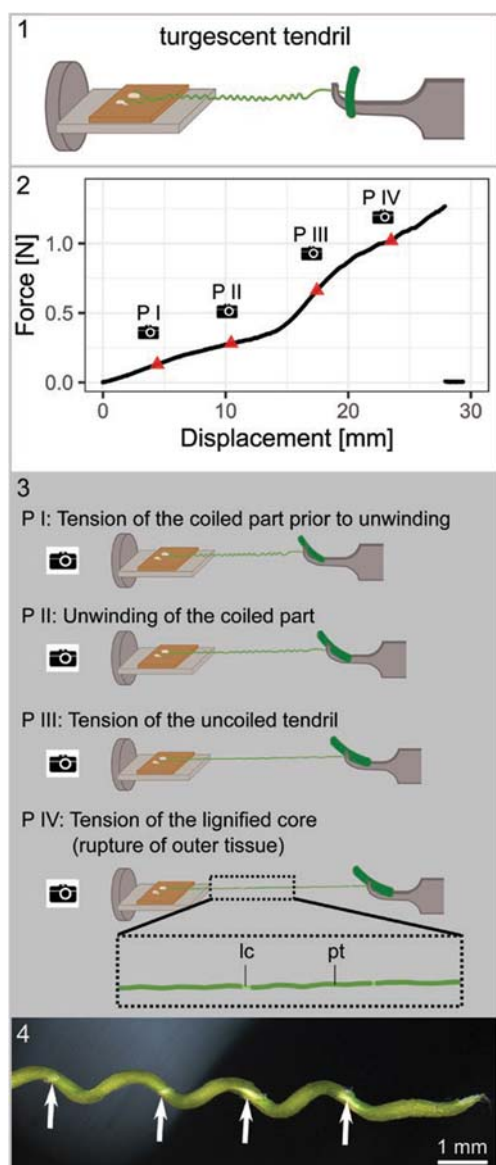


Fig. 2: Pull-off test on a turgescens tendril of *Parthenocissus discophora*. The tendril still attached to its substrate was subjected to increasing tension (1). On the resulting force-displacement curve (2), red triangles indicate the respective positions at which the tendril state was redrawn from video stills (3). Stereomicroscopic images taken after testing show various rupture points in the parenchymatous tendril tissue (4). Abbreviations: lc, lignified core; pt, parenchymatous tissue. Figure adapted from [6].

As to the entire plant, both species possess multiple tendrils positioned alternately along their shoots. Thus, for the anchoring of the entire plant, not only the individual tendril's or even pad's failure force plays an important role, but also the way tendrils act and fail to-

gether. This is even more so since in their natural habitat these plants are submitted to loading conditions not included in our studies so far, such as dynamical loads and loads at varying angles. Nevertheless, we infer that the "fail-safe" approach plays a central role for the secure anchorage of these climbing plants as a whole, based on the fact that we and Steinbrecher et al. [7] found attachment systems that via different ways both function optimized as to displacement and dissipated energy rather than force-optimized.

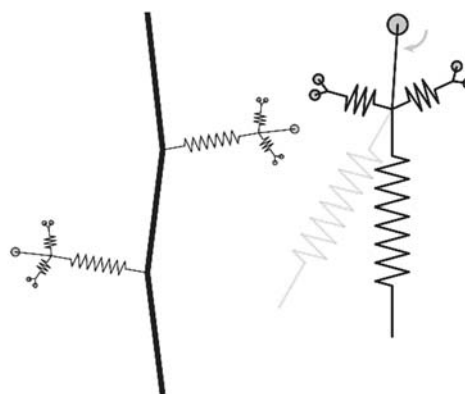


Fig. 3: Schematic representation of attachment structures of *Passiflora discophora* and their arrangement along the plant shoot. Tendrils of *P. discophora* consist of a long spring-like main axis branching 3-fold, carrying up to 5 pads at its tips. Deflection of the main axis and the expected resulting torsional shear loads are indicated in gray. Figure adapted from [6].

*P. discophora*'s ability to permanently attach to a variety of support structures and thereby to climb upwards is linked to striking movements of the tendrils and shoot. This includes a "searching" movement and the coiling movement to form the spring-like structure, typical for climbing plants [1]. We investigate climbing plant movements within the project "GrowBot - Towards a new generation of plant-inspired growing artefacts". This project aims to develop new, low-mass and low-volume bio-inspired robots, able to navigate environments not accessible to conventional robots equipped with wheels, legs or other types of animal inspired climbing devices. To that end it proposes a disruptively new paradigm of movements in robotics based on the inspiration from plant role models. Plant movements are relatively unexplored as concept generators for movements in soft-robots. In addition,

they fundamentally differ from animal movements, since plants move from one point to another mainly using growth and thereby continuously and adaptively changing their size and shape. These movements are particularly apparent and fast in climbing plants.

### References

- [1] C. Darwin (1882): The movements and habits of climbing plants. London: John Murray.
- [2] S. Isnard & W.K. Silk (2009): Moving with climbing plants from Charles Darwin's time into the 21st century. *American Journal of Botany* 96, 1205-1221.
- [3] K.C. Vaughn & A.J. Bowling (2011): Biology and physiology of vines. – In: Horticultural reviews Vol. 38. (ed. J. Janick), 1-21, Hoboken, NJ: John Wiley & Sons, Inc..
- [4] N.P. Rowe & T. Speck (2015): Stem biomechanics, strength of attachment, and developmental plasticity of vines and lianas. – In: Ecology of lianas (eds. S.A. Schnitzer, F. Bongers, R.J. Burnham & F.E. Putz), 323-341, Chichester: John Wiley & Sons Ltd.
- [5] H.F. Bohn, F. Günther, S. Fink & T. Speck (2015): A passionate free climber: structural development and functional morphology of the adhesive tendril in *Passiflora discophora*. *International Journal of Plant Sciences* 176, 294-305.
- [6] F. Klimm, S. Schmier, H.F. Bohn, S. Kleiser, M. Thielen & T. Speck (2021): Biomechanics of tendrils and adhesive pads of the climbing passionflower *Passiflora discophora*. *Journal of Experimental Botany*, erab456. (doi.org/10.1093/jxb/erab456)
- [7] T. Steinbrecher, E. Danninger, D. Harder, T. Speck, O. Kraft & R. Schwaiger (2010): Quantifying the attachment strength of climbing plants: a new approach. *Acta Biomaterialia* 6, 1497-1504.

## Artificial Venus flytraps demonstrators outperforming the biological model

Falk Tauber<sup>1,2</sup> and Thomas Speck<sup>1,2</sup>

<sup>1</sup>Plant Biomechanics Group (PBG) Freiburg, Botanic Garden of the University of Freiburg,  
<sup>2</sup>Cluster of Excellence livMatS @ FIT – Freiburg Center for Interactive Materials and Bioinspired Technologies

Project funding: Funded by the Deutsche Forschungsgemeinschaft (DFG, German Research Foundation) under Germany's Excellence Strategy – EXC-2193/1 – 390951807

The Cluster of Excellence “Living, adaptive and energy-autonomous Materials Systems (*livMatS*)” at the University of Freiburg aims at developing novel materials systems that show dynamic, life-like and non-equilibrium (energy-autonomous) features. Within the *livMatS* research area “Demonstrators”, technical demonstrators like an artificial Venus flytrap are envisaged, which will demonstrate the feasibility of the developed materials systems. Such demonstrators will be the first step towards future implementation of novel technologies into industrial products and everyday life applications.

Biological material systems are diverse and complex systems, which are highly adapted to their environment. Optimized in 3.8 billion years of evolution today biological materials systems serve as concept generators and “biological models” for bioinspired material systems. Research in this field is being conducted with the goal of translating the functions of living nature into technical applications, thus enabling novel functions such as embodied intelligence and embodied energy. For example current artificial Venus flytrap systems (AVF) representing plant-inspired (soft-)robotic systems draw their inspiration from various plant movements, actuation and adaptability strategies as role models utilizing e.g. principles of carnivorous snap-trap plants for hinge-less movements.

Here, we present novel bio-inspired “artificial Venus flytrap” demonstrators [1, 2] which not only incorporate the snap-trap movement principles of two carnivorous plant species (Venus flytrap (*Dionaea muscipula*) and waterwheel

plant (*Aldrovanda vesiculosa*) [3-6]), but also show adaptive responses to different environmental triggers [2]. As a first example, the presented actuator systems successfully implement several principles based on plant movement actuation and deformation systems into one versatile adaptive technical compliant mechanism. These systems have been characterized and compared as to their movement speed, energy requirement and overall performance. During the last 25 years over a dozen different AVF systems were developed [2], but none of the developed systems incorporates all Venus flytrap functions (i.e. prey detection, trapping and digestion; decision making; energy harvesting; self-healing). One of the newest additions to these artificial systems, our compliant foil based AVF, is the first to pass

the Turing test (in comparison to the Venus fly-trap) on a specific function. In abstracting and transferring the snap trap motion of both biological models into one artificial system, the compliant foil based AVF is able to perform a natural like opening and closing motion surpassing the biological models in speed and energy consumption (Fig. 1).

Within our *livMatS* project, envisaged technical demonstrators like an “artificial Venus fly-trap” will demonstrate the feasibility of the developed materials systems with dynamic, life-like and non-equilibrium features for implementation in soft-machines. The demonstrators are a first step towards future implementation of novel technologies into industrial products and everyday life applications.

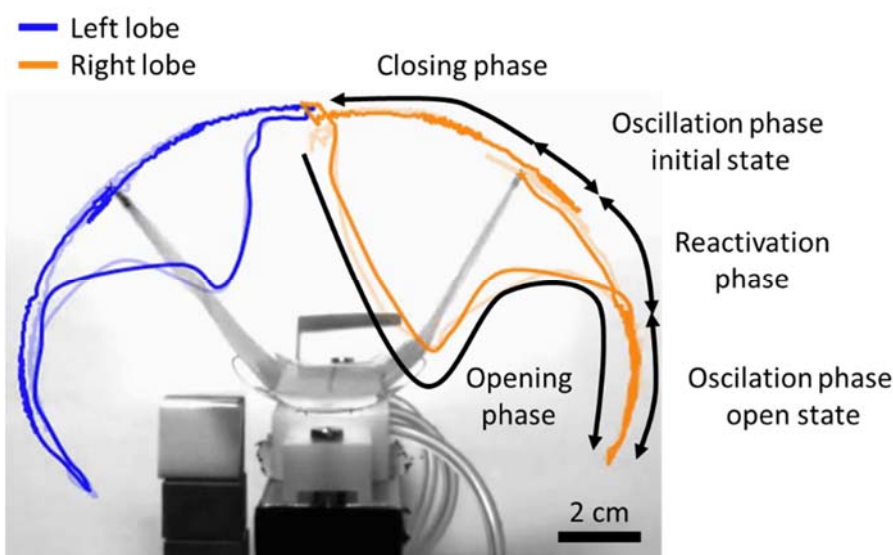


Fig. 1: AVF motion cycle. The pneumatic system is able to outperform its biological models in speed and energy requirements. The five phasic motion mimics the biological motion of the Venus flytrap passing the Turing test for motion and speed already. © Plant Biomechanics Group Freiburg

In the *livMatS* AVFs, the compliant foil demonstrators, the basic snap-trap geometry of the plants was abstracted into a foil model. Through four different actuation systems (using pneumatics, magnetics, thermal actuations and a combination of humidity and temperature) is the AVF able to perform a closure movement of its “lobes” via kinematic coupling and motion amplification by curved folds (inspired by *Aldrovanda vesiculosa*) and an inverse snap-buckling movement for opening (inspired by *Dionaea muscipula*) [2-6]. The

pneumatic system was used to characterize this complex motion, enabling the identification of the five different phases of the motion cycle: 1. Closing phase, the outer pneumatic cushions inflate and cause closing the lobes within ca. 300ms. 2. Opening phase, the central pneumatic cushion inflates and evoke bending the backbone (pressure of the outer cushions is released simultaneously) and triggering snap buckling motion opening the lobes within in ca. 70ms and releasing the stored elastic energy within the lobes. 3. Oscillation

phase (open state), the lobes oscillate in an up- and downward motion in the open state. 4. Reactivation phase, all pressure is released from the system and the lobes move back their initial position. 5. Oscillation phase (initial state), the lobes oscillate in the initial position, ready for the next cycle (Fig. 1). One cycle lasts less than 400ms and is with this well inside the timeframe of the Venus flytrap (500ms for a snap buckling closure motion) [3,4]. The Venus flytrap needs roughly 10J to close their trap [2], our first characterization showed that the pneumatic system needs with ca. 50mJ less energy to close its lobes.

The different systems were characterized in terms of movement kinematics and input requirements (force and energy). A direct comparison to the biological model highlights that our system was not only able to outperform the biological model *Dionaea muscipula* (the pneumatic driven system open and closed faster and need less energy), but also to create a life-like motion which would pass a functional Turing test [2,7]. The identification and characterization of the energy requirements and kinematics concerning novel motion principle can be seen as a first basis for the development of more advanced demonstrators. These are regarded as guideline values for future materials systems and AVF currently under development within *livMatS*.

#### References

- [1] Esser F., Scherag F.D., Poppinga S., Westermeier A., Mylo M.D., Kampowski T., Bold G., Rhe J. & Speck T. (2019) Adaptive Biomimetic Actuator Systems Reacting to Various Stimuli by and Combining Two Biological Snap-Trap Mechanics. In: Martinez-Hernandez U. et al. (eds.) *Biomimetic and Biohybrid Systems. Living Machines 2019*, 114-121. Lecture Notes in Computer Science, vol. 11556. Springer, Cham
- [2] Esser F.J., Auth P. & Speck T. (2020). Artificial Venus flytraps: A research review and outlook on their importance for novel bioinspired materials systems. *Frontiers in Robotics and AI*, 7, 75.
- [3] Poppinga S. & Joyeux M. (2011). Different mechanics of snap-trapping in the two closely related carnivorous plants *Dionaea muscipula* and *Al-drovanda vesiculosa*. *Physical Review E*, 84(4), 041928.
- [4] Poppinga S., Bauer U., Speck T. & Volkov A.G. (2017) Motile traps. In: Ellison A.M., Adamec L. (eds.), *Carnivorous plants: physiology, ecology,*

*and evolution*, 180-193. Oxford University Press, Oxford.

[5] Sachse, R., Westermeier, A., Mylo, M., Nadasdi, J., Bischoff, M., Speck, T. & Poppinga, S. (2020). Snapping mechanics of the Venus flytrap (*Dionaea muscipula*). *PNAS*, 117(27), 16035-16042.

[6] Westermeier, A., Sachse, R., Poppinga, S., Vgele, P., Adamec, L., Speck, T. & Bischoff, M. (2018). How the carnivorous waterwheel plant (*Al-drovanda vesiculosa*) snaps. *P. Roy. Soc. B-Biol. Sc.*, 285, 20180012.

[7] Speck T., Poppinga S., Speck O. & Tauber F. (2021). Bio-inspired life-like motile materials systems: Changing the boundaries between living and technical systems in the Anthropocene. *The Anthropocene Review*.

### Biosensor-enabled multiplexed on-site therapeutic drug monitoring of antibiotics

H. Ceren Ates<sup>1,2</sup>, Hasti Mohsenin<sup>3</sup>, Christin Wenzel<sup>4</sup>, Regina Glatz<sup>1,2</sup>, Hanna J. Wagner<sup>3,5</sup>, Richard Bruch<sup>2</sup>, Nico Hfflin<sup>3</sup>, Sashko Spassov<sup>4</sup>, Lea Streicher<sup>4</sup>, Sara Lozano-Zahonero<sup>4</sup>, Bernd Flamm<sup>4</sup>, Rainer Trittler<sup>6</sup>, Martin J. Hug<sup>6</sup>, Maja Khn<sup>3</sup>, Johannes Schmidt<sup>4</sup>, Stefan Schumann<sup>4</sup>, Gerald A. Urban<sup>1,7</sup>, Wilfried Weber<sup>3</sup>, Can Dincer<sup>1,2</sup>

<sup>1</sup>University of Freiburg, FIT – Freiburg Centre for Interactive Materials and Bioinspired Technology; <sup>2</sup>University of Freiburg, IMTEK – Department of Microsystems Engineering, Laboratory for Sensors; <sup>3</sup>University of Freiburg, Faculty of Biology and Signalling Research Centers BIOSS and CIBSS; <sup>4</sup>University of Freiburg, Department of Anesthesiology and Critical Care, Medical Center -, Faculty of Medicine; <sup>5</sup>ETH Zurich, Department of Biosystems Science and Engineering; <sup>6</sup>Medical Center – University of Freiburg, Department of Pharmacy; <sup>7</sup>University of Freiburg, Freiburg Materials Research Centre (FMF)

Project funding: German Research Foundation (DFG) – miPAT - Personalisierte Antibiotikatherapie: Entwicklung und Evaluierung einer mikrofluidischen Biosensor-Plattform fr die nicht-invasive, patientennahe Multianalyt-Diagnostik

The cooperation project focuses on the development of a biosensor that allows simultaneous measurement of several specimens and test substances, which will enable personalized dosing of medicines against infectious diseases and help to minimize the antimicrobial resistance. This wide-ranging interdisciplinary

nary research programme is conducted by engineers of the Disposable Microsystems Group from the Faculty of Engineering (PI: Dr. Can Dincer), biologists of the Cluster of Excellence CIBSS – Centre for Integrative Biological Signalling Studies (PI: Prof. Wilfried Weber), clinicians (PI: Prof. Dr. rer. nat. Stefan Schumann), and pharmacists (PI: Prof. Dr. Martin J. Hug) at Medical Center – University of Freiburg [1].

The starting point of this project is the fact that antibiotic-resistant bacteria are on the rise with new strains capable of evading front-line medications springing up all over the world. While researchers scramble to identify new classes of drugs to bridge this gap, we are falling behind and are approaching an era where even a simple infection could once again kill [2]. In the current clinical practice, the aim is to keep the blood drug concentrations of the patient within a predetermined therapeutic range by adjusting the dosage and its frequency. However, this range is predetermined during the clinical trials over a small population, although in reality it varies significantly from one individual to the other. It means, most of the time, patients cannot receive the optimal doses for their current condition.

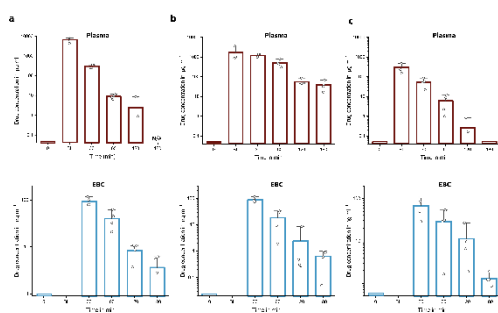


Fig. 1: Calculated free drug concentrations for plasma and EBC samples of animals given (a) overdose (b) normal dose and (c) underdose antibiotic. A similar clearance behaviour and concentration decrease with respect to drug dosing regimen were observed for both plasma and EBC measurements over a time period starting from before antibiotic administration (0), after 5 (BL), 30, 60, 120 and 180 minutes. Adapted with permission from [1] Copyright 2021, Wiley-VCH GmbH

Considering the success of the antibiotherapy strongly depends on our ability to keep the blood antibiotic concentrations within the “personalized” therapeutic range, the individual drug metabolism must be understood[2]. Such

personalized scheme, however, requires frequent sampling and analysis, which is hard to achieve using conventional methods like chromatography or immunoassays. Therefore, there is an urgent need for a simple, yet accurate technique, which could provide insights about the drug levels in the body with a cost-effective manner.

To answer this need, a versatile, polymer-based, disposable microfluidic sensor platform along with an antibody-free and highly sensitive antibiotic detection assay has developed and validated with animal experiments conducted on Landrace pigs treated with three different (under-, over- and normal) dosages of antibiotic. Herein, the detection and temporal monitoring of piperacillin/tazobactam in EBC, along with a correlation study exploring the link between plasma and EBC drug levels was demonstrated, for the first time (Fig. 1). The developed biosensor with a highly-performant, synthetic biology-empowered assay enabling measurement of very low ( $\text{ng ml}^{-1}$  range) drug concentrations, which is not possible to achieve with conventional chromatography-based methods.

To demonstrate its suitability for the clinical usage, the biosensor was benchmarked with HPLC measurements (gold standard) via temporal analysis of plasma samples of animal giving normal dosage of antibiotic (Fig. 2.f). Both the measured concentrations and the clearance behaviour are in a good agreement with the gold standard analysis.

Another important outcome of the study is the development of the multiplexed sensing technology, which can help to improve the overall reliability of any healthcare monitoring platform by providing physiological information for active calibration and correction of target concentrations (Fig. 2.a). The multiplexed biosensor is capable of gauging antibiotic concentrations from complex biofluids simultaneously (Fig. 2.c). It is also possible to co-currently analyze different analytes on the same chip (Fig. 2.d).

A successful realization of either blood-based or noninvasive on-site monitoring of antibiotics using such a versatile platform that can operate with multianalyte/sample tasks could be a

game-changer for the global combat against antibiotic resistances.

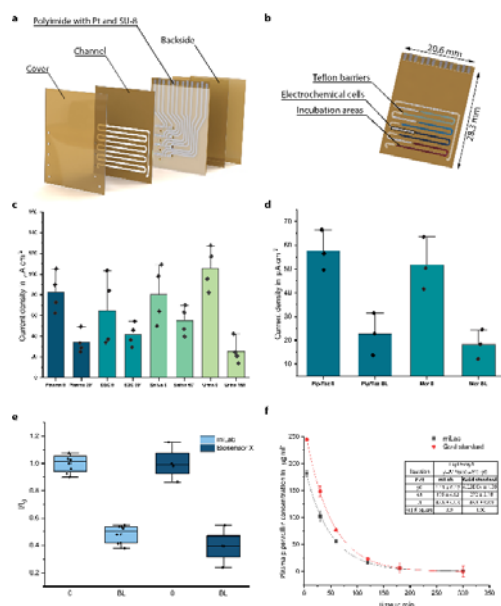


Fig. 2: Multianalyte/sample capability of the biosensing technology. (a) 3D rendering of the stacked multiplexed biosensor and (b) four different incubation areas, individual electrochemical cells and Teflon barriers preventing electrode fouling. Demonstration of multisample (c) and multianalyte (d) measurement capability via temporal evaluation of four different sample types and two different antibiotics on the same chip. (e) Validation of multiplexed biosensor via comparing clearance behaviour of antibiotic in plasma samples obtained with multianalyte and single-analyte biosensor (f) Benchmarking against gold-standard (HPLC) measurement. Reproduced with permission from [1] Copyright 2021, Wiley-VCH GmbH

References

[1] H. C. Ates et al., “Biosensor-Enabled Multiplexed On-Site Therapeutic Drug Monitoring of Antibiotics,” *Adv. Mater.*, p. 2104555, 2021.  
 [2] H. C. Ates, J. A. Roberts, J. Lipman, A. E. G. Cass, G. A. Urban, and C. Dincer, “On-Site Therapeutic Drug Monitoring,” *Trends Biotechnol.*, vol. 38, no. 11, pp. 1262–1277, 2020.

## DINAMIK - Digital detection of interactome biomarkers for cancer diagnostics using HER2/HER3 interaction as an example

Tobias Groß<sup>1</sup>, Peter Koltay<sup>1</sup>, Csaba Jeney<sup>1</sup>

<sup>1</sup>Department of Microsystems Engineering – IMTEK laboratory for MEMS applications of the University of Freiburg and Bioinspired Technologies (FIT)

Project funding: Ministerium für Wissenschaft, Forschung und Kunst Baden-Württemberg – “Ideenwettbewerb Biotechnologie – Von der Natur lernen – DINAMIK-7533-7-11.10-6

In the near future, personalized diagnostic approaches based on the parallel detection of many different analytes (biomarkers), in particular including also proteins and protein-protein-interactions (PPI) will be indispensable for a more precise molecular biological medical diagnosis. In the project presented here, the HER2-HER3 protein interaction will be investigated with a novel digital assay with high sensitivity. Presence and interaction of the HER2 and HER3 proteins plays an important role in the development of carcinomas, especially in mammary carcinoma (breast cancer) [1]. However, the HER2-HER3 protein interactions cannot be detected with currently available medical diagnostic methods. Even in specialized analytical laboratories, the detection is only possible at high concentrations and with quite unreliable methods, only. In contrast to the widely used genetic analysis, the analysis of the proteome and even more so of the interactome, is much more difficult and therefore hardly used in molecular biological diagnostics so far. Here we show a novel method called Emulsion Coupling (EMUC) assay [2] that can close this gap and thus become of great importance for cancer diagnostics and for the life sciences in general.

The method uses two pairs of antibodies with unique DNA labels that can bind to the target simultaneously. The targets can be proteins from cell lysate, recombinant protein, peptides or protein modifications. After incubation, the antibodies and the target molecules form ternary complexes, the so-called Couplexes. Af-

ter strong dilution of the sample these Couplexes can be detected in a digital PCR reaction, and the actually number of Couplexes per reaction is determined with a bioinformatics algorithm. In addition, a mathematical concept was developed that enables quantification of the targets.

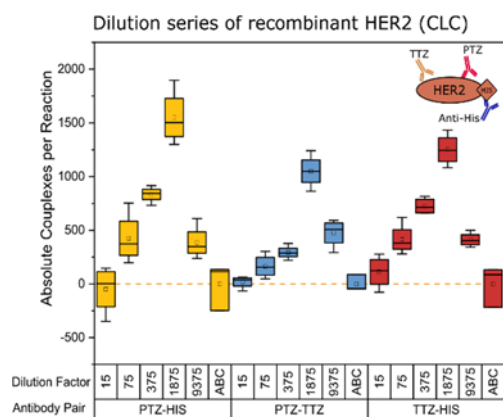


Fig. 1: Measurement of recombinant HER2 using EMUC. The detected number of Couplexes per reaction is shown for a dilution series of recombinant HER2. (© Laboratory of MEMS applications)

The high sensitivity and reliability of the EMUC assay was tested and demonstrated using computer simulations and by measuring recombinant HER2 at a known concentration in titration experiments. Since the recombinant HER2 also exhibits a His tag, three antibodies (namely PTZ, TTZ and HIS) could bind to it simultaneously and each pair of antibodies could be used to evaluate the measurement results independently. It was expected that each of the three different possible antibody combinations would measure the same concentration for HER2. This assumption was proven by the experiments shown in Fig. 1. Here, a dilution series of the protein was plotted and the number of Couplexes were evaluated three times using different pairs of antibodies. The measured number of the couplexes was used to calculate the HER2 concentration. The individual measurements were multiplied by the dilution factor to obtain the stock concentration and to calculate the mean concentration. Prepared concentration of the HER2 sample was  $5.71 \times 10^{-7}$  M and EMUC detected  $2.8 \times 10^{-7}$  M (CV 72.67%) HER2, which is quite accurate considering protein aggregation and imprecision of protein concentration measured by the provider. Furthermore, the

found recombinant HER2 concentrations were confirmed by independent SIMOA measurement, as well.

To demonstrate the general usability of the assay for diagnostic purposes, the HER2-HER3 complex was measured in BT474 breast cancer cell lines with verified pathological classification, subsequently. As shown in Fig. 2, the assay demonstrated high sensitivity and can measure not only individual HER2 or HER3 levels, but also the HER2-HER3 interaction, in case one of the antibodies is directed towards HER2 and the other one towards HER3. Couplex values do not scale linearly with increasing antigen concentration but follow a bell-shaped curve (see also figure 1), with the highest Couplex values being measured where antibody and antigen have approximately equimolar concentrations. Figure 2 shows high HER2 concentrations, less HER3, and even lower measured HER2-HER3 interactions. Studies with other cell lines have shown that HER2-HER3 concentrations can also be determined very accurately in other cell types. (Data not shown).

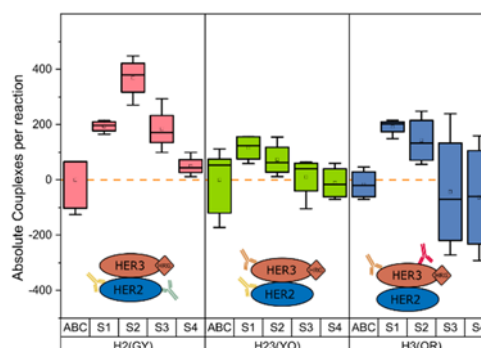


Fig. 2: Measurement of the HER2-HER3 complex of BT474 cells with EMUC. The number of detected Couplexes are shown per reaction for a dilution series (S1 – S4) prepared from a cell lysate of BT474 cells. Left: HER2 measurement, Middle: HER-HER3 PPI measurement, Right: HER3 measurement (© Laboratory of MEMS applications)

EMUC has proven to be an invaluable improvement in diagnostic predictions in the clinical setting. If the exact concentration of the underlying biochemical keystone of the pathological cancer pathways can be determined, this would allow the treating physician to apply the exact right drug for treatment and better predict therapeutic success. Future studies

will use patient material to validate its use in a field trial in comparison to established methods.

References

[1] Lee-Hoeflich, S. T., Crocker, L., Yao, E., Pham, T., Munroe, X., Hoeflich, K. P., ... & Stern, H. M. (2008). A central role for HER3 in HER2-amplified breast cancer: implications for targeted therapy. *Cancer research*, 68(14), 5878-5887.

[2] Karakus, U., Thamamongood, T., Ciminski, K., Ran, W., Günther, S. C., Pohl, M. O., Eletto, D., Jeney, C., Hoffmann, D., Reiche, S., Schinköthe, J., Ulrich, R., Wiener, J., Hayes, M. G. B., Chang, M. W., Hunziker, A., Yángüez, E., Aydilto, T., Krammer, F., ... Stertz, S. (2019). MHC class II proteins mediate cross-species entry of bat influenza viruses. *Nature*, 567(7746), 109–112.

### Fused Deposition Modeling of Microfluidic Chips in Transparent Polystyrene

Christof Rein,<sup>1</sup> Markus Mader,<sup>1</sup> Eveline Konrat,<sup>1</sup> Sophia L. Meermeyer,<sup>2</sup> Cornelia Lee-Thedieck,<sup>2</sup> Frederik Kotz-Helmer,<sup>1</sup> Bastian E. Rapp<sup>1,3</sup>

<sup>1</sup>Laboratory of Process Technology, Department of Microsystems Engineering of the University of Freiburg; <sup>2</sup>Institute of Cell Biology and Biophysics, University of Hannover, <sup>3</sup>Freiburg Center for Interactive Materials and Bioinspired Technologies (FIT)

Project funding: German Ministry of Education and Research (BMBF), funding code 03\_5527 “Fluoropor”, Deutsche Forschungsgemeinschaft (DFG, German Research Foundation) under Germany’s Excellence Strategy – EXC-2193/1 – 390951807, Research Cluster “Interactive and Programmable Materials (IPROM)” funded by the Carl Zeiss Foundation, Baden-Württemberg Stiftung GmbH within the program “Biofunctional Materials and Surfaces” (BiofMo-2, 3D Mosaic), European Research Council (ERC) under the European Union’s Horizon 2020 research and innovation programme (grant agreement No. 816006)

Polystyrene (PS) is one of the most-used thermoplastic materials worldwide due to its facile processability, its excellent optical and mechanical properties as well as its biocompatibility [1]. However, PS is only rarely used in microfluidic prototyping since structuring of PS is mainly done using industrial scale replication processes. So far, microfluidic chips in PS

have not been accessible to rapid prototyping via 3D printing. In consequence, microfluidic prototypes are most commonly prepared by soft-replication methods like polydimethylsiloxane (PDMS). While PDMS is a material with ease of handling and many established lab protocols for processing, it is not a material for mass market manufacturing like PS. Therefore, prototype development on a lab scale with PDMS generates difficulties when transitioning protocols from lab-scale to industry-scale [2]. Furthermore, rapid prototyping also allows the direct print of ready-to-use microfluidic chips, which do not require additional bonding, as well as enabling arbitrary true 3D design. In order to increase the accessibility of PS in rapid prototyping we developed protocols for creating a 3D-printable PS filament and generation of functional microchannels. As polystyrene is a material of choice for biomedical applications, we showed that FDM-printed PS has a high biocompatibility compared to commercial tissue culture PS (TCPS), making FDM printing a suitable method for preparation of microfluidic chips in life science applications.

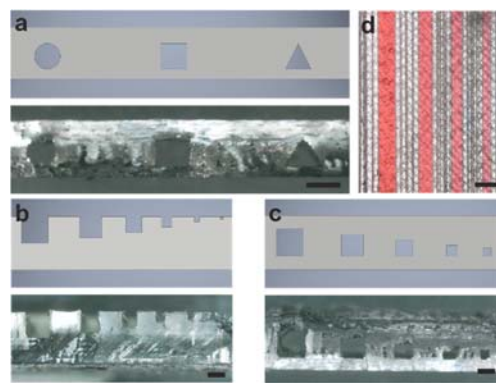


Fig. 1: Investigation of PS FDM printing accuracy. 600 µm Channels with circular, square and triangular cross section were printed with high accuracy (a). Open channels (b) and embedded channels (c) were printed to investigate the minimum resolution. Scale bars a-c: 600 µm. Embedded channels were filled with dyed water to prove that they are free of leakage (d). Scale bar: 1 mm [4]. © Laboratory of Process Technology, IMTEK, University of Freiburg.

In order to generate a filament for FDM printing commercial PS-granule ( $\bar{M}_w = 350\,000$  g/mol) was extruded with an extruder (Noztek Pro Filament Extruder, Noztek) at 220 °C. The filament was printed with a commercial FDM-

printer (Ultimaker 2+, Ultimaker B.V.) at 240 °C and a bed temperature of 70 °C. The resolution of FDM-printed PS was investigated by printing various channel geometries at a scale of 600  $\mu\text{m}$  (Fig. 1 a)<sup>4</sup> as well as square-shaped open and embedded channels with diameters ranging from 1000-200  $\mu\text{m}$  (Fig. 1 b, c)<sup>4</sup>. All geometries were printed with good accordance to the CAD model and embedded channels as small as 300  $\mu\text{m}$  and open channels as small as 200  $\mu\text{m}$  were printed with high accuracy. Furthermore, embedded channels showed no leakage (Fig. 1 d)<sup>4</sup>.

Furthermore, it was found that air inclusions reduced the transparency of FDM-printed PS, therefore the flowrate was increased to 120 %, which effectively reduced the air inclusions and thus higher transparencies were achieved (Fig. 2 a)<sup>4</sup>. In order to further increase the optical transparency chips with open channels were printed directly on a commercial PS substrate. With this setup the transmission into the channel is only limited by the optical properties of the commercial PS (Fig. 2 b)<sup>4</sup>.

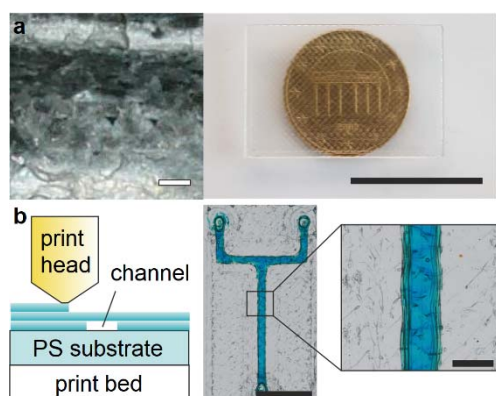


Fig. 2: Strategies to improve transparency of FDM-printed PS. A flowrate of 120 % effectively eliminates air inclusions from the bulk phase (a). Scale bar left: 200  $\mu\text{m}$ , scale bar right 20 mm. Printing on a commercial PS substrate causes no laminate structure that would otherwise reduce the transmission into the microchannel (b). Scale bar left 5 mm, scale bar right 600  $\mu\text{m}$  [4]. © Laboratory of Process Technology, IMTEK, University of Freiburg.

UV/Vis studies were conducted with FDM-printed PS substrates with various thickness in order to investigate the optical transmission. Substrates with a thickness of 100  $\mu\text{m}$  showed

transparencies of more than 50 % in the optical range, whereas 1100  $\mu\text{m}$  substrates showed transparencies around 40 %.

Microfluidic chips were generated with channel cross-sections of 600  $\mu\text{m}$  and filled with a pump to demonstrate typical microfluidic applications. Exemplary tesla mixers and mixer cascades were printed to show mixing of dyed water. Furthermore, chips were generated with geometries which are inaccessible otherwise by 2,5D-prototyping methods like soft replication. Additionally, FDM-printing allows the generation of custom-built structures like well-plates with highly customizable dimensions or geometries (Fig. 3)<sup>4</sup>.

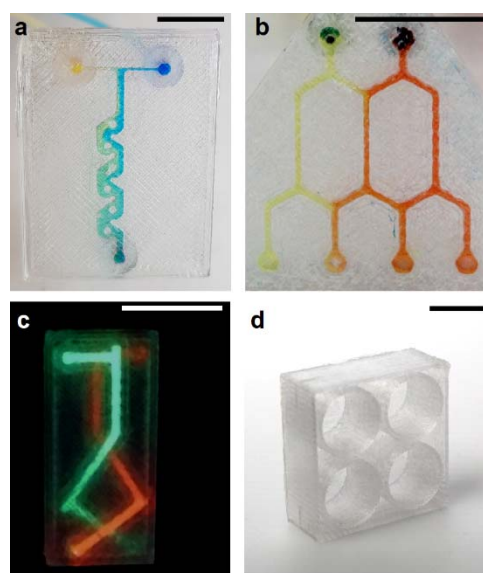


Fig. 3: Applications for FDM-printed structures. 2.5D structures like tesla mixers (a) and mixer cascades (b) were printed. Furthermore 3D channels are possible (c) and customized geometries that vary from industry standards (d). Scale bar: 10 mm [4]. © Laboratory of Process Technology, IMTEK, University of Freiburg.

In order to prove that FDM-printed microfluidics from PS can be successfully used for biomedical applications, cell culture experiments were carried out. Mouse L929-fibroblasts were seeded on FDM-printed PS substrates and commercial TCPS as a control. Live-dead-staining was carried out at three times to investigate the cell viability. Both the rough substrate surface and the smooth substrate side facing towards while printing were utilized for seeding cells in two distinct cell culture groups. By using different substrate topologies the influence of surface characteristics on the cell

growth should be investigated. It was shown that during all three times the cell viability of all three groups was comparably high (Fig. 4)<sup>4</sup>. Confocal microscopy revealed that the proliferation on the sample group with rough surfaces mostly took place inside of the low regions, as the cell growth was mostly guided by the laminate structure. In all cases, the results demonstrate a high cell viability of FDM-printed PS, which enables cell adhesion and proliferation.

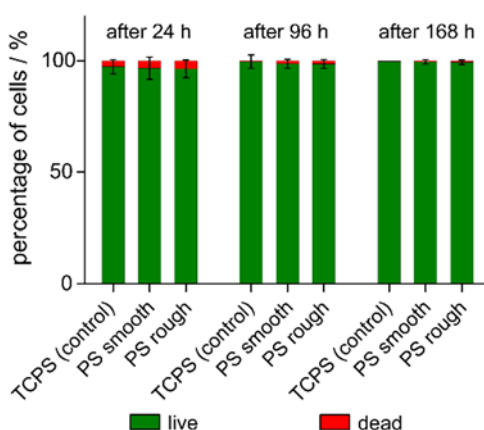


Fig. 4: Results of live-dead-staining of smooth and rough FDM-printed PS samples and commercial TCPS at three distinct times during culturing [4]. © Laboratory of Process Technology, IMTEK, University of Freiburg.

By using our new protocols for microfluidics prototyping by FDM printing it will be possible to generate new microfluidic structures in an important mass-marketing material. This will facilitate and increase the development speed of new chip designs for life science applications.

References

[1] Rubin, H. Altering Bacteriological Plastic Petri Dishes for Tissue Culture Use, Public Health Rep. 1966, 81, 843–844

[2] Becker, H. Mind the Gap! Lab Chip 2010, 10, 271–273

[3] Naderi, A.; Bhattacharjee, N.; Folch, A. Digital Manufacturing for Microfluidics. Annu. Rev. Biomed. Eng. 2019, 21, 325–364

[4] M. Mader, C. Rein, E. Konrat, S.L. Meermeyer, C. Lee-Thedieck, F. Kotz-Helmer, B. E. Rapp, Fused Deposition Modeling of Microfluidic Chips in Transparent Polystyrene, Micromachines, 2021, 12, 1348

FUTURE FIELD “(MICRO)SYSTEMS FOR ENERGY CONVERSION, STORAGE AND ENERGY-AUTONOMY”

CO<sub>2</sub> electrolysis

Joey Disch<sup>1,2</sup>, Khaled Seteiz<sup>1,2</sup>, Severin Vierrath<sup>1,2</sup>

<sup>1</sup>Freiburg Center for Interactive Materials and Bioinspired Technologies (FIT); <sup>2</sup>Electrochemical Energy Systems Group, IMTEK - Department of Microsystems Engineering, University of Freiburg

Project funding: Vector Foundation, Project: CO<sub>2</sub>-to-X

Carbon emission from fossil fuels causing global warming is posing a serious threat to human life on earth. Electrochemical CO<sub>2</sub> reduction has emerged in recent years as an outstanding approach to convert captured CO<sub>2</sub> into feedstock [1]. In an electrolyzer, the CO<sub>2</sub> reduction is catalyzed on the electrode surface in the cathode compartment, resulting in various products controlled by the choice of the catalyst.

The aim of the project CO<sub>2</sub>-to-X, funded by the Vector Foundation, is to tackle efficiency and cost barriers in CO<sub>2</sub> electrolysis. The main focus is set on the conversion of CO<sub>2</sub> to Carbon Monoxide (CO).

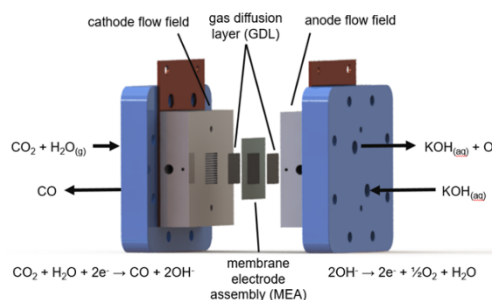


Fig. 1: Schematic of custom built CO<sub>2</sub> electrolysis cell. (© Electrochemical Energy Systems Group)

The electrolyzer design selected in CO<sub>2</sub>-to-X, consists of two half-cell compartments, which are divided by an anion exchange membrane (Figure 1). The cathode compartment is fed with gaseous CO<sub>2</sub>, whereas the anode is fed

with an alkaline solution. By applying a potential to the cell,  $\text{CO}_2$  is reduced to  $\text{CO}$  at the cathode and oxygen evolves at the anode, while anions migrate through the membrane [2]. For an efficient catalyst it is desirable to drive  $\text{CO}_2$  conversion at high current densities with high selectivity, especially suppressing the hydrogen evolution. Similarly important are low overpotentials to reduce the energy demand for the  $\text{CO}_2$  conversion and to achieve economic feasibility [3].

One part of the work focuses on silver nanoparticles, a typical  $\text{CO}_2$ -reduction catalyst. Figure 2 shows the scanning electron micrographs of two silver (Ag) electrodes synthesized by different approaches. The Micrograph on the top depicts the porous structure of silver nanoparticles deposited on a carbon gas diffusion layer via a spray coating process.

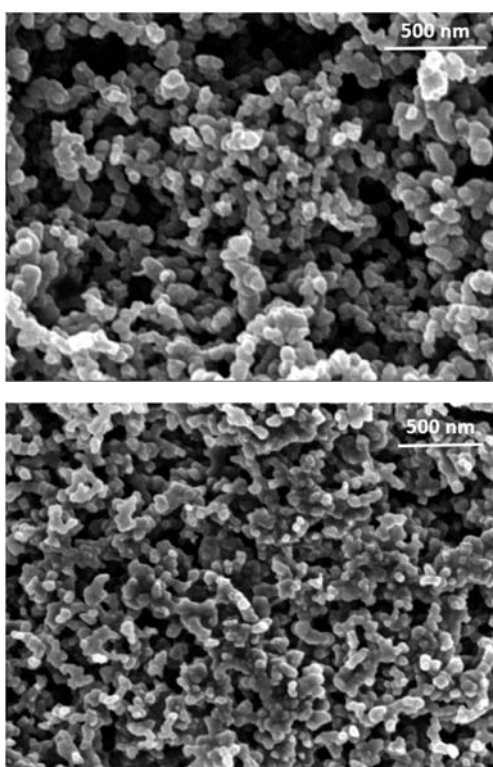


Fig. 2: Electron micrographs of a catalyst layer, fabricated via spray coating with commercial silver nanoparticles (top), and a chlorine doped silver catalyst layer electrochemically deposited on a carbon gas diffusion layer (bottom). (© Electrochemical Energy Systems Group)

The Micrograph on the bottom on the contrary shows a chlorine (Cl) doped silver catalyst layer, which was produced by electroplating

silver directly onto a carbon gas diffusion layer followed by an electrochemical doping procedure. Following this procedure a 3-dimensional porous coral-like structure could be achieved.

Measurements in the electrolyzer cell demonstrated promising performance with the Cl doped silver electrodes (Figure 3). At  $30^\circ\text{C}$  a maximum  $\text{CO}$  partial current density of  $154 \text{ mA/cm}^2$  was achieved, as shown in Figure 3. In contrast, a maximum  $\text{CO}$  partial current density of  $128 \text{ mA/cm}^2$  was obtained at a high cell potential of 3.4 Volts by testing the commercial Ag nanoparticles at  $30^\circ\text{C}$ .

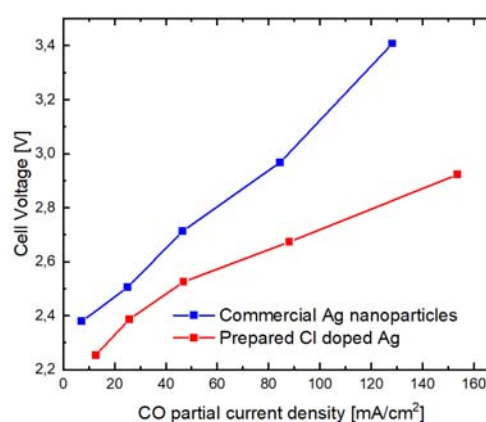


Fig. 3: Cell voltage and partial current density of  $\text{CO}$  of a cell using commercial Ag nanoparticles (blue curve) and a cell using the coral-like Cl doped silver electrodes. (© Electrochemical Energy Systems Group)

One disadvantage of  $\text{CO}_2$  electrolysis in alkaline environment is that  $\text{CO}_2$  reacts with hydroxide to form bicarbonate anions and then carbonate anions. The consequence of this process is precipitation of carbonate salt in the electrode on the cathode side, which impedes  $\text{CO}_2$  transport and leads to hydrogen evolution. Furthermore, it may lead to cell failure, if the channels in the flow-fields are completely blocked. A way to remove the salt is to flush the cathode periodically with liquid water. However, that is accompanied by performance loss [4].

The employment of bipolar membranes instead of an anion exchange membranes have recently been studied to reduce carbonate crossover but face unique challenges such as

delamination of the bipolar membrane interface and hydrogen evolution when the cation exchange membrane faces the cathode. The focus of the next phase of the project is set on the development of novel membrane concepts and on continuing the development of highly active cathodes for CO<sub>2</sub> electrolysis.

### References

- [1] Le Nguyen, Dang Tri; Do, Ha Huu; Nguyen, Manh Tung; Vo, Dai-Viet N.; Nguyen, Van-Huy; Nguyen, Chinh Chien et al. (2021): Electrochemical conversion of carbon dioxide over silver-based catalysts. Recent progress in cathode structure and interface engineering. In: *Chemical Engineering Science* 234, S. 116403. DOI: 10.1016/j.ces.2020.116403.
- [2] Lees, Eric W.; Mowbray, Benjamin A. W.; Salvatore, Danielle A.; Simpson, Grace L.; Dvorak, David J.; Ren, Shaoxuan et al. (2020): Linking gas diffusion electrode composition to CO<sub>2</sub> reduction in a flow cell. In: *J. Mater. Chem. A* 8 (37), S. 19493–19501. DOI: 10.1039/D0TA03570J.
- [3] Salvatore, Danielle; Berlinguette, Curtis P. (2019): Voltage Matters When Reducing CO<sub>2</sub> in an Electrochemical Flow Cell. In: *ACS Energy Lett.* 5 (1), S. 215–220. DOI: 10.1021/acsenerylett.9b02356.
- [4] Mardle, Peter; Cassegrain, Simon; Habibzadeh, Faezeh; Shi, Zhiqing; Holdcroft, Steven (2021): Carbonate Ion Crossover in Zero-Gap, KOH Anolyte CO<sub>2</sub> Electrolysis. In: *J. Phys. Chem. C* 125 (46), S. 25446–25454. DOI: 10.1021/acs.jpcc.1c08430.

## Quantitative STEM Tomography for Proton Exchange Membrane Fuel Cell Applications

Philipp A. Heizmann<sup>1,2</sup>, Carolin Klose<sup>1,2</sup>, Matthias Breitwieser<sup>2</sup>, Severin Vierrath<sup>1,2</sup>

<sup>1</sup>Freiburg Center for Interactive Materials and bio-inspired Technologies (FIT), University of Freiburg and <sup>2</sup>Electrochemical Energy Systems Group, IMTEK – Department of Microsystems Engineering, University of Freiburg

Project funding: Federal Ministry of Education and Research (BMBF), Project “FC-CAT fuel cell CFD and through-plane modelling”

Polymer electrolyte membrane fuel cells (PEMFCs) are one of the key technologies for a hydrogen-based energy economy [1]. The performance of PEMFCs is strongly dependent on the activity and stability of the electrocatalyst, which often consists of Pt or PtM alloy

(M e.g. Co, Ni, Ru) nanoparticles deposited on nanoporous carbon supports [2]. The development of highly active electrocatalysts while using the lowest possible quantities of precious metal requires a thorough understanding of these materials.

One goal of the project “FC-CAT”, which is in cooperation with the Fraunhofer Institute for Solar Energy Systems (ISE) and AVL Deutschland GmbH, is the development and improvement of comprehensive model systems for the performance of state-of-the-art electrocatalysts used in PEMFCs. Within the framework of this project, the Electrochemical Energy Systems Group contributes with experimental ex-situ and in-situ characterization of suitable model materials, improving the understanding of structure-activity relationships. One of these methods involves determining the size and position of precious metal nanoparticles on the carbon support (e.g. Pt/C) via scanning transmission high-angle angular dark-field (S/TEM-HAADF) electron tomography, as both parameters have shown to be decisive factors on the performance of PEMFCs [3,4].

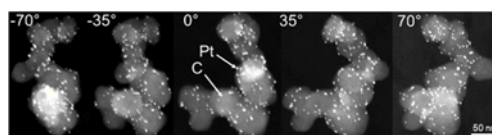


Fig. 1: Selected projections from a S/TEM-HAADF tilt series of 20 wt% Pt/C. (© Electrochemical Energy Systems Group)

For example, using FIT’s Talos F200X (S)TEM, 2D HAADF images from +70° to -70° were acquired for two model materials with 20 wt% and 40 wt% platinum nanoparticles on carbon (Fig. 1). Using Python and the software ImageJ and TomViz, the sample volumes were reconstructed by an ordered subset expectation maximization algorithm [5], segmented and visualized with a theoretical isotropic voxel resolution of 0.89 nm (Fig. 2).

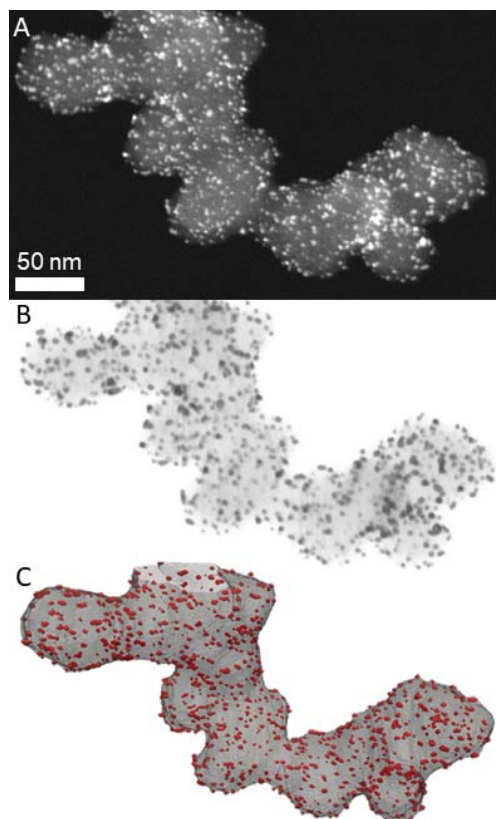


Fig. 2: Post-processing of the HAADF tilt-series of 40 wt% Pt/C. A) Raw STEM-HAADF projection at  $0^\circ$ . B) Reconstructed volume at  $0^\circ$ . C) Segmented volume (red: Platinum, grey: Carbon) at  $0^\circ$ . Note the images in B) and C) contain depth. (© Electrochemical Energy Systems Group)

In the shown case, mean particle diameters of  $(3.50 \pm 1.40)$  nm (20 wt%) and  $(3.09 \pm 1.24)$  nm (40 wt%) were determined (Fig. 3). Although the 2D analysis of the raw HAADF images can already provide sufficient information about the average and mean size diameter of the Pt nanoparticles and their statistical size distribution, statements about the position of the nanoparticles can only be made to a limited extent. Consistent with previous findings from Padgett *et al.* [4] for various Pt/C materials, 3D analysis reveals that the Pt nanoparticles inside the carbon pores are significantly smaller than the Pt nanoparticles sitting on the surface of the carbon support. Furthermore, increasing the platinum loading from 20 wt% to 40 wt% led to higher proportion of internal particles (17.5 % to 27.4 %). With these insights, the goal of the project now is to elucidate the impact of the nano-particle position onto the electrochemical performance.

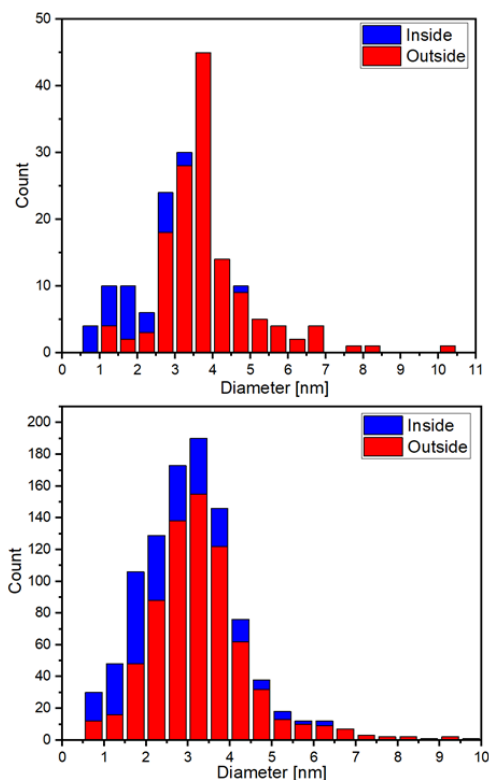


Fig. 3: Particle size distribution with subdivision of particles inside and outside the pores for 20 wt% Pt/C (top) and 40 wt% Pt/C (bottom). (© Electrochemical Energy Systems Group)

## References

- [1] M. Breitwieser, M. Klingele, S. Vierrath, R. Zengerle & S. Thiele (2018): Tailoring the Membrane-Electrode Interface in PEM Fuel Cells: A Review and Perspective on Novel Engineering Approaches. - In *Adv. Energy Mater.*, **8**, 1701257-1701276.
- [2] X. Ren, Q. Lv, L. Liu, B. Liu, Y. Wang, A. Liu & G. Wu (2020): Current progress of Pt and Pt-based electrocatalysts used for fuel cells. - In *Sustain. Energy Fuels*, **4**, 15-30.
- [3] Harzer, G.S., Orfanidi, A., El-Sayed, H., Madkikar, P. & Gasteiger, A. (2018): Tailoring Catalyst Morphology towards High Performance for Low Pt Loaded PEMFC Cathodes. - In *J. Electrochem. Soc.*, **165**, F770.
- [4] Padgett, E., Andrejevic, N., Liu, Z., Kongkanand, A., Gu, W., Moriyama, K., Jiang, Y., Kumaraguru, S., Moylan, T.E., Kukreja, R. & Müller, D.A. (2018): Connecting Fuel Cell Catalyst Nanostructure and Accessibility Using Quantitative Cryo-STEM Tomography. - In *J. Electrochem. Soc.*, **165**, F173.
- [5] Hudson, H. & Larkin, R. (1994): Accelerated Image Reconstruction using Ordered Subsets of Projection Data. - In *IEEE Transactions on Medical Imaging*, **13**, 601-609.

## Theoretical studies of hybrid perovskites at room temperature

Julian Gebhardt<sup>1,2</sup>, Wei Wei<sup>1,2</sup> and Christian Elsässer<sup>1,2,3</sup>

<sup>1</sup>Fraunhofer IWM, 79108 Freiburg, Germany; <sup>2</sup>Cluster of Excellence livMatS at FIT - Freiburg Center for Interactive Materials and Bioinspired Technologies, University of Freiburg, 79110 Freiburg, Germany; <sup>3</sup>Freiburg Materials Research Center (FMF), University Freiburg, 79104 Freiburg, Germany

Project funding: Fraunhofer LIGHTHOUSE PROJECT MaNiTU, Deutsche Forschungsgemeinschaft (DFG, German Research Foundation) under Germany's Excellence Strategy – EXC-2193/1 – 390951807

Hybrid organic-inorganic halide perovskites are the most promising photovoltaic (PV) absorber materials to substitute or complement silicon for high-efficiency solar cells. Furthermore, they have strong ionic character and, thus, they are also considered as Li-ion conducting materials. Hence, they hold the potential to combine solar-cell and ion-battery functions in one device, which is the research objective of the SolStore activities in the *livMatS* cluster.

In order to balance PV properties, ion conductivity, compound stability, and sustainability, computational studies are vital for understanding and designing such materials. An accurate description of electronic structures at operation temperatures of solar cells or ion batteries are notoriously difficult. In order to make accurate predictions, we developed an efficient computational workflow, based on density-functional theory, which is suitable to calculate band gaps for arbitrary compounds with good predictive power. This workflow is validated quantitatively by comparison to experimental band-gap data obtained at finite temperatures.[1]

With this methodology we demonstrate the large impact that the dynamical nature of the perovskite structure has on the PV properties of  $(\text{HC}(\text{NH}_2)_2)_x\text{Cs}_x\text{Pb}(\text{I}_y\text{Br}_y)_3$  ( $x$  and  $y$  may vary from 0 to 1), an intensively studied absorber material employed in the most successful devices currently fabricated in SolStore. As

schematically shown in Fig. 1(a), despite being observed as temporal and spatial average in experimental investigations, the ordered cubic phase does not occur at a temperature of 300 Kelvin. Instead, the crystal structure is dynamically distorted and tilted, as evident from analyzing bond distances (Fig. 1(b)) and bond angles (Fig. 1(c)) from *ab initio* molecular dynamics (MD) calculations. These structural changes have a severe influence on the electronic structure: they raise the electronic band gap from  $\sim 1.0$  eV at 0 K to  $\sim 1.78$  eV at 300 K (Fig. 1(d)).

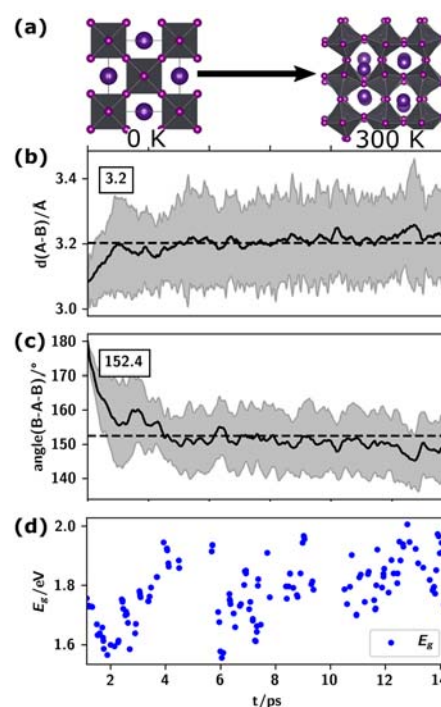


Fig. 1: (a) Sketch of the structural changes that occur in the cubic perovskite structure of CsPbI<sub>3</sub> at 300 K, represented here as the averaged structure from the MD run. Atoms are colored in purple (Cs), magenta (I), and gray (Pb). Changes in (b) Pb-I bond distances and (c) Pb-I-Pb bond angles during the MD run. Average values are plotted in black for each time step, and their standard deviations are indicated as  $\pm\sigma$  by the gray regions. (d) Band gap  $E_g$  vs time. © Julian Gebhardt

With this understanding and the efficient as well as accurate methodology of [1] to calculate PV properties of perovskite materials, we extend our efforts in SolStore to investigate Li-ion diffusion in these materials.

### Reference

[1] J. Gebhardt, W. Wei & C. Elsässer (2021): Efficient Modeling Workflow for Accurate Electronic Structures of Hybrid Perovskites. In: J. Phys. Chem. C, 125, 34.

## Pan-European Network of Fundamental pH Research: UnipHied

Valentin Radtke<sup>1,2</sup>, Denis Priester<sup>1,2</sup>, Monika Bäuerle<sup>1,2</sup>, Niklas Gebel<sup>1,2</sup>, Ingo Krossing<sup>1,2,3</sup>

<sup>1</sup>Institut für Anorganische und Analytische Chemie,  
<sup>2</sup>Freiburger Materialforschungszentrum (FMF) and  
<sup>3</sup>Freiburger Zentrum für interaktive Werkstoffe und bioinspirierte Technologien (FIT)

Project funding: This work was funded through the European Metrology Programme for Innovation and Research (EMPIR) Project 17FUN09 "Realisation of a Unified pH Scale" The EMPIR is jointly funded by the EMPIR participating countries within the European Association of National Metrology Institutes (EURAMET e.V.) and the European Union.

Due to the conventional definition of standard states of solutes in solution pH values of different solvent solutions cannot be compared to each other reasonably. On a conceptual and theoretical level the  $\text{pH}_{\text{abs}}$  scale was created by establishing a (hypothetical) gaseous reference state, which enables this comparability.[1] The modified scale  $\text{pH}_{\text{abs}}^{\text{H}_2\text{O}}$  can be considered as continuation of the aqueous pH scale that can be applied on all media.

On a practical level, however, a number of questions still need to be clarified, from which the objectives of the project derive:

- Development and Validation of a reliable and universally applicable measurement procedure for the determination of  $\text{pH}_{\text{abs}}^{\text{H}_2\text{O}}$  values in non-aqueous and mixed solvents, colloids, etc.

- Creation of a reliable method for the evaluation of the liquid junction potential between aqueous and non-aqueous solutions.

- Development of a coherent and validated suite of calibration standards for standardizing routine measurements systems in terms of  $\text{pH}_{\text{abs}}$  values for a variety of media.

The project consortium consists of 12 partners across Europe, of which 8 are National Metrology Institutes (NMIs: LNE, France; BFKH, Hungary; CMI, Czech Republic; DFM, Denmark; IPQ, Portugal; PTB, Germany; SYKE, Finland; TUBITAK, Turkey), one is private (ANBSensors, UK), one is a private non-profit

association (FC-ID, Portugal) and two are universities (UT, Estonia; ALU Freiburg, Germany). A complete summary of the project results can be found on the EURAMET website.[2] The main focus of ALU is on objective 2.

In the potentiometric pH measurement a liquid junction is formed at the interface between two solvents, typically water and the non-aqueous solvent. The liquid-junction potential (LJP) that arises has a magnitude that is generally difficult to evaluate and control, and is, therefore, considered to be the major source of bias in classical pH measurement. Salt bridges (SB) are commonly used to minimize LJP contributions to the electric cell potential by creating two liquid-liquid junctions whose LJPs tend to cancel each other out. The underlying idea is that a highly concentrated electrolyte, whose cations and anions have the same transference numbers, takes over the charge transport between both half-cells of an electrochemical cell. In case of identical solvents in both half-cells the LJP can be calculated moderately well with e.g. the Henderson-equation. For all-aqueous cells (i.e. the solvent in both half-cells is water) the KCl-SB (potassium chloride is the electrolyte) is most common, and the LJPs nearly cancel out, depending on the particular case. However, in case of different solvents, the Henderson-equation and similar approaches are not suitable. The reason is the direct contact of two different solvents at least at one of the junctions, from which solvent-solvent interactions (not accounted for by the Henderson equation) arise contributing to the LJP.

Ionic liquids (IL) are electrolytes in liquid state of aggregation without being solvated, i.e. no solvent is present. Thus, solvent-solvent interactions are excluded if a SB is filled with an IL (ILSB). Further, due to their high concentration virtually only the IL-ions cross the S|IL-junction between the solvent S and the IL undertaking the charge transport in the cell.

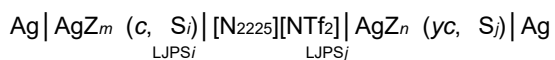
The minimisation of the liquid junction potential by using a salt bridge formed by an "ideal" ionic liquid (IL) was studied in a number of systems formed by water and non-aqueous solvents such as acetonitrile, ethanol and methanol. The ideal character of the IL requires,

## Highlights

among others, close to identical transference numbers, or ionic mobilities, for cation and anion both in the pure IL and in solution, close to identical solvation Gibbs energies of the ions, while being inert by respect to the solvents. The IL [N2225][NTf2] selected for the project satisfies these requirements.

Although this IL enables close to ideal elimination of the LJP, there still remains a degree of uncertainty as to how complete is the elimination. Thus, the initial task of evaluating the LJP changed into evaluating the residual uncertainty due to possibly incomplete elimination of LJP. To this purpose, a new methodology aiming to determine the uncertainty due to possibly incomplete elimination of LJP was proposed by ALU and UT. The approach is based on the network analysis and was implemented by ALU. The network is an overdetermined system, i.e. a system of equations with more equations than unknowns. Generally, the more closely meshed the network the more reliable the result. The approximate solution can be found by statistical analysis using the method of least squares.

The network is used to determine the Gibbs transfer energy of the redox system  $\text{Ag}^+/\text{Ag}$  from water to various solvents  $\Delta_{\text{tr}}G^\circ(\text{Ag}^+, \text{H}_2\text{O} \rightarrow \text{S})$ . Combinations with the solvents  $S_i$  and  $S_k$  being water ( $\text{H}_2\text{O}$ ), acetonitrile (AN), propylene carbonate (PC), dimethylformamide (DMF), ethanol (EtOH) and methanol (MeOH) have been studied. The cell used for measurements is:



The network includes variations of concentrations  $c$  of the redox active salt  $\text{AgZ}$  (and the concentration ratio expressed by  $y$ ) as well as the nature of counterion  $Z^-$  of the  $\text{Ag}^+$  ion which is the electroactive species, expressed by  $n$  and  $m$ , resp. (whereby  $m$  may or may not be identical with  $n$ ), and the solvents with  $i = j = 1 - 6$ , i.e. the above defined six solvents.

As such, the network analyzed during the project comprises 145 individual measurements. Comparison of the obtained experimental values to the calculated values enabled assessment of the overall liquid junction potential

hence establishing whether contributions arising from solvent-solvent interactions equals to zero.

The Gibbs transfer energy of the redox system  $\text{Ag}^+/\text{Ag}$  from water to acetonitrile (AN),  $\Delta_{\text{tr}}G^\circ(\text{Ag}^+, \text{H}_2\text{O} \rightarrow \text{AN})$ , was determined to  $-25.1 \text{ kJ mol}^{-1}$  with the accuracy level of 6 mV, see below. A widely accepted literature value is  $-23.2 \text{ kJ mol}^{-1}$  having an estimated uncertainty of 3 – 6  $\text{kJ mol}^{-1}$ . The literature value was obtained using the so-called reference electrolyte assumption that is considered to be the most reliable. The closeness between experimental value obtained in the project and literature value validate the setup used by ALU and also the proposed network approach. Moreover, the difference of the LJPs in the given setup, i.e.  $\text{LJP}(\text{H}_2\text{O-IL}) - \text{LJP}(\text{AN-IL})$ , is stable and remains within 6.3 mV, equivalent to  $0.61 \text{ kJ mol}^{-1}$  or 0.11 pH-units, respectively, in the case of low ionic strength solutions. This 0.11 in pH is used as the standard uncertainty contribution due to possibly incomplete LJP elimination in other tasks of this project. For water-acetonitrile, LJPs are remarkably insensitive against the change of the ionic strength of the electrolyte solutions (silver salts of type  $\text{Ag}^+Z^-$ ) as long as it remains within 0.1 to 10  $\text{mmol L}^{-1}$  and against influx of solvent into the ILSB. In addition, this indicates that the redox system  $\text{Ag}^+/\text{Ag}$  under investigation doesn't affect the LJPs either. The Gibbs transfer energy of the redox system  $\text{Ag}^+/\text{Ag}$  from water to EtOH,  $\Delta_{\text{tr}}G^\circ(\text{Ag}^+, \text{H}_2\text{O} \rightarrow \text{EtOH})$  was determined to  $1.6 \text{ kJ mol}^{-1}$  and from water to MeOH,  $\Delta_{\text{tr}}G^\circ(\text{Ag}^+, \text{H}_2\text{O} \rightarrow \text{MeOH})$  to  $3.8 \text{ kJ mol}^{-1}$ . These findings can be considered reliable since they are in good agreement with literature data. The consistency of the values is  $0.55 \text{ kJ mol}^{-1}$ . If the ionic liquid [N2225][NTf2] forms the salt bridge, the LJP contributions are strictly valid for the studied solvents i.e. water, acetonitrile, ethanol, methanol, dimethylformamide and propylene carbonate. However, it is reasonably expected that they are equally valid for a variety of other solvents with not too low dielectric constant.

The main achievement of this project was to show that the “close to ideal” IL studied within

the project allows the experimental implementation of the  $\text{pH}_{\text{abs}}^{\text{H}_2\text{O}}$  scale for several complex organic solvents. This contributes to obtain  $\text{pH}_{\text{abs}}^{\text{H}_2\text{O}}$  values that serve as a thermodynamically well-defined link between the acidity in water and the acidity in any other medium with respect to the aqueous system. The work undertaken in this project was also incorporated into the efforts already started by IUPAC to address pH assessment in non-aqueous and mixed solvents. The Uniphied project was promoted in the News Magazine of IUPAC as an important opportunity to secure intercomparability of pH measurement results in different media. After a careful evaluation process by 8 reviewers that lasted over one year, a Technical Report presenting the state-of-the-art of the meaning and assessment of pH in solvents other than water has been published by the IUPAC official journal, Pure and Applied Chemistry.[3] A second Technical Report aiming to present the progress achieved toward practical implementation of  $\text{pH}_{\text{abs}}^{\text{H}_2\text{O}}$  as well as the Quality of Measurement Values is currently in progress. The measurements and methods carried out in this project impress by their simplicity. They can be incorporated into existing measurement setups without difficulty. In addition, the IL is chemically inert, i.e. also non-toxic, is commercially available and can be easily repurified.

The project is also present on the Internet and can be accessed via the web site [uniphied.eu](http://uniphied.eu).

#### References

- [1] D. Himmel, S. K. Goll, I. Leito, I. Krossing, *Angew. Chem. Int. Ed.* 49, 6885, (2010)
- [2] [https://www.euramet.org/research-innovation/search-research-projects/details/?tx\\_euramettcp\\_project\[project\]=1526&tx\\_euramettcp\\_project\[controller\]=Project&tx\\_euramettcp\\_project\[action\]=show](https://www.euramet.org/research-innovation/search-research-projects/details/?tx_euramettcp_project[project]=1526&tx_euramettcp_project[controller]=Project&tx_euramettcp_project[action]=show)
- [3] V. Radtke, D. Stoica, I. Leito, F. Camões, I. Krossing, B. Anes, M. Roziková, L. Deleebeeck, S. Veltzé, T. Näykkki, F. Bastkowski, A. Heering, N. Dániel, R. Quendera, L. Liv, E. Uysal, N. Lawrence, *Pure Appl. Chem.* 93, 1049, (2021)

## Development of integrated and flexible manufacturing processes for micro-Thermoelectric generators – MiTEG

Negin Sherkat<sup>1</sup>, Uwe Pelz<sup>1,2</sup>, Peter Woias<sup>1,2</sup>

<sup>1</sup>Laboratory for the Design of Microsystems, Department of Microsystems Engineering (IMTEK);  
<sup>2</sup>Cluster of Excellence livMatS @ FIT – Freiburg Center for Interactive Materials and Bioinspired Technologies, University of Freiburg

Project funding: German Research Foundation (DFG)

The main aim of this cooperation project focuses on a cost-effective fabrication process for micro thermoelectric generators ( $\mu\text{TEG}$ ) based on printed circuit device technologies. This research program is conducted together with the group of Dr. Heiko Reith from Leibniz Institute for Solid State and Materials Research (IFW). This paper discusses and demonstrates the work which are being carried out in IMTEK.

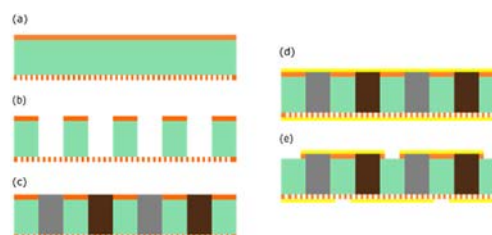


Fig. 1: Single-sided PCB-based  $\mu\text{TEG}$ -fabrication process: (a) filter layer on the bottom side of the PCB is created by lithography and Cu etching; (b) holes are created on one side of the PCB by CNC milling; (c) paste dispensing of TE materials into the thermolegs (p-type (grey)) (n-type (brown)); (d) gold electrochemically deposited on the Cu layers; (e) patterning the electrical contacts © IMTEK/Laboratory for Design of Microsystems

According to the literature, most of  $\mu\text{TEG}$  fabrication processes are complex, costly and need clean room micro fabrication technologies [1]. Additionally,  $\mu\text{TEG}$  devices with low efficiency suffer over-proportionally from non-optimized device design resulting in sometimes negligible power output [1]. To enhance the output efficiency of the  $\mu\text{TEG}$ , two fabrication processes are proposed, of which one is shown in this work. Finite element analysis on  $\mu\text{TEG}$  design is done in order to accurately predict the final performance of the fabricated  $\mu\text{TEG}$ .

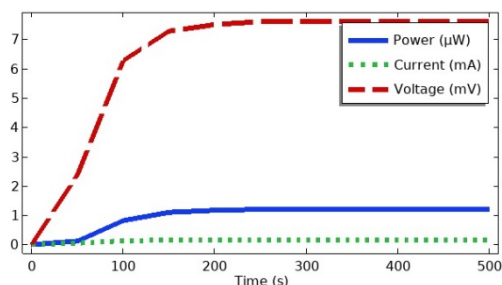


Fig. 2: Time dependent simulation results for the designed 8TC- $\mu$ TEG at 50.5  $\Omega$  load resistance with a  $\Delta T$  of 8.6 K © IMTEK/Laboratory for Design of Microsystems

The  $\mu$ TEG that has been designed and fabricated is based on a one-sided  $\mu$ TEG fabrication process forming 8 thermocouples (8-TC- $\mu$ TEG). Figure 1 shows the overview of the fabrication processes based on double-sided 500  $\mu$ m thick printed circuit board (PCB). Small holes ( $\sim \varnothing$  40  $\mu$ m) are created on the bottom copper layer with the help of laser lithography and copper etching processes first. Then the larger 500  $\mu$ m holes for the thermolegs are created on the top side of the PCB using a milling machine. After forming the holes, they are filled by p-type and n-type thermoelectric material paste and the solvent of the paste is removed by vacuum filtration through the small bottom holes. Next a very thin layer of gold is deposited on both sides of the substrate in order to reduce both electrical and contact resistance between thermolegs and copper connections. The final step is patterning the electrical contacts between thermocouples by using CNC milling [2].

Table 1: comparison between simulation results and measured value of designed  $\mu$ TEG at the corresponding  $\Delta T$ ; Values taken from [2]

	U [mV]	I [ $\mu$ A]	P [mW]	$R_{TEG}$ [ $\Omega$ ]	$\Delta T$ [K]
$\mu$ TEG	7.95	154.96	1.23	51.28	7.8
$\mu$ TEG <sub>sim</sub>	7.6	157.56	1.2	50.5	8.6

In a simulation study of the designed  $\mu$ TEG, performed in COMSOL Multiphysics (5.6), the theoretical designs simulation results are compared to measurement results for fabricated  $\mu$ TEGs. Figure 2 shows the time dependent simulation results for the designed 8TC- $\mu$ TEG.

Table 1 illustrates a fairly well-matched behavior of the simulated and measured electrical output values of the designed and fabricated  $\mu$ TEGs [2].

References

[1] Pelz, U., J. Jaklin, R. Rostek, F. Thoma, M. Kröner, and P. Woias. "Fabrication process for micro thermoelectric generators ( $\mu$ TEGs)." *Journal of Electronic Materials* 45, no. 3 (2016): 1502-1507.

[2] N. Sherkat, S. K. Subhash, T. Gerach, U. Pelz and P. Woias, "Development of Manufacturing Processes for Vertical Micro-Thermoelectric Generators based on Printed Circuit Boards," 2021 IEEE 20th International Conference on Micro and Nanotechnology for Power Generation and Energy Conversion Applications (PowerMEMS), 2021, pp. 112-115, doi: 10.1109/PowerMEMS54003.2021.9658353.

### Realistic Aging Modelling in Fuel Cells

Julian Stiegeler<sup>1,2</sup>, Hien Nguyen<sup>1,2</sup>, Matthias Breitwieser<sup>2</sup>, Carolin Klose<sup>2</sup>

<sup>1</sup>Freiburg Center for Interactive Materials and Bio-inspired Technologies (FIT), University of Freiburg and <sup>2</sup>Electrochemical Energy Systems Group, IMTEK-Department of Microsystems Engineering, University of Freiburg

Project funding: Federal Ministry of Education and Research (BMBF), Project "FC-RAT: Fuel cell Realistic aging trend modelling"

Mobility is changing towards sustainable, emission free electrical powertrains. One key element of electric powertrains will be fuel cells due to short refuelling times and high energy-storage density. These two advantages are particularly important for heavy-duty applications. When employed in trucks, however, the lifetime requirement for fuel cells has to be increased by a factor of 4 - 8 compared to the state of the art for light duty vehicles. [1-4]

In cooperation with the Fraunhofer Institute for Solar Energy Systems (ISE) and AVL Deutschland GmbH, the project "FC-RAT" aims to significantly improve and expand the understanding of aging and degradation processes. For this purpose, models for realistic lifetime assessments under real load profiles will be developed in the project. In this sub-

project the aim is to characterize and understand the aging and degradation mechanisms of different key components of the fuel cell. For now, the sub-projects' focus is on the aging and degradation of the membrane and the metal catalyst in the electrodes.

To improve the understanding of aging processes within a reasonable time frame, membrane electrode assemblies (MEAs) are aged with established accelerated stress tests (ASTs). Each AST is chosen depending on the component and degradation mechanism, which is to be studied.

To study membrane degradation in respect to chemical and mechanical degradation, the MEA is held at the open circuit voltage while the relative humidity is varied [3]. In this AST, the operation at the open circuit voltage accelerates chemical degradation, while the variation of the relative humidity leads to swelling and shrinking of the membrane, which accelerates mechanical degradation. While the AST is running, the membrane integrity is characterised in-situ in regular intervals.

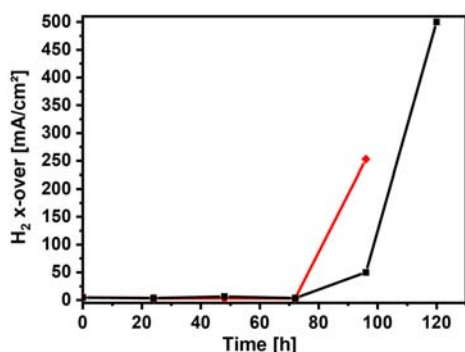


Fig. 1: Hydrogen cross-over over time in fuel cells with Nafion™ N211 membrane (red) and Fumatech FS715 (black) (© Electrochemical Energy Systems Group)

Since the start of this sub-project in May 2021, the mentioned AST protocol established from the U.S. Department of Energy [3] was adapted to the available test equipment and commercially available membranes were tested towards their lifetime in a combined mechanical/ chemical AST. Here, a non-reinforced Nafion™ N211 membrane and an ePTFE reinforced and chemically stabilized state-of-the-art membrane (Fumatech) were evaluated. In this test, the state-of-the-art

membrane with reinforcements is stable for longer than the non-reinforced Nafion™ membrane. This can be seen in Figure 1, which shows the current proportional to hydrogen crossing from the anode to the cathode. Hence, the crossover of the reinforced membrane (red) increases less after 78h of operation compared to the non-reinforced (black). To understand whether this is related to the reinforcement in the Fumatech membrane, ex-situ post lifetime experiments are planned.

Future work will focus on electrode degradation to enhance the understanding of platinum dissolution and the influence of the polymer binder. For this purpose, the degradation of platinum nanoparticles in electrodes with different polymer binders will be investigated. In the AST designed for metal catalyst degradation, the cell potential is varied between 0.6 and 0.9 V to oxidize and reduce and thus dissolve the platinum catalyst. Two different types of polymer binders will be compared: a standard PFSA (perfluoro-sulfonic acids) based binder and a new hydrocarbon-based binder polymer, sulfophenylated terphenylene copolymer (PEMION™, Ionomr Innovations Inc.). It is believed that the presence of the polymer and its influence on water accumulation has a strong effect on the platinum dissolution.

#### References

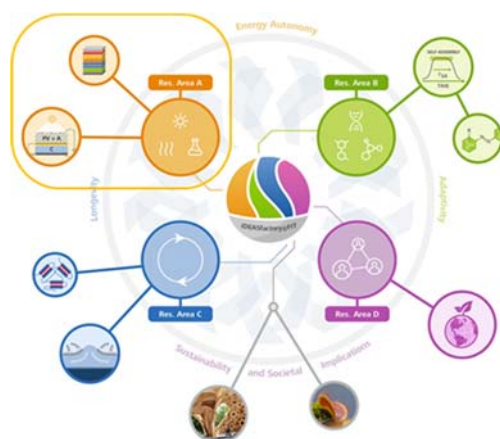
- [1] European Commission: Communication COM/2020/301: A hydrogen Strategy for a climate-neutral Europe, 2020
- [2] Bundesministerium für Wirtschaft und Energie (MWi), Die Nationale Wasserstoffstrategie, 2020
- [3] The Fuel Cell Technical Team, Fuel Cell Technical Team Roadmap, 2017. [https://www.energy.gov/sites/prod/files/2017/11/f46/FCTT\\_Roadmap\\_Nov\\_2017\\_FINAL.pdf](https://www.energy.gov/sites/prod/files/2017/11/f46/FCTT_Roadmap_Nov_2017_FINAL.pdf), accessed 1.12.2021
- [4] Marcinkoski, J. et al.: *Hydrogen Class 8 Long Haul Truck Targets* (US Department of Energy, 2019); [https://www.hydrogen.energy.gov/pdfs/19006\\_hydrogen\\_class8\\_long\\_haul\\_truck\\_targets.pdf](https://www.hydrogen.energy.gov/pdfs/19006_hydrogen_class8_long_haul_truck_targets.pdf), accessed 1.12.2021

## Integrated Photosupercapacitors based of Perovskite Solar Cells and Electrochemical Double Layer Supercapacitors

Taisiia Berestok,<sup>1,2,3</sup> Christian Diestel,<sup>1,2</sup>  
 Jan Büttner,<sup>1,2,3</sup> Niklas Ortlieb,<sup>1,2,3</sup>  
 Stefan Glunz,<sup>1,2,4,5,6</sup> Anna Fischer<sup>1,2,3,4</sup>

<sup>1</sup>Cluster of Excellence *livMatS* @ FIT – Freiburg Center for Interactive Materials and Bioinspired Technologies, University of Freiburg; <sup>2</sup>Freiburg Center for Interactive Materials and Bioinspired Technologies (FIT); <sup>3</sup>Institute for Inorganic and Analytical Chemistry (IAAC), University of Freiburg; <sup>4</sup>Freiburg Materials Research Center (FMF), University of Freiburg; <sup>5</sup>Department of Sustainable Systems Engineering (INATECH), University of Freiburg; <sup>6</sup>Fraunhofer ISE, Freiburg

Project funding: *livMatS* Cluster of Excellence “Living, Adaptive and Energy-autonomous Materials Systems” – Project A.1 - Funded by the Deutsche Forschungsgemeinschaft (DFG, German Research Foundation) under Germany’s Excellence Strategy – EXC-2193/1 – 390951807



© *livMatS* / Daniel Hellweg

The inorganic SolStore (*iSolStore*) project is running within the framework of the Cluster of Excellence *livMatS* at the University Freiburg and is part of the Research Area A, developing materials and systems concepts for energy autonomy.

The project focuses on the development of highly integrated solar-charging energy devices that can harvest, convert and store solar energy from their surroundings. The most promising way to realize such hybrid multi-functional systems at a high level of integration

is by using a monolithic three-electrode inter-connection scheme, with a shared/common electrode integrated at the interface between a photovoltaic (PV) unit, a solar cell, and an electrochemical storage unit, for example a battery or a supercapacitor – mode referred herein as integration mode II. In this case the charge carriers photogenerated by the solar cell under illumination migrate to and through the shared electrode, the latter simultaneously acting as charge acceptor electrode for the electrochemical storage unit. The two remaining electrodes are connected during photo-charging to close the circuit between the photovoltaic cell and the electrochemical storage unit (see Figure 1).<sup>1</sup>

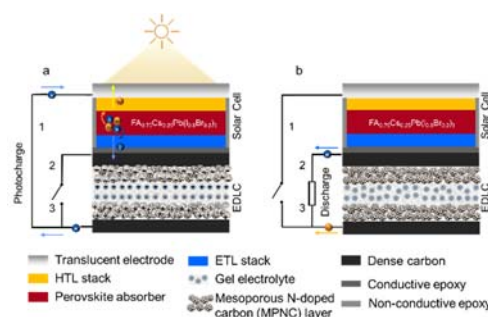


Fig. 1: Working principle of the device. Reproduced with permission from ref.1.

In mode II, depending on the type of electrochemical storage technology chosen, two types of devices are possible – mode II photo-batteries and mode II photosupercapacitors. To build such a device, one must take into consideration the compatibility of the chosen solar cell with the storage unit e.g. voltage mismatch, interfacial layers, chemical stability, etc. In this token, compared to batteries and pseudocapacitors, where charging is associated with a given redox process, electrochemical double layer capacitors (EDLCs) are much easier to integrate with solar cells, as they don’t require a given voltage for charging but rely on the build-up of the electrochemical double layer. Even if achievable energy densities are limited, EDLCs feature fast operation, voltage flexibility and high power densities compared to batteries and pseudocapacitors, which made them the system of choice in this project.

First, a proper architecture of the EDLC towards large energy and power density had to be defined. This included: (i) developing a proper 3D porous capacitive conductive material for high performance EDLCs, including its synthesis, characterization and optimization; (ii) designing and processing the supercapacitor electrodes out of it; and (iii) identifying the proper electrolyte that would provide high ionic conductivity especially in a gel state and at the same time would be compatible (in terms of stability) with the chosen solar cell.

As the EDLC electrode active material, we used mesoporous N-doped carbon nanospheres (MPNCs) produced via a hard-template synthesis, developed in the Fischer group.<sup>2,3</sup> The approach is based on aniline oxidative polymerization in the presence of SiO<sub>2</sub> nanoparticles as templates. This resulted in a highly monodisperse 140 nm MPNC particles with well-defined porous structure with ~7 nm mesopores and large specific surface area of 825 m<sup>2</sup>/g (Figure 2 a inset).

To process the developed MPNCs into suitable supercapacitor electrodes, we developed and optimized a doctor-blading procedure, which resulted in 3D porous electrodes with homogeneously packed MPNCs particles with potentially high electrolyte accessibility (Figure 2 a, b).

The produced electrodes were used to fabricate EDLC in a symmetric configuration using a semi-solid gel electrolyte, which reduced the overall device complexity, making any housing or packaging unnecessary and allowing a freestanding structure. The assembled MPNC-EDLCs showed an outstanding supercapacitive performance, featuring large capacitances up to 400 F/g at 0.5 A/g, energy densities up to 13.8 Wh/kg (10.4  $\mu$ Wh/cm<sup>2</sup>), power densities up to 14.8 kW/kg (11 mW/cm<sup>2</sup>), and a high charge/discharge Coulombic efficiency of 98 %.<sup>1</sup>

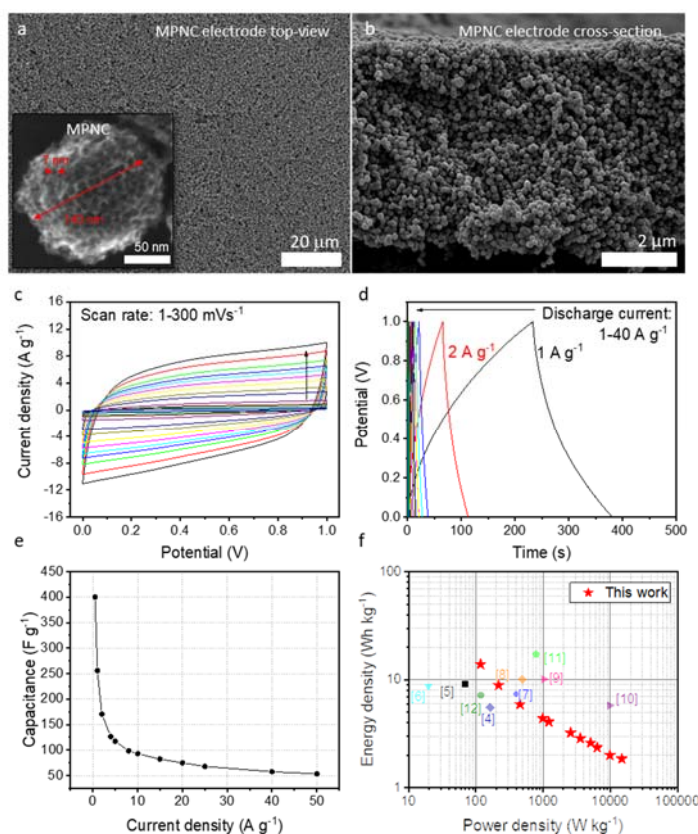


Fig. 2: SEM images in top-view (a) and cross-section (b) of an MPNC-based supercapacitor electrode. SEM image of an MPNC with a particle diameter of 140 nm and an average pore size of ~7 nm in the inset. Performance of the MPNC-EDLC: cyclic voltammograms (c); galvanostatic-charge-discharge experiments (d); dependence of the capacitance with the current applied (e). Ragone plot (f).<sup>4-12</sup> Adapted from ref.1 with permission.

As the photovoltaic device, we used  $\text{FA}_{0.75}\text{Cs}_{0.25}\text{Pb}(\text{I}_{0.8}\text{Br}_{0.2})_3$  perovskite solar cell (Area =  $1 \text{ cm}^2$ , Figure 3). Prior to the assembly we optimized the solar cell design with a layer sequence suitable for the integration and to protect the sensitive perovskite absorber from the electrolyte used in the supercapacitor. In addition, the utilization of a semi-solid gel-electrolyte in our MPNC-EDLC allowed to minimize the solar cell exposure to moisture and solvents. The solar cell showed a high  $V_{oc}$  of 1.08 V since this is a main driver for a high system performance of the photo-supercapacitor device, while the current  $J_{sc}$  is not limiting for most applications (Figure 3).

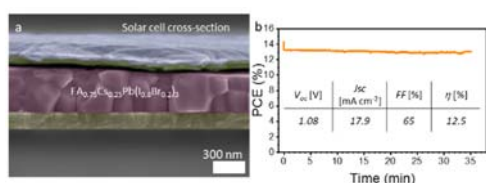


Fig. 3: Dependence of PCE of the solar cell with time (a). Scheme of the integrated photosupercapacitor device (b) and photocharge-discharge behavior at  $1 \text{ mA/cm}^2$  (f). Adapted from ref.1 with permission.

To assess the photoelectrochemical performance of such devices, a test station comprised of a potentiostat/galvanostat together

with a solar simulator were utilized to perform a set of measurements such as photocharging, photo-assisted charging as well as charging and discharging of the device.

The monolithic integration of the  $\text{FA}_{0.75}\text{Cs}_{0.25}\text{Pb}(\text{I}_{0.8}\text{Br}_{0.2})_3$  perovskite solar cell with the MPNC-EDLC resulted in a free-standing photosupercapacitor that could be photocharged up to 1 V in less than 5 s (upon illumination) and discharged on demand (Figure 4 a).<sup>1</sup> The device could deliver an energy density up to  $4.27 \text{ } \mu\text{Wh/cm}^2$  at a power density of  $0.29 \text{ mW/cm}^2$  and  $1.68 \text{ } \mu\text{Wh/cm}^2$  at  $2.2 \text{ mW/cm}^2$ , resulting in an unprecedented peak overall photoelectrochemical energy conversion efficiency of 11.5 %, which is higher than for the other few devices reported so far in which an EDLC is integrated with perovskite solar cell (Figure 4 b, c, d).<sup>1</sup> This only demonstrates the efficiency of our materials, devices and integration, paving the way towards photo-charging energy autonomous devices.

Ongoing work is focused on the integration of MPNC-based EDLCs with other types of solar cells, depending on the intended application.

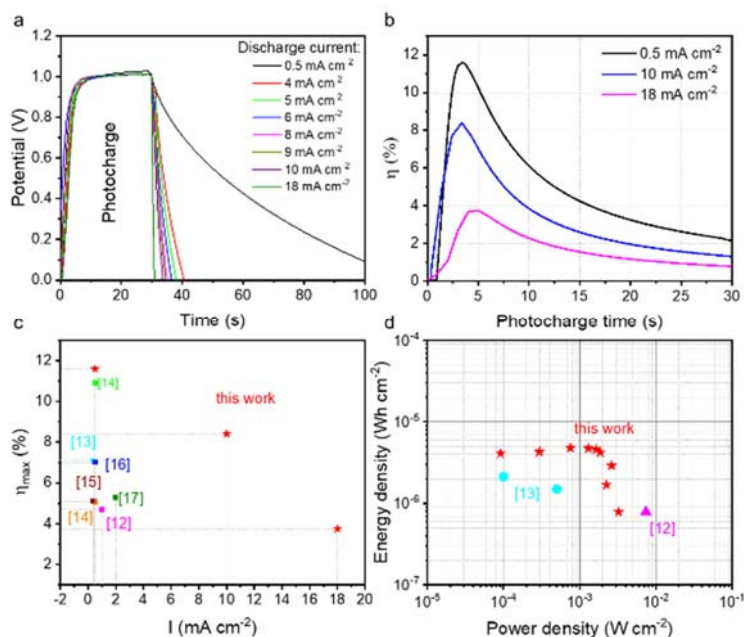


Fig. 4: Photocharge-discharge of the photosupercapacitors (a). Dependence of the overall photoelectrochemical energy conversion efficiency on photocharging time at different currents applied (b). Comparison of efficiencies of the photosupercapacitors (c). Ragone plot (d).<sup>13-17</sup> Adapted from ref.1 with permission.

## References

1. T. Berestok, C. Diestel, N. Ortlieb, J. Buettner, J. Matthews, P. S. C. Schulze, J. C. Goldschmidt, S. W. Glunz and A. Fischer, *Sol. RRL*, 2021, 5, 1–13.
2. J. Melke, R. Schuster, S. Möbus, T. Jurzinsky, P. Elsässer, A. Heilemann and A. Fischer, *Carbon N. Y.*, 2019, 146, 44–59.
3. J. Melke, J. Martin, M. Bruns, P. Hugenell, A. Schökel, S. M. Isaza, F. Fink, P. Elsässer and A. Fischer, *ACS Appl. Energy Mater*, 2020, 3, 11627.
4. Y. Qiu, M. Hou, J. Gao, H. Zhai, H. Liu, M. Jin, X. Liu and L. Lai, *Small*, 2019, 15, 1–10.
5. S. Liu, X. Chen, X. Li, P. Huo, Y. Wang, L. Bai, W. Zhang, M. Niua, Z. Li, *RSC Adv.* 2016, 6, 89744.
6. M. Li, J. Xue, *J. Phys. Chem. C* 2014, 118, 2507.
7. K. Liang, W. Wang, Y. Yu, L. Liu, H. Lv, Y. Zhang, A. Chen, *New J.Chem.* 2019, 43, 2776.
8. L. Sun, C. Tian, M. Li, X. Meng, L. Wang, R. Wang, J. Yin, H. Fu, *J. Mater. Chem. A* 2013, 1, 6462.
9. M. Liu, L. Liu, Y. Yu, H. Lv, A. Chen, S. Hou, *Front. Mater. Sci.* 2019, 13, 156
10. J. Zhou, T. Zhu, W. Xing, Z. Li, H. Shen, S. Zhuo, *Electrochim. Acta* 2015, 160, 152
11. B. Liu, L. Liu, Y. Yu, Y. Zhang, A. Chen, *New J. Chem.* 2020, 44, 1036.
12. L. F. Chen, X. D. Zhang, H. W. Liang, M. Kong, Q. F. Guan, P. Chen, Z. Y. Wu, S. H. Yu, *ACS Nano* 2012, 6, 7092.
13. J. Xu, Z. Ku, Y. Zhang, D. Chao, H. J. Fan, *Adv. Mater. Technol.* 2016, 1, 1.
14. J. Liang, G. Zhu, Z. Lu, P. Zhao, C. Wang, Y. Ma, Z. Xu, Y. Wang, Y. Hu, L. Ma, T. Chen, Z. Tie, J. Liu, Z. Jin, *J. Mater. Chem. A* 2018, 6, 2047.
15. J. Kim, S. M. Lee, Y. H. Hwang, S. Lee, B. Park, J. H. Jang, K. Lee, *J. Mater. Chem. A* 2017, 5, 1906.
16. J. Liang, G. Zhu, C. Wang, P. Zhao, Y. Wang, Y. Hu, L. Ma, Z. Tie, J. Liu, Z. Jin, *Nano Energy* 2018, 52, 239.
17. K. Gao, D. Ti, Z. Zhang, *Sustain. Energy Fuels* 2019, 3, 1937

## Understanding Electrocatalyst Dynamics under electrochemical conditions by In-Situ Electrochemical (Scanning) Transmission Electron Microscopy "In-Situ EC-(S)TEM"

S. Esmael Balaghi<sup>1,2</sup>; Anna Fischer<sup>1,2,3</sup>

<sup>1</sup>Institute for Inorganic and Analytical Chemistry (IAAC), University of Freiburg; <sup>2</sup>Freiburg Center for Interactive Materials and Bioinspired Technologies (FIT), University of Freiburg; <sup>3</sup>Freiburg Materials Research Center (FMF), University of Freiburg

Project funding: Volkswagen Foundation, Momentum, Project duration: 01.01.2021 – 31.12.2025

The "In-Situ EC-(S)TEM" project is dedicated to studying nanostructured energy materials for electrochemical energy conversion and storage under operational conditions at the nanoscale using in-situ electrochemical scanning transmission electron microscopy (EChem-(S)TEM).

Recent advances in the micro-fabrication of electrochemical devices and their combination with electron microscopy techniques have opened new horizons for studying the dynamic behavior of electrochemical energy materials at the nanoscale under in situ electrochemical conditions. In that context, EChem-(S)TEM studies on the dynamic behavior of (i) electrocatalysts for a wide range of reactions, including water electrolysis [1], electrocatalytic CO<sub>2</sub> reduction [2], and oxygen reduction in fuel cells [3], and (ii) battery materials for electrochemical energy storage [4] have recently been reported. The knowledge gained in such types of in-situ studies will improve the understanding of electrochemical materials "at operational condition" and therefore help to pave the way to design and manufacture materials with improved performance in terms of activity, storage capacity, and long-term stability.

The EChem-(S)TEM holder, which is going to be used in this Momentum project, contains a microelectromechanical system (MEMS) connected to a microfluidic pumping setup [5]. In the MEMS part, two silicon chips equipped with two electron-beam transparent silicon nitride windows (Figure 1) are stacked and used to build a vacuum-tight nanofluidic cell, which, once connected with the microfluidic pumping

system, can be filled and flowed with liquid electrolyte. To perform the electrochemical experiment, one of the silicon chips supports embedded electrodes, i.e., an electron transparent working electrode (WE in Figure 1), a counter electrode (CE in Figure 1), and a reference electrode (RE in Figure 1), all are in contact with the electrolyte. The electron transparent electrode, preferably carbon-based, then needs to be coated or contacted with the sample of interest in order to run an EChem-(S)TEM experiment.

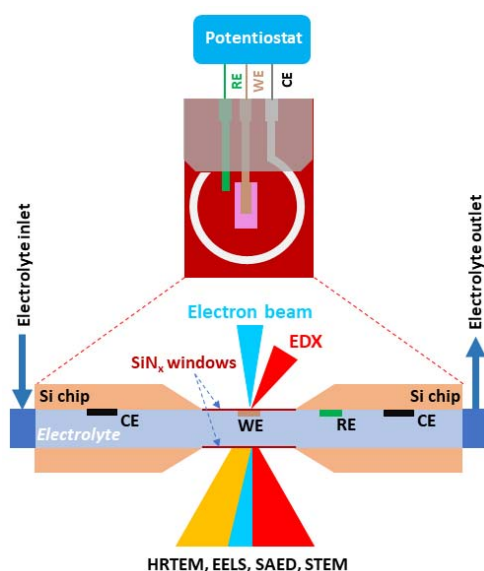


Fig. 1: Schematic view of an in-situ electrochemical liquid TEM holder. © Fischer Lab

This microfluidic MEMS setup allows to run a variety of electrochemical reactions inside the transmission electron microscope column and thereby investigate "quasi operando" a plethora of electrochemically active materials at the catalyst/electrolyte interface with different imaging and analytical techniques, including (scanning) transmission electron microscopy ((S)TEM), high-resolution transmission electron microscopy (HRTEM), electron diffraction (ED) and spectroscopic methods such as energy dispersive X-ray (EDX) and electron energy loss spectroscopy (EELS).

Most of the experiments will be performed at the Talos 200X microscope of the core facility "Imaging of materials systems" at FIT and will be complemented in cooperation if higher resolution and EELS measurements are required. The project "In-situ EC-(S)TEM" will focus on three classes of materials, including electrocatalysts for fuel cell reactions and electrolysis as well as battery materials with a particular focus on green battery systems.

#### References

- [1] N. Ortiz Peña, D. Ihiwakrim, M. Han, B. Lasalle-Kaiser, S. Carencio, C. Sanchez, C. Laberty-Robert, D. Portehault, O. Ersen, Morphological and Structural Evolution of Co<sub>3</sub>O<sub>4</sub> Nanoparticles Revealed by in Situ Electrochemical Transmission Electron Microscopy during Electrocatalytic Water Oxidation, *ACS nano* 13 (2019) 11372.
- [2] R.M. Arán-Ais, R. Rizo, P. Grosse, G. Algarsiller, K. Dembélé, M. Plodinec, T. Lunkenbein, S.W. Chee, B.R. Cuenya, Imaging electrochemically synthesized Cu<sub>2</sub>O cubes and their morphological evolution under conditions relevant to CO<sub>2</sub> electroreduction, *Nat. Commun.* 11 (2020) 3489.
- [3] V. Beermann, M.E. Holtz, E. Padgett, J.F. de Araujo, D.A. Muller, P. Strasser, Real-time imaging of activation and degradation of carbon supported octahedral Pt–Ni alloy fuel cell catalysts at the nanoscale using in situ electrochemical liquid cell STEM, *Energy Environ. Sci.* 12 (2019) 2476.
- [4] M. Yousaf, U. Naseer, Y. Li, Z. Ali, N. Mahmood, L. Wang, P. Gao, S. Guo, A mechanistic study of electrode materials for rechargeable batteries beyond lithium ions by in situ transmission electron microscopy, *Energy Environ. Sci.* 14 (2021) 2670.
- [5] Y. Yuan, K. Amine, J. Lu, R. Shahbazian-Yassar, Understanding materials challenges for rechargeable ion batteries with in situ transmission electron microscopy, *Nat. Commun.* 8 (2017) 15806.

## Simulation of S-based Li-ion batteries

Sunel de Kock,<sup>1</sup> Rolf Würdemann,<sup>2</sup> Michael Walter<sup>1-4</sup>

<sup>1</sup>Freiburg Center for Interactive Materials and Bio-inspired Technologies (FIT); <sup>2</sup>Freiburger Materialforschungszentrum, <sup>3</sup>Cluster of Excellence *iv*MatS @ FIT; <sup>4</sup>Fraunhofer IWM, Wöhlerstraße 11, D-79108 Freiburg

Project funding: German Research Foundation (DFG) SPP 2248 (DFG-Geschäftszeichen WA 1687/12-1)

As fossil fuel energy is replaced by renewable energy sources, the demand for energy storage increases unabatedly. Lithium-sulfur (Li-S) batteries are a highly promising energy storage technology due to their light weight, abundant active material, high theoretical capacity, and high energy density relative to existing Li-ion batteries.<sup>1</sup> Organic polymers with isolated redox-active sites are attractive materials for battery electrodes because of their structural tunability, solution-processability, the absence of heavy metals and possible commercial scale production.<sup>2,3</sup> Such redox polymers feature redox reactions at distinct potentials and, consequently, enable the construction of organic batteries with stable charge/discharge voltages. However, limitations exist in terms of specific capacities and energies.

Our project involves the design, synthesis, characterization (Chemnitz University of Technology) and theoretical modelling (University of Freiburg) of novel materials for Li-S batteries with additional organic redox couples, and their investigation using highly advanced in-operando X-ray spectroscopies (Physikalisch-Technische Bundesanstalt). Inverse vulcanization of sulfur with redox active divinyl monomers of varying redox potential will be done to produce sulfur/ comonomer networks in which additional charge can be stored on the redox active comonomer. The University of Freiburg contributes to these investigations by using DFT simulations to probe the stability and the electronic structure of the various species involved, as well as the prediction of NEXAFS and XES spectra on an absolute scale. With this joint theoretical and experimental project

we hope to gain an enhanced mechanistic understanding as well as more stable, and eventually more efficient, materials for both Li-S and organic batteries.

As a first step in our theoretical investigation, we developed a conformational sampling procedure to predict the lowest energy conformers of comonomer-capped S-chains and Li-polysulfide species. First, a set of conformers is generated with RDKit,<sup>4</sup> open source software for cheminformatics and machine learning. With the use of an API developed at FIT this is done within the Atomic Simulation Environment (ASE).<sup>5</sup> The conformers are then pre-optimized with GFN2-xTB,<sup>6</sup> a self-consistent tight-binding quantum chemical method (also available in ASE as an API). A smaller set is then selected from the lowest energy conformers for further optimization at the DFT level of theory, using the PBE functional<sup>7</sup> and GPAW<sup>8,9</sup> within ASE.

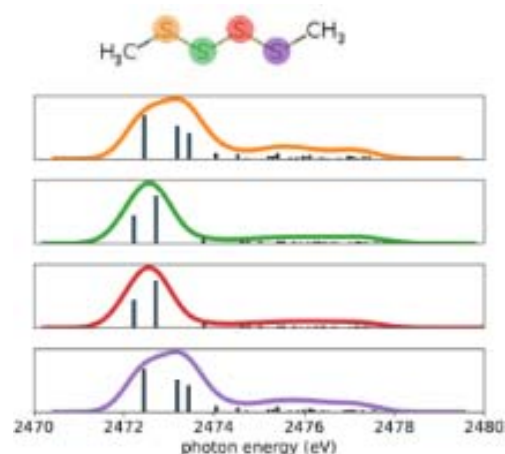


Fig. 1: X-ray absorption spectra of individual S atoms in S<sub>4</sub>(CH<sub>3</sub>)<sub>2</sub>. (© Functional Nanosystems Group)

Using the above method we determined the lowest energy conformers of methyl-capped S-chains containing 1 to 8 S atoms, and proceeded to calculate their x-ray absorption spectra with GPAW, applying a semiempirical correction<sup>10</sup> to attain the absolute x-ray photoelectron energies. Examining the atomic x-ray absorption spectra, it is easy to distinguish between terminal S atoms (bonded to C) and the internal S atoms (bonded only to S) (Fig. 1).

When the atomic spectra are summed (Fig. 2), two peaks may be identified (with sufficiently low line broadening) – the higher energy peak originates mostly from the terminal S atoms, while the higher energy peak has contributions from the terminal and internal S atoms. As the number of internal S atoms is increased, the lower energy peak grows, while the higher energy peak remains the same size. A linear relationship exists between the peak height ratios and the number of internal S atoms, allowing for the estimation of the number of S atoms in the chain. Fig. 2 also shows that the two most important features are visible up to a rather large unavoidable experimental broadening.

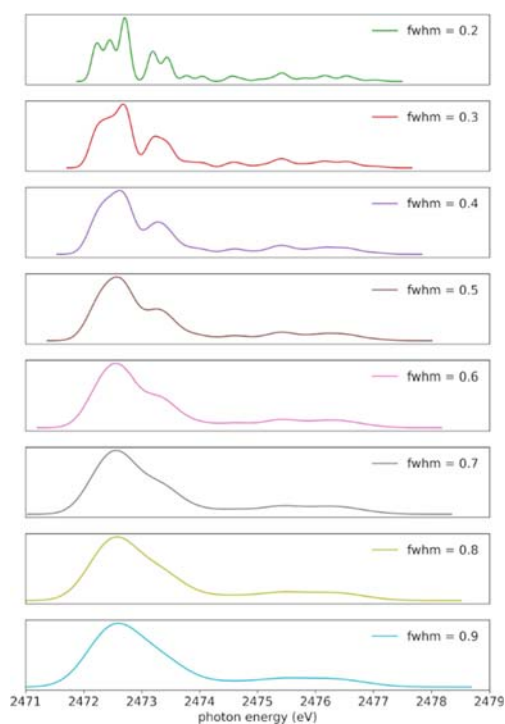


Fig. 2: X-ray absorption spectra of  $S_4(CH_3)_2$  with different degrees of line broadening applied. (© Functional Nanosystems Group)

Following the same procedure for the Li-poly-sulfides  $Li_2S_x$  ( $x = 2$  to  $8$ ), we again found that two peaks may be identified in the spectra corresponding to terminal and internal S atoms, with the terminal peak appearing at lower energy and the internal at higher energy, suggesting that the average S-content for these species may also be determined by the peak height ratio.

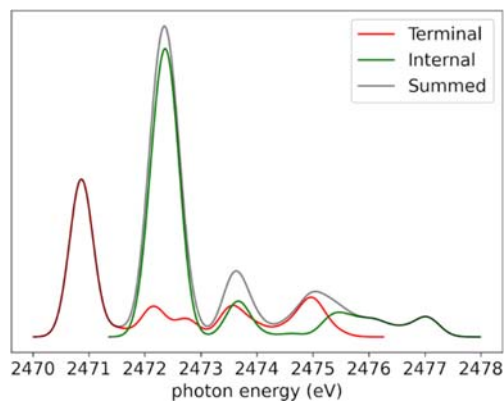


Fig. 3: X-ray absorption spectrum of  $Li_2S_4$ . (© Functional Nanosystems Group)

Most recently we have investigated the preferred conformations for  $Li^+$  attachment to methyl-capped S-chains, to shed light on the mechanism by which Li reacts to form Li-poly-sulfides. As this is a non-covalent interaction, RDKit is not suitable for generating conformers. Instead we made use of ASE to randomly attach Li to the S-chain species, followed by preoptimization with GFN2-xTB and further geometry optimization with PBE. It was found that the lowest energy conformers were those with multiple Li-S short contacts, especially with the terminal S atoms (Fig. 4). Li attachment in solvent is currently being investigated.

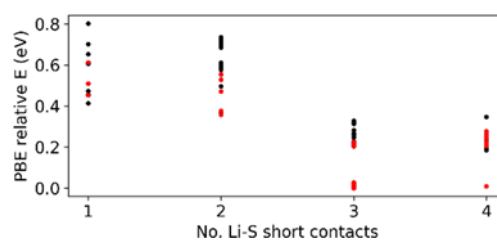


Fig. 4: Relative energy as a function of the number of Li-S short contacts, with terminal S contacts indicated in red. (© Functional Nanosystems Group)

## References

- [1] Z. Zeng & X. Liu, *Adv. Mater. Interfaces* 5, 1701274 (2018)
- [2] S. Muench, A. Wild, C. Friebe, B. Häupler, T. Janoschka & U.S. Schubert, *Chem. Rev.* 116, 9438 (2016)
- [3] T. Janoschka, M. D. Hager & U.S. Schubert, *Adv. Mater.* 24, 6397 (2012)
- [4] RDKit: Open-source cheminformatics; <http://www.rdkit.org>

[5] A.H. Larsen, J.J. Mortensen, J. Blomqvist, I.E. Castelli, R. Christensen, M. Duřak, J. Friis, M.N. Groves, B. Hammer, C. Hargus, E.D. Hermes, P.C. Jennings, P.B. Jensen, J. Kermode, J.R. Kitchin, E.L. Kolsbjerg, J. Kubal, K. Kaasbjerg, S. Lysgaard, J.B. Maronsson, T. Maxson, T. Olsen, L. Pastewka, A. Peterson, C. Rostgaard, J. Schiøtz, O. Schütt, M. Strange, K.S. Thygesen, T. Vegge, L. Vilhelmsen, M. Walter, Z. Zeng & K.W. Jacobsen, *J. Phys.: Condens. Matter* 29, 273002 (2017)

[6] C. Bannwarth, S. Ehlert & S. Grimme, *J. Chem. Theory Comput.* 15, 1652 (2019)

[7] J.P. Perdew, K. Burke & M. Ernzerhof, *Phys. Rev. Lett.* 77, 3865 (1996)

[8] J.J. Mortensen, L.B. Hansen & K.W. Jacobsen, *Phys. Rev. B* 71, 035109 (2005)

[9] J. Enkovaara, C. Rostgaard, J.J. Mortensen, J. Gavnholt, C. Glinsvad, V. Haikola & H.A. Hansen, *J. Phys. Condens. Matter* 22, 253202 (2010)

[10] M. Walter, M. Moseler & L. Pastewka, *Phys. Rev. B* 94, 041112 (2016)

## PGM-free Anode Catalysts and Improved Water Management in Anion Exchange Membrane Fuel Cell

Patrick Elsässer<sup>1,2,3</sup>, Jan Oechsler<sup>1,2,3</sup>, Jakob Salewsky<sup>1,4</sup>, Matthias Breitwieser<sup>1</sup>, Anna Fischer<sup>1,2,3,5</sup>, and Severin Vierrath<sup>1,4</sup>

<sup>1</sup>Freiburg Center for Interactive Materials and Bioinspired Technologies (FIT), University of Freiburg; <sup>2</sup>Inorganic Functional Materials, Institute for Inorganic and Analytical Chemistry, University of Freiburg; <sup>3</sup>Cluster of Excellence *livMatS @ FIT*, University of Freiburg; <sup>4</sup>Electrochemical Energy Systems, Laboratory for MEMS Applications, IMTEK, University of Freiburg; <sup>5</sup>Freiburg Materials Research Center (FMF), University of Freiburg

Project funding: Vector Stiftung, project "Alka-Cell"

Anion-exchange membrane fuel cells (AEM-FCs) are considered as a viable alternative to established proton-exchange membrane fuel cells (PEM-FCs). In contrast to PEM-FCs, AEM-FCs bare the inherent advantage that cheaper fluorine-free ionomers and abundant catalyst materials (such as iron-based at the cathode and nickel-based at the anode) can be used to form membrane-electrode assemblies. [1,2]

## Enhancing the HOR activity of NiMo/Carbon catalysts (Jan Oechsler, Patrick Elsässer, and Anna Fischer)

Due to the higher stability of non-precious group metals (non-PGM) in the alkaline environment, the expensive platinum at the anode can be replaced by other transition metals.[3] Among these non-PGM catalysts, nickel molybdenum alloys (NiMo) show promising activity towards the hydrogen oxidation reaction (HOR), since the alloying with Mo modifies the electronic structure of nickel and improves the hydrogen adsorption energy. [3,4]

Last year, a novel NiMo@N-C HOR electrocatalyst was developed using mesoporous N-doped carbon supports in our group. The high porosity and defined pore size of the supports increased the accessibility of the NiMo active species resulting in a 4-times increased HOR activity when compared to less porous polymer-derived NiMo@N-C catalysts reported first in this project (Fig. 2).

To further increase the HOR activity, the NiMo metal loading as well as the pore size of the supports were varied.

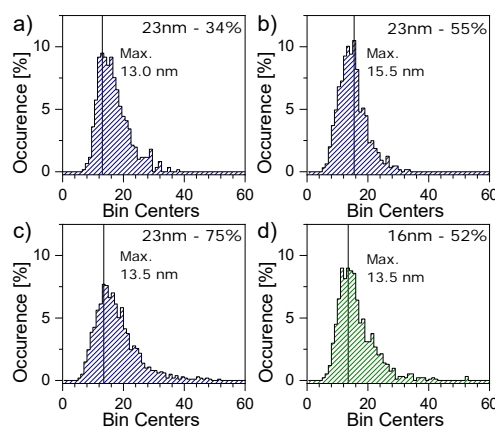


Fig. 1: STEM particle size distributions of NiMo@N-C-23 with a) 34wt.%, b) 55wt.%, and c) 75wt.% metal loading. (© Fischer group)

**Effect of metal loading:** First, the metal loading on the carbon support with an average pore size of 23 nm was varied between 34 wt.%, 55 wt.% and 75 wt.%. For 34 wt.% and 55 wt.%, catalysts with highly distributed NiMo alloy nanoparticles (NP) with comparable particle size distributions (SEM-derived, Fig. 1) and an average crystallite size of

~17 nm (XRD-derived), and high surface areas (~200-600 m<sup>2</sup>/g) were obtained, while for 75 wt%, lower surface area (~200 m<sup>2</sup>/g), a broader particle size distribution, and an average NiMo crystallite size of ~26 nm (XRD-derived) due to NP agglomeration and growth were received.

Increasing the NiMo metal loading from 34 wt.% to 55 wt.% resulted in a 1.6-times higher HOR activity (see Fig. 2), in line with the 1.6-times higher metal loading. However, further increasing the metal loading resulted in a lower HOR activity, in line with NiMo NPs agglomeration and loss of electrochemical active surface area.

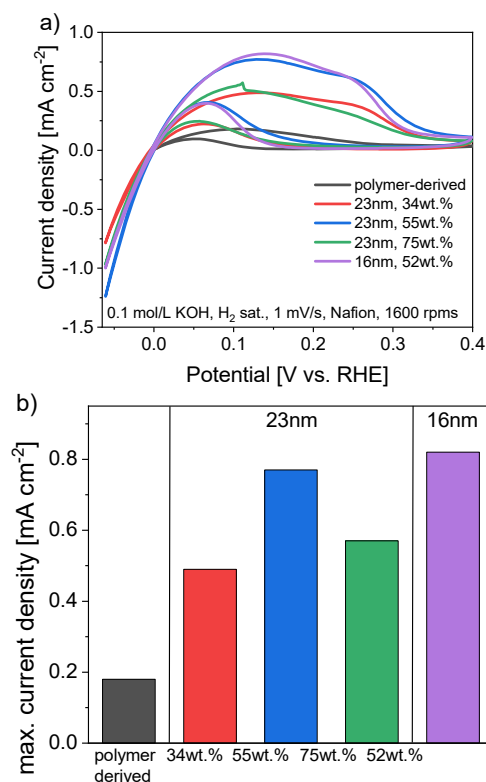


Fig. 2: a) Cyclic voltammograms and b) maximum current densities of polymer-derived NiMo@N-C catalyst (black) and NiMo@N-C catalysts with different metal loadings and pore sizes. (© Fischer group)

**Effect of pore size:** The influence of the pore size of the supports on the resulting NiMo NP size distribution, accessibility and HOR activity, was investigated. For this, supports with pore sizes of 23 nm and 16 nm were used. Decreasing the pore size from 23 to 16 nm while maintaining a metal loading between 55 and 52 wt.%, resulted in a catalyst with slightly

higher surface area (~450 m<sup>2</sup>/g), comparable NiMo particle size distributions (SEM-derived, Figure 1) and an average crystallite size of 18 nm (XRD-derived), and hence comparable HOR activity (Fig. 2).

The next steps towards increasing the HOR activity are the optimization of the particle dispersion and size distribution on the porous carbon supports, and the synthesis of new Ni-containing materials.

**Improving the water management with hydrophilic metal oxide additives** (Jakob Salewsky, Matthias Breitwieser, Severin Vierath)

The advantages of AEMFCs come with several technical hurdles, which still require further investigation. In particular the water management in AEMFCs is particularly delicate and more complex than in PEMFCs: On the cathode side water is consumed to generate the OH<sup>-</sup> charge carrier in the presence of water and oxygen gas. On the anode side, the OH<sup>-</sup> charge carrier reacts with H<sub>2</sub> to liquid water. Given this water consumption and generation in the MEA, the balance of humidification in the cell is very challenging [5]. E.g., a dry-out on the cathode side can cause irreversible degradation of ionic conductivity, whereas flooding on the anode electrode may result in undesired gas transport losses towards the active catalyst sites [6].

In our work, we approach this problem by increasing the hydrophilicity of the cathode electrode. By integrating low amounts of hydrophilic metal oxide nanoparticles (antimony-doped tin oxide, ATO) we were able to maintain more water inside the cathode layer to prevent dry out and thus irreversible loss of functionality.

In Fig. 3, TEM and STEM/EDX images of the catalyst aggregates are shown. It can be seen that the ATO nanoparticles are dispersed within the Pt/C catalyst particles and the content scales with the wt% of ATO.

The contact angle of the cathode electrodes scales strongly with the amount of ATO in the electrode as additive. As expected, the addition of hydrophilic metal oxides improves the

wettability of the electrodes. This trend is confirmed in the in-situ fuel cell characterizations. Fuel cells were assembled by using the direct membrane deposition approach [7,8] to enable a very low total membrane thickness of only about 5  $\mu\text{m}$ .

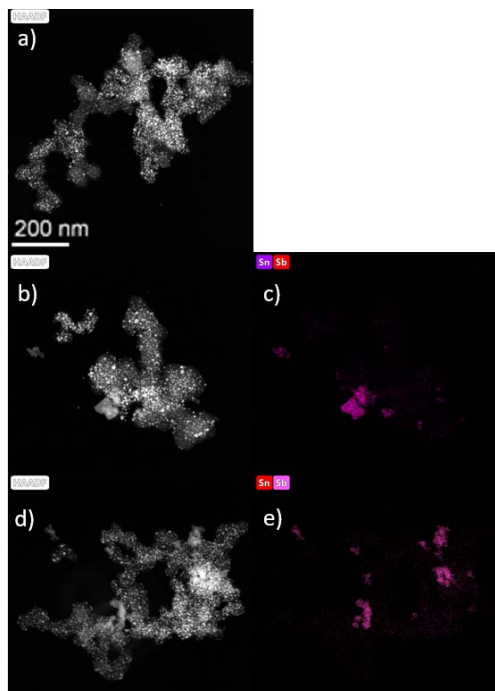


Fig. 3: representative TEM imaging and STEM-EDX measurements of the high-angle annular dark field (HAADF) of catalyst aggregates (Sb signal): a) 0% ATO, b) 4wt% ATO, c) 10 wt% ATO. (© Vierrath group)

In Fig. 4, performance of single cells is reported. The baseline sample achieves a peak power density of about 1.4  $\text{W}/\text{cm}^2$ , which is in line with typical AEMFC results with commercially available ionomers. The addition of ATO clearly lower the ohmic resistance of the fuel cells, as can be seen in Figure 4c) over the entire range of current density

Table 1: Overview on contact angle measurements of standard cathodes without ATO and ATO-loaded electrodes

standard cathode	4% ATO	10% ATO
<b>89.9°</b>	57.2°	58.8°

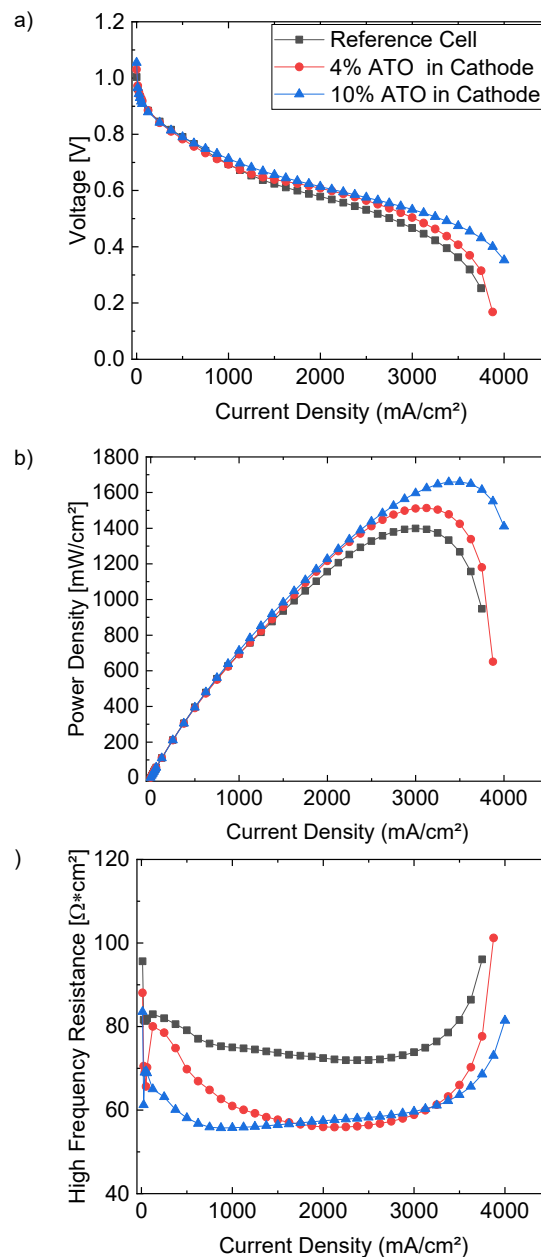


Fig. 4: Electrochemical data from single cell evaluation. a) polarization data I/V, b) polarization data I/P, c) evolution of the ohmic resistance, measured by impedance spectroscopy (high frequency resistance, HFR). Cell operation conditions:  $\text{H}_2/\text{O}_2$ , 100 % RH, 300/300 kPa absolute operation pressure. (© Vierrath group)

In particular at low current densities (low water consumption rate in cathode), the HFR is significantly lower for the 10 wt% sample, confirming the positive impact of the hydrophilic ATO onto the humidification and thus ionic conductivity within the membrane-electrode-assembly. As the contribution of ATO to the electrical conductivity of the catalyst layer is negligible (measurements not included here) and all other cell components (membrane

thickness, choice of gas diffusion media etc.), the observed differences in HFR can only be related to improved water management. This is reflected in the increased cell performance shown in Figure 4b).

In this work, a novel way to encounter the know issue of cathode dry-out in AEM fuel cells was developed. The integration of ATO as dispersed nanoparticle additive enabled an improvement of the electrode wettability, which enabled lower ionic resistances and finally higher cell performances in in-situ single cell diagnostics.

#### References

- [1] Truon, V.M., Tolchard, J., ..., Barnett, A.O., *Energies*, 2020, 13, 582
- [2] Firouzjaie, H.A., Mustain, W.E., *ACS Catal.*, 2020, 10, 225-234.
- [3] Sheng, W., Bivens, A.P., ..., & Yan, Y., *Energy Environ. Sci.*, 2014, 7, 1719
- [4] Davydova, E., Lemire, K., ..., & Dekel, D., *J. Mater. Chem. A*, 2017, 5, 24433
- [5] Gottesfeld, S., Dekel, D. R., Page, M., Bae, C., Yan, Y., Zelenay, P., & Kim, Y. S. (2018). *Journal of Power Sources*, 375, 170-184.
- [6] Omasta, T. J., Park, A. M., LaManna, J. M., Zhang, Y., Peng, X., Wang, L., ... & Mustain, W. E. (2018). *Energy & Environmental Science*, 11(3), 551-558.
- [7] Klingele, M., Breitwieser, M., Zengerle, R., & Thiele, S. (2015). *Journal of Materials Chemistry A*, 3(21), 11239-11245.
- [8] Veh, P., Britton, B., Holdcroft, S., Zengerle, R., Vierrath, S., & Breitwieser, M. (2020) *RSC Advances*, 10(15), 8645-8652

## ThermoBatS – Thermoelectric Battery Systems

Swathi Krishna Subhash<sup>1,3</sup>, Uwe Pelz<sup>1,3</sup>, Harald Hillebrecht<sup>2,3</sup>, Peter Woias<sup>1,3</sup>

<sup>1</sup>Laboratory for the Design of Microsystems, Dept. of Microsystems Engineering (IMTEK); <sup>2</sup>Laboratory for Solid State Chemistry, Faculty of Chemistry and Pharmacy; <sup>3</sup>Cluster of Excellence *livMatS* @ FIT – Freiburg Center for Interactive Materials and Bioinspired Technologies Bioinspired Technologies (FIT), University of Freiburg

Project funding: Funded by the Deutsche Forschungsgemeinschaft (DFG, German Research Foundation) under Germany's Excellence Strategy – EXC-2193/1 – 390951807

The *livMatS* project ThermoBatS is part of the thermal energy thrust in research area A and aims at harvesting this abundant and easily accessible form of energy by developing a micro-thermoelectric generator ( $\mu$ TEG) with two different phase change materials (PCM) on both sides, acting as heat reservoirs. This package will be capable of powering e.g. a small sensor or being used as a sensor itself. Thermoelectric generators (TEG) in general are, based on the Seebeck effect, able to generate an electric voltage when subjected to a temperature difference. The integration of the  $\mu$ TEG together with PCMs in a  $\mu$ TEG-PCM stack enables the  $\mu$ TEG to create its own temperature difference for a short amount of time, making time dependent temperature fluctuations (e.g. by the daylight cycle) accessible for the harvester.

The fabricated ThermoBatS  $\mu$ TEG in Fig. 1a is based on ball milled *nano*-Bi<sub>2</sub>Te<sub>3</sub> in double sided PCB housing. The substrate was pre-structured using laser micromachining, followed by filling the holes via dispensing formulated thermoelectric paste and compacting via hot-pressing. Forming the upper contact by lithography and copper etching resulted in the final  $\mu$ TEG with 8 thermocouples.

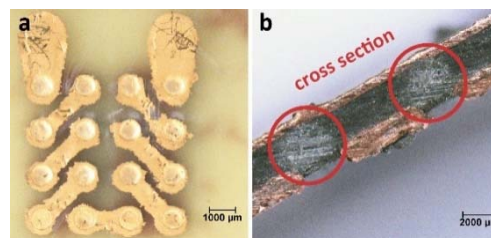


Fig. 1: a) ThermoBatS 10 x 10 mm<sup>2</sup>  $\mu$ TEG; b) Cross section view of the  $\mu$ TEG with TEG legs marked with red circles (both © IMTEK/Laboratory for Design of Microsystems)

In a parallel study the development of PCM- $\mu$ TEG stacks was started. Phase change materials (PCMs) are latent heat storage systems, which release or absorb large amounts of heat during phase transition, while keeping the temperature at a constant level. Integrating two dissimilar PCMs on the top and bottom of the  $\mu$ TEG will allow thermal energy harvesting twice per natural thermal cycle (e.g. day-night).

Preliminary investigations were carried out on commercially available organic PCMs. Four PCMs of different transition temperatures were obtained from CRODATHERM, and tested with multiple heating and cooling cycles. Primary observations concluded ineffective heat transfer through the PCM, phase separation and long charging discharging cycle time as a consequence of low thermal conductivity of these PCMs. An additional challenge with these PCMs are volume shrinkage during the solidification process.

For an effective heat transfer and improved performance of PCMs, low thermal conductivity needs to be addressed. The measured thermal conductivity values for the pure PCMs are in the range of 0.14 – 0.16 W/mK. We employed shavings of three different metals, Aluminium, brass and copper as thermal conductivity enhancers (TCEs). The results are listed in Table 1. The most promising results were obtained with copper shavings with an enhancement of more than two-fold with only a 4 % v/v addition. However, the goal is to achieve a thermal conductivity above 1 W/mK either with increased volume of TCEs or an alternative high thermally conductive PCM. Both approaches are under investigation at the moment.

Table 1: Thermal conductivity measurement of PCM37, pure and with three different metal TEs.

	<b>PCM 37</b>	<b>+ Al</b> (8.8%)	<b>+ Brass</b> (26.8%)	<b>+ Cu</b> (4%)
Th. Con- ductivity in W/mK	0.1682 ± 0.0009	0.355 ± 0.001	0.434 ± 0.001	0.412 ± 0.001

FUTURE FIELD “NEW MATERIALS: SOCIETAL CHALLENGES“

### Multimethod approach to assess Cognitive-Affective Maps for changing attitudes – A quantitative validation study

Wilhelm J. Gros<sup>1,2</sup>, Julius Fenn<sup>2</sup>, Sabrina Livanec<sup>1,2</sup>, Lisa Reuter<sup>1,2</sup>, Michael Stumpf<sup>1,2</sup>, Andrea Kiesel<sup>1,2</sup>

<sup>1</sup>Cluster of Excellence *livMatS*, University of Freiburg; <sup>2</sup>Institute of Psychology, University of Freiburg

Project funding: Funded by the Deutsche Forschungsgemeinschaft (DFG, German Research Foundation) under Germany's Excellence Strategy – EXC-2193/1 – 390951807

A Cognitive-Affective Map (CAM) is a concept graph that is able to represent cognitions and affective assessment of somebody's point of view (please see Fig. 1 for an example). A huge advantage of CAMs is that they enable to comprehensibly depict attitudes of individuals towards a specific topic. Up to now, we assessed the suitability of CAMs to assess individual attitudes and experiences [1,2,3]. In this current project, we extended the scope of CAMs. Specifically, we aimed to explore the impact that a close consideration of somebody else's CAM might have on the own attitude towards an ambivalent topic.

In detail, we elaborated the potential to change somebody's point of view just by elaborating an opposing CAM of another person. To examine this potential of CAMs, our participants first drew an own CAM on a controversial topic, i.e. a fictional technological implant to control the sleep-wake cycle. Such an implant could be used for good (e.g. mitigating sleep disorders, optimizing energy balance, replacing drugs) or bad (surveillance, class division, abuse by employers) as well which induced rich and controversial CAMs. A week later, participants of the experimental group were asked to explore a CAM with a different attitude as their own. Specifically participants who drew a CAM of positive affective connotation at the first measurement time point elaborated a negative CAM and vice versa. After

this, the participants drew a second CAM. A control group only elaborated their first CAM.

To measure attitude changes, we assessed differences in the CAMs at the two measurement time points. In addition, participants filled in a modified version of the established Technology Acceptance Model 3 (TAM3) questionnaire to validate our findings with a standard method.

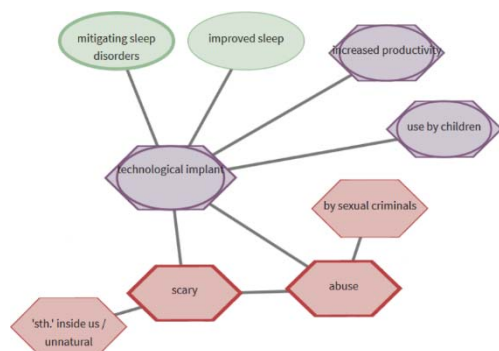


Fig. 1: Excerpt of the negative CAM which was presented to participants who drew a positive CAM at the first measurement time point. (© livMatS)

Participants were recruited at prolific.co. Single inclusion criterion was English as first language, since we used a demanding scenario text and difficult items. The participants predominantly answered from the United Kingdom (N = 56). Out of 90 participants at the first measurement time point, we managed to keep 75 participants at the second measurement time point resulting in a dropout rate of 16.6%. 18 participants of the experimental group (N = 35) drew a positive CAM, 17 participants drew a negative CAM and the control group consisted of 40 participants. The mean age was 32.69 years (SD = 12.14), while ranging from 19 to 72. We had 46 male participants, 28 female and one intersex.

Analyses of the CAMs and the questionnaire data confirm the potential of CAMs to change the attitude of an observer: The pre-post difference concerning the CAM's average valence was larger in the experimental group than in the control group. And the pre-post difference concerning the TAM3's aggregated score was larger in the experimental group than in the control group. This means, that the elaboration of a CAM of opposite affective

connotation was able to change the point of view of the participants in the experimental group. The TAM3 questionnaire provided a first hint at the validation of CAMs for the purpose of opinion change.

References

[1] Mansell, J., Reuter, L., Rhea, C., & Kiesel, A. (2021). A Novel Network Approach to Capture Cognition and Affect: COVID-19 Experiences in Canada and Germany. *Frontiers in Psychology*, 12, 2082. <https://doi.org/10.3389/fpsyg.2021.663627>

[2] Reuter, L., Fenn, J., Bilo, T. A., Schulz, M., Weyland, A. L., Kiesel, A., & Thomaschke, R. (2021). Leisure walks modulate the cognitive and affective representation of the corona pandemic: Employing Cognitive-Affective Maps within a randomized experimental design. *Applied Psychology: Health and Well-Being*, 13(4), 952-967. <https://doi.org/10.1111/aphw.12283>

[3] Reuter, L., Mansell, J., Rhea, C., & Kiesel, A. (2021). Direct Assessment of Individual Connotation and Experience: An Introduction to Cognitive-Affective Mapping. *Politics and the Life Sciences*. <https://doi.org/10-1017/pls.2021.31>

**Tiered Approach for Prospective Assessment of Benefits and Challenges (TAPAS)**

Rainer Grießhammer<sup>1,2</sup>,  
Martin Möller<sup>2,3</sup>

<sup>1</sup> Faculty of Environment and Natural Resources of the University of Freiburg,  
<sup>2</sup>Cluster of Excellence livMatS @ FIT Freiburg Center for Interactive Materials and Bioinspired Technologies, University of Freiburg, Germany and <sup>3</sup>Öko-Institut e.V. – Institute for Applied Ecology, Freiburg

Project funding: Funded by the Deutsche Forschungsgemeinschaft (DFG, German Research Foundation) under Germany's Excellence Strategy – EXC-2193/1 – 390951807

The ultimate goal of the project is the design of a new interdisciplinary development-integrated sustainability assessment method. It can be characterized as a heuristic-systematic approach that aims to pose the "right" questions at early stages of technology development as well as to assess sustainability at later stages (demonstrators, applications). At any stage, TAPAS develops recommendations in order to accompany and enhance the livMatS developments.

TAPAS acts as a strategic radar and assessment methodology within *livMatS* for the cross-cutting topic of “Resilience and Sustainability”, which shows guiding boundaries and recommends shifts to more sustainable options. Regarding the methodology’s key aspects and functionalities, TAPAS aims to detect existing chances and opportunities as well as challenges and possible threats that may be associated with novel living materials systems. Thus, the method serves both as an “early warning system” for less sustainable options and as an “early encouraging system” for favorable paths of innovation. As part of the overall approach TAPAS operationalizes relevant normative settings for the sustainability assessment. In particular, this refers to the 2030 Agenda with its 17 Sustainable Development Goals (SDGs) [1] and the concept of Planetary Boundaries [2].

After having completed the review of existing assessment systems regarding sustainability issues of technology / product development, the fundamentals of the TAPAS framework have been outlined. Major guiding principles for the tiered approach and suitable tools for the various iteration steps have been published in the journal "TATuP" in March 2021 together with several co-authors from the *livMatS* cluster [3].

In addition, responses to the challenges of the Anthropocene were highlighted from the perspective of sustainability research for a publication in the journal "Elementa" [4], based on a fruitful interdisciplinary exchange in the *livMatS* cluster between Area C and Area D. As part of the “early warning system”, a prospective assessment of “substances of very high concern” was described, inter alia.

Building on the foundations of the "TATuP" publication, the methodological description for a detailed benefit analysis representing the “early encouraging system” was submitted for publication in the "Journal for Industrial Ecology" [5]. With this approach, a set of indicators was developed for the first time that allows the assessment of societal benefits with regard to the 2030 Agenda, its 17 SDGs as well as the 169 SDG targets.

Furthermore, TAPAS also mirrors ongoing transformation processes in major areas of need and identifies their implications with regard to the research activities in *livMatS*. Based on a review of the current state of knowledge with regard to the early sustainability assessment of technologies, the example of the energy sector was used in a further publication [6] to discuss how analyzing the determinants of ongoing transformation processes can contribute to the further development of the technology assessment framework in order to ensure an agile, targeted and future-proof assessment system.

Currently, ongoing work in the project is focusing on testing the applicability and usefulness of the TAPAS framework on the basis of actual material developments in the *livMatS* cluster. The testing covers the tools of prospective chemicals assessment, benefit analysis as well as orienting life cycle assessment studies and is carried out in close cooperation with two projects from Area A (SolStore and ThermoBatS). Preliminary results have already yielded concrete recommendations for the substitution of critical substances and materials in the above-mentioned projects.

#### References

- [1] United Nations (2016): Report of the Inter-agency and Expert Group on Sustainable Development Goal Indicators, see also: <https://unstats.un.org/unsd/statcom/48th-session/documents/2017-2-IAEG-SDGs-E.pdf>
- [2] Rockström, J., Steffen, W., Noone, K. et al., (2009): A safe operating space for humanity. *Nature* 461(7263): 472–475. DOI: 10.1038/461472a
- [3] Möller, M., Höfele, P., Reuter, L., Tauber, F., & Griebshammer, R. (2021): How to assess technological developments in basic research? Enabling formative interventions regarding sustainability, ethics and consumer issues at an early stage. *TATuP – Journal for Technology Assessment in Theory and Practice*, 30(1), 56-62. DOI: 10.14512/tatup.30.1.56
- [4] Möller, M., Höfele, P., Kiesel, A., Speck, O. (2021): Reactions of sciences to the Anthropocene: Highlighting inter- and transdisciplinary practices in biomimetics and sustainability research. *Elementa Science of the Anthropocene* 8(1). DOI: 10.1525/elementa.2020.035
- [5] Möller, M. & Griebshammer, R. (2021): Product-related benefit analysis based on the Sustainable Development Goals – integrating the voice of society into Life Cycle Sustainability Assessment. *Journal for Industrial Ecology* (submitted).

[6] Möller, M. & Griebhammer, R. (2021): Prospective technology assessment in the Anthropocene - transition towards a culture of sustainability. The Anthropocene Review, special edition 'Nature in the Anthropocene' (in print).

### CORE FACILITY "FUNCTIONAL PROCESSING"

#### **A Soft Biomimetic Actuator Inspired by the Self-Sealing Motion of Succulent Plants**

Claas Müller<sup>1,2</sup>, Jing Becker<sup>2</sup>, Olga Speck<sup>1,3</sup>, Thomas Speck<sup>1,3</sup>

<sup>1</sup>Cluster of Excellence *livMatS* @ FIT – Freiburg Center for Interactive Materials and Bioinspired Technologies; <sup>2</sup>Department of Microsystems Engineering – IMTEK, University of Freiburg; <sup>3</sup>Plant Biomechanics Group (PBG) Freiburg, Botanic Garden; University of Freiburg

Project funding: Funded by the Deutsche Forschungsgemeinschaft (DFG, German Research Foundation) under Germany's Excellence Strategy – EXC-2193/1 – 390951807

This collaborative project between botanists and engineers is a *livMatS* booster project in Area C (Longevity) and Demonstrators. The goal of this project is to develop a biomimetic bending actuator for soft robots inspired by the self-sealing deformation of the succulent leaves of *Delosperma cooperi* (Fig. 1).

In this study, we focus on the functional principle of the mechanically driven leaf movement after an injury [1,2], which we transfer to shape memory polymer (SMP) based multilayer systems. By utilizing the shape memory effect of the SMP thin films, process-induced stress would be easily built up into the polymer based soft multilayer systems. This flexible multilayer structure, which is a fully soft polymer mechanism, will work as a bending actuator based on the minimum energy mechanism. Similar to the plant leaf, multi-layer SMP/elastomer materials system can bend after an external damage. The plant-inspired movement can serve as an actuator or controller of a technical mechanism or system, or alternatively, the deformation can bring damage-related areas

close together that a subsequent chemical reaction completely heals the crack. In terms of engineering, it is desirable to find a simple technique, which is not only capable of preparing various polymeric single- and multi-layers, but also to tailor the structures and properties of the layers in order to fulfill the functional requirements of the whole bio-inspired materials systems and to simulate the self-sealing deformation of the succulent leaves of *Delosperma cooperi*.



Fig. 1: Stand of Pink Carpet (*Delosperma cooperi*) in the outdoor area of the Botanic Garden Freiburg. The succulent leaf shows a permanent deformation after sealing and healing of an external damage. © Plant Biomechanics Group Freiburg

#### References

- [1] O. Speck, M. Schlechtendahl, F. Borm, T. Kampowski, T. Speck (2018): Humidity-dependent wound-sealing in succulent leaves of *Delosperma cooperi* – An adaptation to seasonal drought stress. *Beilstein J Nanotech* 9: 175–186. DOI: 10.3762/bjnano.9.20
- [2] W. Konrad, F. Flues, F. Schmich, T. Speck, O. Speck (2013): An analytic model of the self-sealing mechanism of the succulent plant *Delosperma cooperi*. *J. Theor. Biol.* 336: 96-109. DOI: 10.1016/j.jtbi.2013.07.013

CORE FACILITY "MODELLING AND SIMULATION OF MATERIALS SYSTEMS"

## Force dependence activation energy for C-S and S-S bond

Wafa Maftuhin<sup>1</sup>, Michael Walter<sup>1,2,3</sup>

<sup>1</sup>Freiburg Center for Interactive Materials and Bio-inspired Technologies (FIT); <sup>2</sup>Cluster of Excellence livMatS @ FIT; <sup>3</sup>Fraunhofer IWM, Wöhlerstraße 11, D-79108 Freiburg

Project funding: German Research Foundation (DFG) – WA 1687/11-1)

Disulfide bonds are known to cross-link polymer networks [1] and disulfide bond loops are also found in proteins. The stability of these bonds is strongly connected to their environment [2]. Disulfide bond breaking is perceived as an important factor in the control of the activity in many proteins and polymer networks such as in self-healing materials [3], sustainable materials and so on. Despite that many studies suggest a S-S bond breaking mechanism in the proteins, low-energy collision induced dissociation (CID) gas-phase experiments could not discover S-S bond rupture due to the higher activation energy as compared to C-S bond [4]. Minor cleavage of C-S bonds also found in gas-phase ionic collisions of model peptides and insulin by mass spectrometry [5]. The overall mechanism of disulfide bond breaking is therefore rather complex and still under debate in the literature.

Research on the mechanochemistry of disulfide bonds has provided key understanding into the coupling between mechanical force and chemical reactivity. Force atomic force microscopy (AFM) experiments by Fernandez et al. [6], measured force induced disulfide bond reduction rates in the range of pulling forces up to 2.0 nN and detected an instantaneous change in the reactivity of the S-S bonds with hydroxide anions (OH<sup>-</sup>) at forces of about 0.5 nN, where the increase of the reaction slows down after 0.5 nN. Several possible scenarios for this effect are discussed, such as the stretching dihedral angle of C-S-S-C to 180° thus exposing the sulfur atoms for an attack by OH<sup>-</sup> (S<sub>N</sub>2 attack), the influence of trimolecular reactions or breaking of the C-S bond.

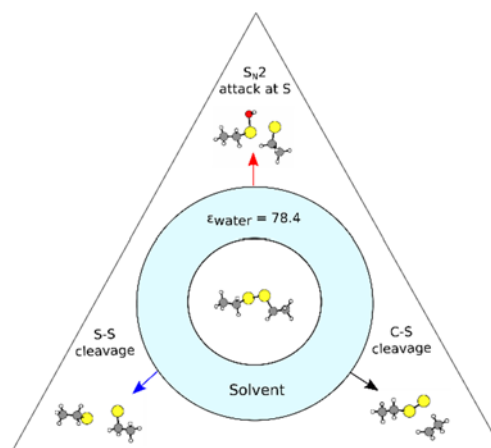


Fig. 1: Scheme of the three different pathways for bond cleavage considered in this study. S: yellow, C: grey, O: red, H: white. (© Functional Nanosystems Group)

It is difficult to analyze the intermediates states and reaction products even in single-molecule AFM experiments, such that the support of theoretical investigations is needed. Haufbauer and Frank [7] studied disulfide bond under mechanical stress using Car–Parrinello molecular dynamics (CPMD) calculations and observed that the bond rupture can arise both from S-S or C-S bonds and did not favor the idea of a nucleophilic attack on the disulfide bonds. In the other hand, Doperalski et al. [8], [9] found in a similar study, that the mechanical force leads to a rotation of the S-S-C-C bond. This study did not support the idea of C-S bond breaking as the activation energy of C-S bond was found to be always higher than that of the S-S bond. They explained the decreased reaction rate for larger forces by a conformational change induced by the force applied. The involved the S-S-C-C dihedral angles get shielded against nucleophilic attack. The study applied computationally expensive large scale ab-initio molecular dynamics calculations.

In this report, we investigate the force dependence activation energy of C-S and S-S bonds and the role of hydroxide anions on disulfide bond reductions by using combination of density functional theory (DFT) with straightforward, reliable, and efficient extension of the constrained geometry of external force (CO-GEF) method.

Potential energies are calculated within DFT as implemented in GPAW software [10], [11], the exchange correlation (XC) potential is modeled as revised Perdew, Burke and Ernzerhof (PBE) [12] within the spin-restricted Kohn-Sham formalism. The aqueous environment is described by continuum solvent model (CSM) [13].

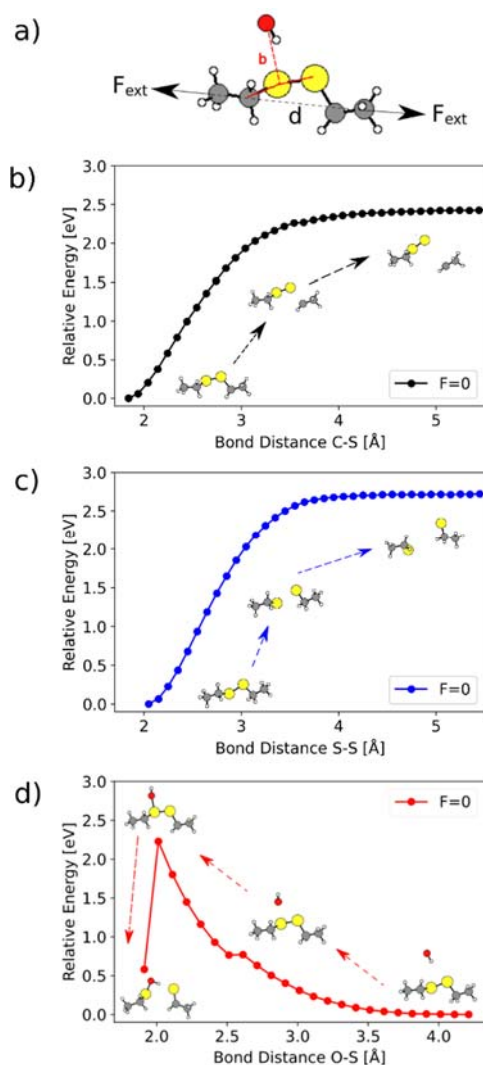


Fig. 2: a). Structures of diethyl disulfide with OH<sup>-</sup>, together with the corresponding bond  $b$  and distance vector  $d$  between the pulling points defining the direction of the external force  $F_{ext}$  and bond dissociation curve for: b) C-S, c). S-S and d). nucleophilic attack at S (© Functional Nanosystems Group)

We consider three different pathways for bond cleavage as illustrated in Fig. 1. The central figure shows the model system applied in the simulations, which consist of a diethyl disulfide molecule.

We first study our model system in the absence of external forces. We find a dihedral angle between C-S-S-C of 87° for equilibrium geometry ( $F=0$ ) in agreement with literature [7], [8]. The exploration of the activation energy via variation of the corresponding bond length  $b$  leads to the energies presented in Figs 2b) and c). The energy needed to cleave the C-S bond and the S-S bond are 2.41 eV and 2.80 eV respectively in agreement with experimental bond energy data (S-S: 2.86 eV, C-S: 2.43 eV [16]–[18]). This is the case in the gas phase or non polar solvents, where the C-S bond is “weaker” at least against thermal cleavage.

A drastic change happens if OH<sup>-</sup> is involved in the mechanism as seen in Fig. 2d. The hydrogen atom of OH<sup>-</sup> initially points toward the sulfur atom, but the OH<sup>-</sup> rotates with decreasing distance between O and S atoms. This causes the energy to flatten slightly for an O-S distance of about 2.5 Å when S and O atoms start to form a bond, which in turn breaks the S-S bond. The energy to cleave the S-S bond via this process is only 2.3 eV and thus 0.2 eV lower than C-S bond. This process is therefore most likely to occur in the experiment for disulfide reduction where OH<sup>-</sup> are available. This result is in qualitative agreement with molecular dynamics simulation [9] which also found this S<sub>N</sub>2 attack at S to require less energy than pure C-S and S-S bond cleavage.

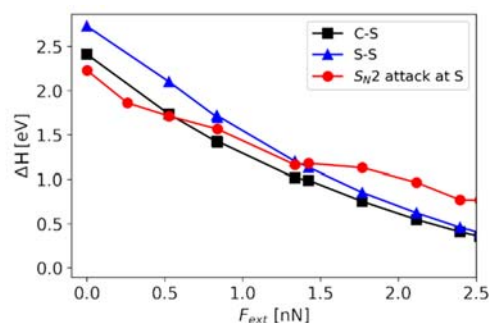


Fig. 3. Force dependent barriers for S-S bond (black), C-S bond (blue) and S<sub>N</sub>2 attack at S (red) (© Functional Nanosystems Group)

To explore the effect of the external force we use the COGEF method and its extension [14], [15], where the energy barriers in dependence of the external force  $F_{ext}$  are determined. In the

first step, the outer distance  $d$  between pulling points is varied to obtain the corresponding external force. All other degrees of freedom are relaxed without constraints. In the second step the C-S, S-S or O-S bond  $b$  are varied under the constraint of the given external force  $F_{ext}$ . The work done by the force is taken into account in the enthalpy via  $(b; F_{ext}) = U_0(d(F_{ext}), b) - dF_{ext}$ .

The effect of the external force to the activation enthalpies  $\Delta H$  on C-S and bond S-S bond were evaluated with force up to 2.5 nN and are depicted in Fig. 3. The activation energy decreases with increasing force. The S-S bond (blue) always stronger than the C-S bond (black), but the activation energy gap between C-S and S-S reduces when the forces are higher. Similar to the situation without external forces, the energy barrier of  $S_N2$  (red) is lower than C-S bond at lower forces (<0.5 nN). The barrier reduction with force of the  $S_N2$  attack is smaller than for the C-S and S-S bonds and reduces further after 0.5 nN. This leads to a switch of the process with lowest barrier at about 0.5 nN. These might be the reason for the experiment observed reduction rate of S-S bond cleavage at 0.5 nN.

In Conclusion, we have investigated the force dependence of C-S and S-S bond by using combination of DFT and the extended COGEF method. We found that the bond that breaks depends on the environment: while the S-S bond appears to be the weakest bond in aqueous environment, the C-S bond is the weakest bond in non-polar solvents or in the gas phase. Our results in a good agreement with other, more expensive calculations. Using this promising strategy, we aim for calculating more complex structures and cross linking systems that we will report in near future.

#### References

- [1] B. Gyarmati, Á. Némethy, and A. Szilágyi, "Reversible disulphide formation in polymer networks: A versatile functional group from synthesis to applications," *Eur. Polym. J.*, vol. 49, no. 6, pp. 1268–1286, 2013, doi: 10.1016/j.eurpolymj.2013.03.001.
- [2] F. Wang and C. E. Diesendruck, "Effect of disulphide loop length on mechanochemical structural stability of macromolecules," *Chem. Commun.*, vol. 56, no. 14, pp. 2143–2146, 2020, doi: 10.1039/c9cc07439b.
- [3] S. Y. An, D. Arunbabu, S. M. Noh, Y. K. Song, and J. K. Oh, "Recent strategies to develop self-healable crosslinked polymeric networks," *Chem. Commun.*, vol. 51, no. 66, pp. 13058–13070, 2015, doi: 10.1039/c5cc04531b.
- [4] H. Lioe and R. A. J. O'Hair, "A Novel Salt Bridge Mechanism Highlights the Need for Nonmobile Proton Conditions to Promote Disulfide Bond Cleavage in Protonated Peptides Under Low-Energy Collisional Activation," *J. Am. Soc. Mass Spectrom.*, vol. 18, no. 6, pp. 1109–1123, 2007, doi: 10.1016/j.jasms.2007.03.003.
- [5] C. H. Sohn, J. Gao, D. A. Thomas, T. Y. Kim, W. A. Goddard, and J. L. Beauchamp, "Mechanisms and energetics of free radical initiated disulfide bond cleavage in model peptides and insulin by mass spectrometry," *Chem. Sci.*, vol. 6, no. 8, pp. 4550–4560, 2015, doi: 10.1039/c5sc01305d.
- [6] S. Garcia-Manyes, J. Liang, R. Szoszkiewicz, T. L. Kuo, and J. M. Fernández, "Force-activated reactivity switch in a bimolecular chemical reaction," *Nat. Chem.*, vol. 1, no. 3, pp. 236–242, 2009, doi: 10.1038/nchem.207.
- [7] F. Hofbauer and I. Frank, "CPMD simulation of a bimolecular chemical reaction: Nucleophilic attack of a disulfide bond under mechanical stress," *Chem. - A Eur. J.*, vol. 18, no. 51, pp. 16332–16338, 2012, doi: 10.1002/chem.201202065.
- [8] P. Dopieralski, J. Ribas-Arino, P. Anjukandi, M. Krupicka, J. Kiss, and D. Marx, "The Janus-faced role of external forces in mechanochemical disulfide bond cleavage," *Nat. Chem.*, vol. 5, no. 8, pp. 685–691, 2013, doi: 10.1038/nchem.1676.
- [9] P. Dopieralski, J. Ribas-Arino, P. Anjukandi, M. Krupicka, and D. Marx, "Unexpected mechanochemical complexity in the mechanistic scenarios of disulfide bond reduction in alkaline solution," *Nat. Chem.*, vol. 9, no. 2, pp. 164–170, 2017, doi: 10.1038/NCHEM.2632.
- [10] J. Enkovaara *et al.*, "Electronic structure calculations with GPAW: A real-space implementation of the projector augmented-wave method," *J. Phys. Condens. Matter*, vol. 22, no. 25, 2010, doi: 10.1088/0953-8984/22/25/253202.
- [11] J. J. Mortensen, L. B. Hansen, and K. W. Jacobsen, "Real-space grid implementation of the projector augmented wave method," *Phys. Rev. B - Condens. Matter Mater. Phys.*, vol. 71, no. 3, pp. 1–11, 2005, doi: 10.1103/PhysRevB.71.035109.
- [12] J. P. Perdew, K. Burke, and M. Ernzerhof, "Generalized Gradient Approximation Made Simple - The PBE functional," *Phys. Rev. Lett.*, vol. 77, no. 18, pp. 3865–3868, 1996, doi: 10.1103/PhysRevLett.77.3865.
- [13] A. Held and M. Walter, "Simplified continuum solvent model with a smooth cavity based on volumetric data," *J. Chem. Phys.*, vol. 141, no. 17, 2014, doi: 10.1063/1.4900838.

[14] M. K. Beyer, "The mechanical strength of a covalent bond calculated by density functional theory," *J. Chem. Phys.*, vol. 112, no. 17, pp. 7307–7312, 2000, doi: 10.1063/1.481330.

[15] O. Brügner and M. Walter, "Temperature and loading rate dependent rupture forces from universal paths in mechanochemistry," *Phys. Rev. Mater.*, vol. 2, no. 11, pp. 1–6, 2018, doi: 10.1103/PhysRevMaterials.2.113603.

[16] J. A. Hawari, F. P. Lossing, and D. Griller, "Thermochemistry of Perthiyl Radicals," *J. Am. Chem. Soc.*, vol. 108, no. 12, pp. 3273–3275, 1986, doi: 10.1021/ja00272a021.

[17] J. B. Pedley, R. D. Naylor, S. P. Kirby, and P. G. Francis, *Thermochemical data of organic compounds, 2nd edn*, vol. 194. 1987.

[18] F. Hofbauer and I. Frank, "Disulfide bond cleavage: A redox reaction without electron transfer," *Chem. - A Eur. J.*, vol. 16, no. 17, pp. 5097–5101, 2010, doi: 10.1002/chem.200902831.

## Development of polarizability calculators in the Atomic Simulation Environment and GPAW

Ekaterina Zossimova, Michael Walter

Freiburg Center for Interactive Materials and Bioinspired Technologies (FIT)

Project funding: German Research Foundation (DFG) – Project WA 1687/10-1

Atomic and electronic structure dependent polarizability models are required to decode information from advanced single molecule bio-sensing experiments. Collaborators at the University of Exeter use a plasmonically-coupled whispering gallery mode sensor to probe the reaction kinetics of single molecules, whereby the target molecule is detected through a shift in the spectral position of the opto-plasmonic resonance. The wavelength shift,  $\Delta\lambda$ , is known to be proportional to the excess polarizability of the target molecule [1], [2].

The aims of this project are to develop accurate and scalable atomic structure informed polarizability calculators for use with the Atomic Simulation Environment (ASE) [3] and GPAW [4], [5]. We compare several different methods to calculate polarizability, all of which consider the atomic composition of the molecule. We benchmark the results against experimentally known values for the parallel and

perpendicular components of polarizability for a nitrogen molecule. We further calculate the polarizabilities of several neurotransmitter molecules that are being investigated by the experimental group in Exeter.

As a simple approximation, the polarizability of a molecule can be considered as the sum of the individual free atomic polarizabilities of its constituent atoms. However, this fails to account for several important factors such as intra-molecular interactions and is thus missing molecular anisotropy. We develop our own Python code based on the Thole model with linear screening [6] and two versions based on the Tkatchenko-Scheffler (TS) methods that describe vdW interactions, namely the TS-vdW method (TS09) [7] and the TS-vdW with self-consistent screening method (TS12) [8]. We also test a development version of the ab initio finite-field method in GPAW. As a further comparison, we include the results generated by the AlphaML machine learning web-app with the SCAN0 functional [9], which is trained on highly converged coupled cluster theory simulations of small molecules from the QM7b dataset [10]. The benchmark results for a nitrogen molecule are summarized in Table 1. The nitrogen molecule is chosen as the test case because it has well-defined parallel and perpendicular axes, denoted by  $\alpha_{\parallel}$  and  $\alpha_{\perp}$ , respectively.  $\alpha_{iso} = (2\alpha_{\perp} + \alpha_{\parallel})/3$  corresponds to the isotropic polarizability of the nitrogen molecule.

Table 1: Nitrogen benchmark for the polarizability calculators.

Polarizability of N <sub>2</sub> [Bohr <sup>3</sup> ]			
	$\alpha_{\parallel}$	$\alpha_{\perp}$	$\alpha_{iso}$
Experiment	16.1	9.8	11.9
Free atoms	n/a	n/a	14.8
Thole [6]	14.5	10.2	11.6
TS09 [7]	n/a	n/a	12.9
TS12 [8]	16.6	9.0	11.5
Finite field	15.7	10.7	12.4
AlphaML (SCAN0) [9]	16.0	6.7	9.8

All models are in reasonable agreement with experiment for  $\alpha_{iso}$ , whereas the results for

asymmetric components are more varied, depending on how screening is modelled. The Thole model and TS12 approximation introduce asymmetry through the dipole-dipole interaction tensor, whereby the molecule is considered as an arrangement of interacting dipoles centred at the atomic positions. Linear screening considers the atoms in the molecule as a distribution of point dipoles. Self-consistent screening considers the atomic dipoles as a set of quantum harmonic oscillators, which avoids divergences in the dipole-dipole interaction tensor for small interatomic separations. Both the finite field model and AlphaML consider all inter-atomic interactions and screening implicitly.

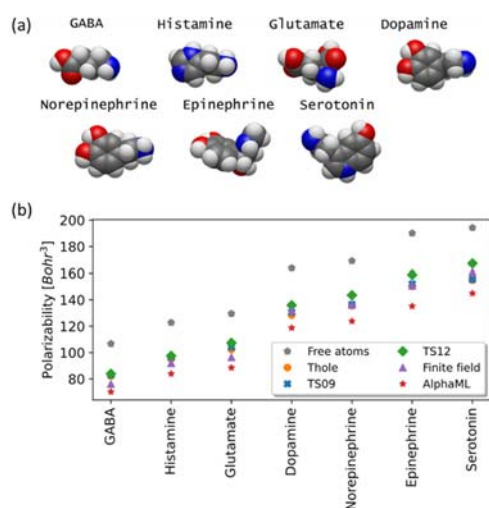


Fig. 1: (a) Van der Waal spheres for several different neurotransmitter molecules. C: grey, O: red, N: blue, H: white. Visualisation with Avogadro2: an open-source molecular builder and visualization tool. Version 1.91.0. <http://avogadro.cc/> (b) Results for static polarizability using different approaches, namely the Thole model, Tkatchenko-Scheffler methods, the finite field method in GPAW and the AlphaML machine learning web-app. (© Functional Nanosystems Group)

The finite field and TS12 polarizability calculators give the smallest error against experimental values in the nitrogen benchmark. The TS12 approximation considers pairwise vdW interaction terms and the screening is accounted for in a self-consistent way. The finite field model implicitly considers all inter-atomic interactions and screening through the GPAW implementation of density functional theory. The benefit of the TS12 method is that it can be extended to calculate frequency-depend-

ent polarizability without incurring the computational costs of calculating excited states with time-dependent density functional theory.

We have also used these polarizability models to predict the isotropic polarizabilities of several different angstrom-sized neurotransmitter molecules, namely GABA, Histamine, Glutamate, Dopamine, Norepinephrine, Epinephrine and Serotonin. The vdW spheres of these molecules are plotted in Fig. 1(a), showing the anisotropic shape of these molecules. The results in Fig. 1(b) compare the polarizability values obtained from the 6 different polarizability calculators assessed in Table 1. As expected, the finite field and TS12 methods perform very similarly, whilst the Thole and TS09 methods also perform well when comparing the isotropic polarizability. These computational results will be compared with single molecule biosensing experiments to verify the proportionality between the wavelength shift of the optoplasmonically coupled biosensor and the excess polarizability of single neurotransmitter molecules.

Several open questions remain to be addressed as part of this project. What is the effect of a solvent on the molecular polarizability and what is the best way to model this? What happens when we add the frequency dependence to the TS12 model and how do the results compare with time-dependent density functional theory? Interesting questions also arise from the experimental side, such as whether it is possible to determine the molecular orientation from the biosensor signals.

## References

- [1] S. Arnold, M. Khoshshima, I. Teraoka, S. Holler, and F. Vollmer, "Shift of whispering-gallery modes in microspheres by protein adsorption," *Opt. Lett.*, vol. 28, no. 4, pp. 272–274, Feb. 2003, doi: 10.1364/OL.28.000272.
- [2] D. Yu and F. Vollmer, "Allan deviation tells the binding properties in single-molecule sensing with whispering-gallery-mode optical microcavities," *Phys. Rev. Res.*, vol. 3, no. 2, p. 023087, May 2021, doi: 10.1103/PhysRevResearch.3.023087.
- [3] A. H. Larsen et al., "The atomic simulation environment—a Python library for working with atoms," *J. Phys. Condens. Matter*, vol. 29, no. 27, p. 273002, Jun. 2017, doi: 10.1088/1361-648X/aa680e.

## Highlights

- [4] J. J. Mortensen, L. B. Hansen, and K. W. Jacobsen, "Real-space grid implementation of the projector augmented wave method," *Phys. Rev. B*, vol. 71, no. 3, p. 035109, Jan. 2005, doi: 10.1103/PhysRevB.71.035109.
- [5] J. Enkovaara et al., "Electronic structure calculations with GPAW: a real-space implementation of the projector augmented-wave method," *J. Phys. Condens. Matter*, vol. 22, no. 25, p. 253202, Jun. 2010, doi: 10.1088/0953-8984/22/25/253202.
- [6] B. T. Thole, "Molecular polarizabilities calculated with a modified dipole interaction," *Chem. Phys.*, vol. 59, no. 3, pp. 341–350, Aug. 1981, doi: 10.1016/0301-0104(81)85176-2.
- [7] A. Tkatchenko and M. Scheffler, "Accurate Molecular Van Der Waals Interactions from Ground-State Electron Density and Free-Atom Reference Data," *Phys. Rev. Lett.*, vol. 102, no. 7, p. 073005, Feb. 2009, doi: 10.1103/PhysRevLett.102.073005.
- [8] A. Tkatchenko, R. A. DiStasio, R. Car, and M. Scheffler, "Accurate and Efficient Method for Many-Body van der Waals Interactions," *Phys. Rev. Lett.*, vol. 108, no. 23, p. 236402, Jun. 2012, doi: 10.1103/PhysRevLett.108.236402.
- [9] D. M. Wilkins, A. Grisafi, Y. Yang, K. U. Lao, R. A. DiStasio, and M. Ceriotti, "Accurate molecular polarizabilities with coupled cluster theory and machine learning," *Proc. Natl. Acad. Sci.*, vol. 116, no. 9, pp. 3401–3406, Feb. 2019.
- [10] Y. Yang, K. U. Lao, D. M. Wilkins, A. Grisafi, M. Ceriotti, and R. A. DiStasio, "Quantum mechanical static dipole polarizabilities in the QM7b and AlphaML showcase databases," *Sci. Data*, vol. 6, no. 1, p. 152, Aug. 2019, doi: 10.1038/s41597-019-0157-8.

## PROJECTS

### LIVMAT S—LIVING, ADAPTIVE AND ENERGY-AUTONOMOUS MATERIALS SYSTEMS

Jürgen Rühle<sup>1,2</sup>, Anna Fischer<sup>1,3</sup>,  
Thomas Speck<sup>1,4</sup>

<sup>1</sup>Cluster of Excellence livMatS @ FIT – Freiburg Center for Interactive Materials and Bioinspired Technologies, University of Freiburg, Georges-Köhler-Allee 105, D-79110 Freiburg, Germany; <sup>2</sup>Laboratory for Chemistry and Physics of Interfaces, Department of Microsystems Engineering (IMTEK), University of Freiburg, Georges-Koehler-Allee 103, D-79110, Freiburg, Germany; <sup>3</sup>Inorganic Functional Materials and Nanomaterials, Institute for Inorganic and Analytical Chemistry, University of Freiburg, Albertstr. 21, 79104 Freiburg, Germany; <sup>4</sup>Plant Biomechanics Group (PBG) & Botany: Functional Morphology and Biomimetics and Botanic Garden of the University of Freiburg

Project Funding: Funded by the Deutsche Forschungsgemeinschaft (DFG, German Research Foundation) under Germany's Excellence Strategy – EXC-2193/1 – 390951807

The Cluster of Excellence “Living, Adaptive, and Energy-autonomous Materials Systems” (livMatS) develops bioinspired materials systems that adapt autonomously to various environments and harvest clean energy from their surroundings. The intention of these purely technical – yet in a behavioral sense quasi-living – materials systems is to meet the demands of humans with regard to pioneering environmental and energy technologies. The societal relevance of autonomous systems and their sustainability thus plays a crucial role in their development within the framework of livMatS. The cluster receives funding from the German Research Foundation (DFG) under Germany's Excellency Strategy – EXC-2193/1 39051807 since January 2019.

Goal of the Cluster is that bioinspired materials, efficient energy materials systems (harvesting, conversion, and storage), and interactive, self-repairing materials with different and often even contradictory properties and functional conditions all meet to form a quasi-living materials system. Energy autonomy, adaptivity, longevity, and sustainability are the core

properties of the materials systems to be developed in livMatS. These challenging topics are investigated and combined with each other in four research areas: A – Energy Autonomy, B – Adaptivity, C – Longevity, and D – Sustainability (cf. Fig. 1). Research from all four areas feeds into demonstrator projects.

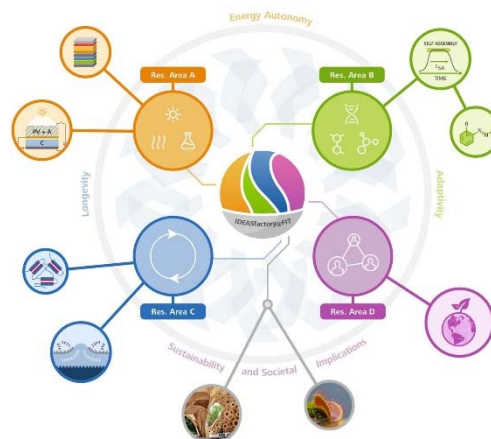


Fig. 1: Interplay of the closely interconnected Research Areas in livMatS (A – Energy Autonomy, B – Adaptivity, C – Longevity, D – Sustainability and Societal Implications). © livMatS / Daniel Hellweg.

Research area A – Energy Autonomy studies novel methods of energy harvesting and/or energy storage within a single highly integrated system, i.e. aims for the development of materials systems with embedded energy and energy management. Light, temperature differences, and vibrations are used as potential sources of energy. Once harvested, the energy is either consumed directly or stored for later use. Another important factor is the transformation of energy to make it available in mechanical, chemical, or thermal form or as light energy for adaptive processes within a materials system.

Research area B – Adaptivity develops new concepts for adaptive materials systems with complex energy landscapes that recognize and can react to sensory input from their environment. The recognition of the sensory input and the reaction to it are not performed by a pre-programmed chip but directly by the material or the materials system, using energy harvested from the environment. The goal of the research in area B is to develop a materials system with a “memory” that can adapt to its environment and improve itself.

Research area C – Longevity develops strategies that focus on the longevity and “self-control” of complex materials systems, drawing inspiration from living nature, particularly plant life, i.e. aims for the development of materials systems with embedded intelligence. Mechanisms for self-repair, the shedding and replacement of damaged parts, or also a training-based strengthening of system parts under special stress help to prevent minor damages from leading to a loss of functioning of the entire system.

Research area D – Sustainability considers the societal dimension of autonomous, quasi-living materials systems and their sustainability. A societal discourse on disruptive technologies, such as autonomous driving or expert systems, is often conducted only after the development and introduction of these technologies. In *livMatS*, this discourse will be initiated even as the technologies are being developed. The goal is to strengthen the development of the materials systems by means of concurrent sustainability analyses and to actively explore their societal dimension by engaging in critical philosophical reflection and conducting psychological studies.

There are myriad potential applications for the materials systems developed in *livMatS*. One example are “soft” machines that can recognize and grasp objects by feeling them, without the help of a computer. The capability of a materials system to adapt itself to temperatures, lighting conditions, or pressure opens up perspectives in a wide range of application areas, such as protective clothing like helmets and back protectors or prostheses that can adjust themselves to fit the wearer automatically, autonomously and without needing external energy supply – for instance through the use of body heat. Other ideas include packaging materials that grow stronger automatically when placed under stress and building envelopes that level out temperature differences, for example to prevent overheating.

*livMatS* is based at the Freiburg Center for Interactive Materials and Bioinspired Technologies (FIT) and unites researchers from the Faculty of Engineering, the Faculty of Chemistry and Pharmacy, the Faculty of Biology, the

Faculty of Mathematics and Physics, the Faculty of Economics and Behavioral Sciences, and the Faculty of Humanities. Our institutional composition reinforces the university’s strategic alliance with Freiburg’s Fraunhofer Institutes, with the Fraunhofer Institute for Solar Energy Systems (ISE) and the Fraunhofer Institute for Mechanics of Materials (IWM) as partner institutions within the Cluster, and is complemented by the Institute for Applied Ecology (Öko-Institut e.V.). The interdisciplinary Spokesperson Team of *livMatS* includes Prof. Dr. Jürgen Rühle (Faculty of Engineering), Prof. Dr. Anna Fischer (Faculty of Chemistry and Pharmacy), and Prof. Dr. Thomas Speck (Faculty of Biology).

*livMatS* uses the ideas factory IDEASfactory@FIT to implement new forms of scientific exchange and interdisciplinary cooperation. Three Shared Laboratories, one for the Research Areas A, B and C each, foster close collaboration between researchers within and across Research Areas. Shared Lab A provides equipment for synthesis, modification, and processing (2D and 3D) of energy materials as well as advanced photo-, electrochemical and microscopic characterization. Shared Lab B focuses on Microscopy, Spectroscopy and Rheology, with additional equipment for wet lab chemistry and sample preparation. Shared lab C provides additional options for microscopy and imaging but has its main focus on materials testing from macro- to microscale, 3D printing and sample preparation. The Shared Labs were officially inaugurated with a Lab Warming Party on October 20<sup>th</sup> 2020, after a continuous build-up period of 1 ½ years.

Over the course of 2021, the Shared Laboratories have acquired strategic additions, including for example: an X-ray photoelectron spectroscopy system for surface analysis with microscopic resolution and depth profiling, a MicroCT system for the quantitative structural analysis of biological structures and biomimetic materials systems, and an electrospinning setup for the processing of polymer and polymer-composite materials into porous felts, among others. In early 2022, the Shared Labs A will be complemented by two Atomic Layer

Deposition reactors that allow for interface optimization in energy materials in both powder and wafer samples. In addition, an ultrahigh performance liquid chromatography time of flight mass spectrometry system (UHPLC/MS/QTOF) for adaptive peptide analysis will be installed in the Shared Labs B.

Since 2019, the Cluster has developed and set up three different types of projects to provide flexible formats for the implementation of its research agenda. Doing so has allowed us to strike a balance between long-term projects (36 months) and complementary booster and impulse projects (six to eight and three months respectively).

A total of 21 long-term projects, each with a duration of 36 months, were set up following the *livMatS* Calls for Projects 2019 and 2020. Long-term projects within the Cluster are collaborative, combining the expertise of several PIs, RIs, Postdocs and PhDs. Since the long-term projects from the *livMatS* Call for Projects 2019 will be completed over the course of 2022, the *livMatS* Call for Projects 2022 was published in December 2021 and will allow for a new set of long-term projects to start in summer 2022. These long-term projects have been complemented by 25 impulse projects which were completed in 2020 and 2021, and 16 booster projects completed in 2021. This has added to the Cluster's scientific positioning and research output. Over the past three years, the Cluster has been able to recruit excellent early career researchers for its projects.

Currently, a total of 107 researchers at all levels, from doctoral researchers to experienced principal investigators, are working in long-term projects directly funded by the Cluster or associated to it. In addition to the 59 PhD and Postdoc researchers working in these long-term projects, a total of 29 PhD researchers and 14 Postdocs have contributed to *livMatS* research in booster and impulse projects over the course of 2020 and 2021.

In 2020 and 2021, after a highly competitive selection process, including leading international reviewers, the Cluster has hired two Junior Research Group Leaders within the *livMatS* Junior Research Group Program and

one Junior Research Group Leader within the Agnes Pockels Junior Research Group Program. Junior Research Groups are funded for five years. These excellent young groups add to the Cluster's research profile and provide attractive career opportunities and early academic independence.

In addition to scientific recruitment, *livMatS* has also been successful in hiring a data steward and an intellectual property manager in 2021. These roles will work to address and further develop the topics of research data management and intellectual property management in close collaboration with the Cluster's researchers.

Given the continued pandemic-related constraints in 2021, *livMatS* has maximized its efforts to promote internal and external scientific exchange and interaction with the public in virtual formats. Scientific exchange was facilitated in several formats throughout 2021. A total of 23 *livMatS* colloquia with external guest speakers offered the *livMatS* community ample opportunity to discuss current developments in their field with renowned international research, covering a wide range of disciplines. PhD, Postdoc and JRG researchers came together for a Young Researchers Retreat from September 30<sup>th</sup> – October 1<sup>st</sup>, 2021, focusing on teambuilding, scientific writing, and time and conflict management. All members of the *livMatS* community came together for the Cluster's third scientific retreat from November 17<sup>th</sup> – 19<sup>th</sup>, 2021, to present their work and discuss challenges, interfaces and goals of collaborative research within *livMatS*.

The Cluster was also able to consolidate activities within the "Convergence Center for Living Multifunctional Material Systems" (LiMC<sup>2</sup>) founded in 2019, uniting researchers from the Penn State University and the University of Freiburg. Following up on a webinar series in 2020, three projects were selected for funding through the LiMC<sup>2</sup> Seed Grants, where researchers from Penn State and *livMatS* join forces to maximize the center's potential for innovation and set the scene for future endeavors. In addition, a student-led virtual event took place in June 2021, focusing on fostering scientific exchange between graduate students

at both sites and building a student community with a focus on peer mentoring.

In November 2021, preparations started for a *European Network on Nature-Inspired Materials*, funded by the Royal Society of Edinburgh within its RSE Saltire Facilitation Network Award Program. Partners currently include *livMatS*, the NCCR Bio-inspired Materials, and the Universities of Strathclyde and Heriot-Watt. The inaugural meeting took place on January 21<sup>st</sup>, 2022.

Throughout 2021, *livMatS* has worked on the implementation and further development of its early career advancement objectives. The Cluster's successful Master Lab program saw its third implementation in 2021. A total of 12 master students are working independently on research ideas in various fields under the supervision of a researcher from the Cluster. Thus, a total of 21 master students will have completed the *livMatS* Master lab by the end of the winter term 2021/2022. In addition to the topics covered during the Young Researchers Retreat, PhDs and Postdocs in *livMatS* received training offers in the areas of good scientific practice and project management. After the implementation of the *livMatS* Writer's Studio in October 2020, a series of writing workshops took place in 2021, including topics such as abstract writing, logical flow, clarity in communication, and a Meet the Editors Event with a focus on the publication process.

Altogether, 2021 has been a very successful year for outreach measures in *livMatS*. The *livMatS* Pavilion, a robotically woven natural fiber construction, was built in the Botanical Garden of the University and is now open to the public. The pavilion stems from the successful collaboration of an interdisciplinary team of architects and engineers from the ITECH master's program at the Cluster of Excellence "Integrative Computational Design and Construction for Architecture (IntCDC)" at the University of Stuttgart and biologists from *livMatS* at the University of Freiburg. The pavilion's supporting structure is made from ro-

botically woven flax fiber, a naturally renewable and biodegradable material. The *livMatS* Pavilion was inspired by the saguaro cactus (*Carnegiea gigantea*) and the prickly pear cactus (*Opuntia* sp.), which are characterized by their special reticulated wood structure. The scientists abstracted the network structures of the biological model and implemented them in the *livMatS* Pavilion by winding. In the future, the pavilion will serve as an outdoor lecture room for *livMatS* to vividly communicate the research of the Cluster. Researchers will present their work to the public there, for example, in guided tours or workshops.

After the inauguration of the pavilion, which was accompanied by a press conference and a wide media coverage, the *livMatS* pavilion was part of two exhibitions in 2021: In the exhibition "Natur Futur – Bioökonomie erleben" at the Natural History Museum Berlin from November to December 2021, models of the robot-wound flax fibers and of the saguaro cactus were on display. In addition, the "Anthropocene" exhibition at the Natural History Museum in Stuttgart displays a model of the pavilion from October 2021 until June 2022. Additionally, the *livMatS* pavilion was awarded the "Materialpreis 2021" in the category "materials".

*livMatS* has also been involved in other outreach events, such as the "Science Days" at Europapark Rust from October 21<sup>st</sup> to 23<sup>rd</sup>, 2021. At the *livMatS* booth, the more than 8,000 visitors to the science festival were able to experiment with shape-memory polymers, try out for themselves how hydrophobic surfaces or metamaterials behave, and learn why thermoresponsive plastics change color. *livMatS* participated in the Science Days for the second time. Due to Corona restrictions, the organizers offered a purely digital program in 2020, to which *livMatS* contributed explanatory videos. In 2021, there were online experiments again in addition to the on-site program at Europapark.



Cacti-inspired /ivMatS Pavilion in the Botanic Garden Freiburg. © ICD/ITKE/IntCDC University of Stuttgart

## GROWBOT—TOWARDS A NEW GENERATION OF PLANT-INSPIRED GROWING ARTEFACTS

T. Speck<sup>1,2</sup>, M. Thielen<sup>1,2</sup>, F. Klimm<sup>1,2</sup>,  
B. Mazzolai<sup>3,4</sup> *et al.*<sup>5</sup>

<sup>1</sup>Plant Biomechanics Group Freiburg, Botanic Garden, University of Freiburg; <sup>2</sup>Freiburg Center for Interactive Materials and Bioinspired Technologies (FIT); <sup>3</sup>Center for Micro-BioRobotics, Istituto Italiano di Tecnologia, Pontedera (PI), Italy; <sup>4</sup>GrowBot Project coordinator; <sup>5</sup>Consortium members of the GrowBot Project

Project funding: This project has received funding from the European Union's Horizon 2020 research and innovation programme under the grant agreement No 824074

[www.growbot.eu](http://www.growbot.eu)

GrowBot proposes a disruptively new paradigm of movement in robotics inspired by the moving-by-growing abilities of climbing plants.



Fig. 1: GrowBot - Towards a new generation of plant-inspired growing artefacts ([www.growbot.eu](http://www.growbot.eu))

Plants are still a quite unexplored model in robotics and ICT technologies, as their sessile nature leads to think that they do not move. Instead, they move greatly, on a different time scale, purposively, effectively and efficiently. To move from one point to another, plants must grow and continuously adapt their body to the external environmental conditions. This continuous growth is particularly evident in climbing plants.

By imitating them, the GrowBot objective is to develop low-mass and low-volume robots capable of anchoring themselves, negotiating voids, and more generally climbing, where

current climbing robots based on wheels, legs, or rails would get stuck or fall. Specifically, the ability to grow will be translated by additive manufacturing processes inside the robot, which creates its body by depositing new materials with multi-functional properties, on the basis of the perceived external stimuli (without a pre-defined design). Perception and behaviour will be based on the adaptive strategies that allow climbing plants to explore the environment. GrowBot is based on a strongly interdisciplinary character and can open the way for a new technological paradigm around the concept of growing robots, fostering a European innovation eco-system for several high-tech sectors [1].

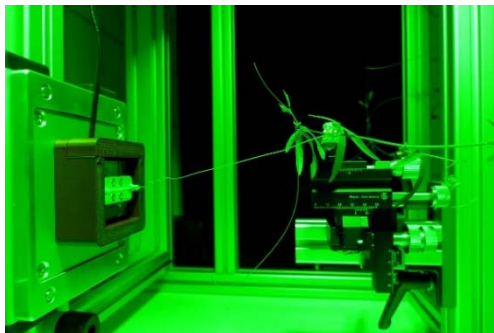


Fig. 2: Experimental set-up for measuring the tensile forces generated during the coiling process in *Passiflora caerulea*. To allow for a 24/7 recording of the time-lapse video, green-light illumination during the night period is essential. © Plant Biomechanics Group Freiburg.

The Plant Biomechanics Group Freiburg will contribute to this task based on their long experience on eco-biomechanics, stem structure and mechanics of climbing plants and on the various attachment systems existing in climbing plants. One of the main focuses will be on how climbers of the genus *Passiflora* manage to attach to very diverse substrates and supports by means of their characteristic coiled tendrils and terminal adhesive pads [2], and on how these are generating forces during the process of coiling. Another focus is on how different plants manage to negotiate large distances between supporting trees by means of so-called searcher shoots, and especially on how several of these searcher shoots provide mutual support by intertwining and increase their reach as a result [3].



Fig. 3: *Mandevilla* sp. can conquer even those spaces in the greenhouse that are inaccessible to other plants (e.g. cable ducts), because of its long searcher shoots that stabilize each other by intertwining. © Plant Biomechanics Group Freiburg.

## References

- [1] Mazzolai, B., Carpi, F., Suzumori, K., Cianchetti, M., Speck, T. et al. (2022). Roadmap on Soft Robotics: multifunctionality, adaptability and growth without borders. *Multifunctional Materials*, (accepted manuscript), <https://doi.org/10.1088/2399-7532/ac4c95>
- [2] Klimm, F., Schmier, S., Bohn, H. F., Kleiser, S., Thielen, M. Speck, T. (2021). Biomechanics of tendrils and adhesive pads of the climbing passion flower *Passiflora discophora*. *Journal of Experimental Botany*, erab456, <https://doi.org/10.1093/jxb/erab456>
- [3] Gallentine, J., Wooten, M. B., Thielen, M., Walker, I. D., Speck, T. & Niklas, K. J. (2020). Searching and Intertwining: Climbing Plants and GrowBots. *Frontiers in Robotics and AI*, 7. 00118, <https://doi.org/10.3389/frobt.2020.00118>

## IPROM—INTERACTIVE AND PROGRAMMABLE MATERIALS

Jürgen Rühle<sup>1,2</sup>, Bastian E. Rapp<sup>1,3</sup>

<sup>1</sup>Cluster of Excellence livMatS @ FIT – Freiburg Center for Interactive Materials and Bioinspired Technologies, University of Freiburg, Georges-Köhler-Allee 105, D-79110 Freiburg, Germany;

<sup>2</sup>Laboratory for Chemistry and Physics of Interfaces, Department of Microsystems Engineering (IMTEK), University of Freiburg; <sup>3</sup>Laboratory of Process Technology (Neptun Lab), Department of Microsystems Engineering

Project Funding: Carl Zeiss Foundation

[www.fit.uni-freiburg.de/iprom](http://www.fit.uni-freiburg.de/iprom)

One of the core principles in the design of technical objects is the static nature of the materials: They have more or less unchangeable properties. In nature, on the other hand, the (bio-)materials used by living systems are geared towards enabling the best possible adaptation to the respective environmental conditions in order to be best react to changes in the surrounding. The aim of the Research Cluster "Interactive and Programmable Materials (IPROM)" funded by the Carl Zeiss Foundation is the development of innovative technical materials that respond to changing environmental conditions with a response, which is preprogrammed into the material and thus triggers a material adaptation to changes in the surrounding and the load conditions. In order to do so, they have to be able to change their internal structure and/or their external shape as a consequence of an external stimulus, e.g. by adapting the adhesion, wettability or mechanical properties of the materials. This concept opens up new opportunities for the production of complex objects in many areas such as optics, medical technology or architecture.

“The IPROM cluster will bring forth a paradigm shift in materials research from static to dynamic materials. The novel materials generated will dynamically adapt their properties to the constantly changing conditions of their environment in a previously programmed manner.”



Fig. 1: IPROM – Interactive and Programmable Materials ([www.fit.uni-freiburg.de/iprom](http://www.fit.uni-freiburg.de/iprom))

IPROM projects include the following topics:

- TP 1: Bio-inspired programmable material systems (PI: Thomas Speck)
- TP 2: Multiparameter / Multimaterial 4D Printing (PI: Bastian E. Rapp)
- TP 3: Light-responsive surfaces (PIs: Jürgen Rühle & Bastian E. Rapp)
- TP 4: Nonlinear micromechanics of programmable materials (PIs: Christoph Eberl & Lars Pastewka)
- TP 5: Sustainable materials for 4D printing (PI: Dorothea Helmer)
- TP 6: Programmable Tribology (PIs: Jürgen Rühle & Lars Pastewka)
- TP 7: Biocompatible, programmable materials for soft micro-robots (PI: Karen Lienkamp)
- TP 8: Bioelectroactive Interfaces for dynamic interaction with biology (PI: Maria Asplund)
- TP 9: Autonomous and reconfigurable metamaterials and soft robots (PI: Andreas Walther)
- TP 10: Digitized dynamic illumination (PI: Hans Zappe)

## PUBLICATIONS

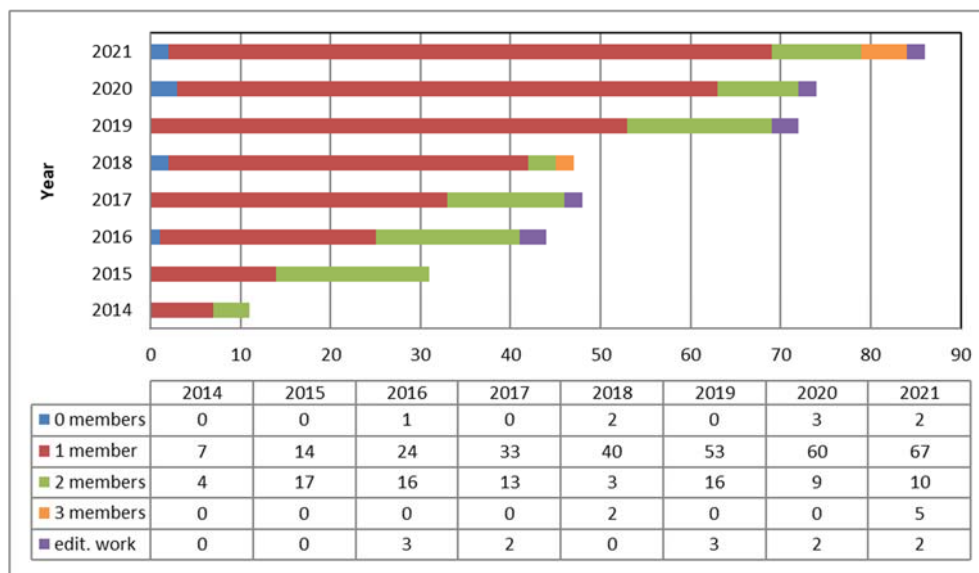


Fig. 1: Peer-reviewed publications and editorial work from 2014 until 2021

## PEER-REVIEWED PUBLICATIONS

AlShetwi YA, Bessif B, Sommer M, Reiter G (2021): Illumination of conjugated polymers reduces the nucleation probability and slows down the crystal growth rate. *Macromolecules* **54**(24), 11478-11485. DOI: 10.1021/acs.macromol.1c02139

Alshetwi YA; Schiefer D, Sommer M, Reiter G (2021): Continuous illumination of a conjugated polymer causes strong enhancement of photoluminescence. *The Journal of Physical Chemistry B* **125**(21), 5636-5644. DOI: 10.1021/acs.jpcc.1c01837

Amine S, Montebault A, Fumagalli M, Osorio-Madrado A, David L (2021): Controlled Polyelectrolyte Association of Chitosan and Carboxylated Nano-Fibrillated Cellulose by Desalting. *Polymers* **13**(12), 2023. DOI: 10.3390/polym13122023

Ates HC, Brunauer A, von Stetten F, Urban GA, Güder F, Merkoçi A, ... Dincer C (2021): Integrated Devices for Non-Invasive Diagnostics. *Advanced Functional Materials* **31**(15), 2010388. DOI: 10.1002/adfm.202010388

Ates HC, Yetisen AK, Güder F, Dincer C (2021): Wearable devices for the detection of COVID-19. *Nature Electronics* **4**(1), 13-14. DOI: 10.1038/s41928-020-00533-1

Berestok T, Diestel C, Ortlieb N, Buettner J, Matthews J, Schulze PS, Goldschmidt JC, Glunz SW, Fischer A (2021): High-efficiency monolithic photosupercapacitors: smart integration of a perovskite solar cell with a mesoporous carbon double-layer capacitor. *Solar RRL* **5**(11), 2100662. DOI: 10.1002/solr.202100662

Bruch R, Johnston M, Kling A, Mattmüller T, Baaske J, Partel S, ... & Dincer C (2021): CRISPR-powered electrochemical microfluidic multiplexed biosensor for target amplification-free miRNA diagnostics. *Biosensors and Bioelectronics* **177**, 112887. DOI: 10.1016/j.bios.2020.112887

Bürger JC, Gutsch S, Thomann Y, Thomann R, Christian B, Ambacher O, Zacharias M (2021): Analysis of the Growth of Laterally Aligned SnO<sub>2</sub> Nanowires by Thermodynamic Considerations and Experiments. *Crystal Growth & Design* **21**(1), 191-199. DOI: 10.1021/acs.cgd.0c00983

Carmesin CF, Fleischmann AS, Klepsch MM, Westermeier AS, Speck T, Jansen S, Poppinga S (2021): Structural gradients and anisotropic hydraulic conductivity in the enigmatic eel traps of carnivorous corkscrew plants (*Genlisea* spp.). *American Journal of Botany* **108**(12), 2356-2370. DOI: 10.1002/ajb2.1779

- Cheng T, Thielen M, Poppinga S, Tahouni Y, Wood D, Steinberg T, Menges A, Speck T (2021): Bio-inspired motion mechanisms: computational design and material programming of self-adjusting 4-printed wearable systems. *Advanced Science* **8**(13), 2100411. DOI: 10.1002/advs.202100411
- Conrad S, Speck T, Tauber F (2021): Tool changing 3D printer for rapid prototyping of advanced soft robotic elements. *Bioinspiration & Biomimetics* **16**(5), 055010. DOI: 10.1088/1748-3190/ac095a
- Dabringhaus P, Barthélemy A, Krossing I (2021): The coordination chemistry and clustering of subvalent Ga<sup>+</sup> and In<sup>+</sup> upon addition of [sigma]-donor ligands. *Zeitschrift für anorganische und allgemeine Chemie* **647**(18), 1660-1673. DOI: 10.1002/zaac.202100129
- Desmaizieres G, Speer ME, Thiede I, Gaiser P, Perner V, Kolek M, Bieker P, Winter M, Esser B (2021): Dibenzo[a,e]cyclooctatetraene-functionalized polymers as potential battery electrode materials. *Macromolecular Rapid Communications*, 2000725. DOI: 10.1002/marc.202000725
- Dürr-Mayer T, Qiu D, Eisenbeis VB, Steck N, Häner M, Hofer A, ... & Jessen HJ (2021): The chemistry of branched condensed phosphates. *Nature Communications* **12**(1), 1-11. DOI: 10.1038/s41467-021-25668-3
- Ernst LD, Krossing I (2021): Fluorination of methanol catalysts to improve productivity and selectivity. *Internationaler Motorenkongress 2021* (pp. 579-587). Springer Vieweg, Wiesbaden. DOI: 10.1007/978-3-658-35588-3\_35
- Esser B, Dolhem F, Becuwe M, Poizot P, Vlad A, Brandell D (2021): A perspective on organic electrode materials and technologies for next generation batteries. *Journal of Power Sources* **482**, 228814. DOI: 10.1016/j.jpowsour.2020.228814
- Fan X, Walther A (2021): Autonomous Transient pH Flips Shaped by Layered Compartmentalization of Antagonistic Enzymatic Reactions. *Angewandte Chemie* **133**(7), 3663-3668. DOI: 10.1002/anie.202009542
- Fehr SM, Nguyen K, Njel C, Krossing I (2021): Enhancement of methanol synthesis by oxidative fluorination of Cu/ZnO catalysts—Insights from surface analyses. *ACS Catalysis* **11**(21), 13223-13235. DOI: 10.1021/acscatal.1c03735
- Fiedler J, Walter M, Buhmann SY (2021): Effective screening of medium-assisted van der Waals interactions between embedded particles. *The Journal of Chemical Physics* **154**(10), 104102. DOI: 10.1063/5.0037629
- Fish GC, Moreno-Naranjo JM, Billion A, Kratzert D, Hack E, Krossing I, Nüesch F, Moser JE (2021): Critical role of H-aggregation for high-efficiency photoinduced charge generation in pristine pentamethine cyanine salts. *Physical Chemistry Chemical Physics* **23**(41), 23886-23895. DOI: 10.1039/D1CP03251H
- Frenking G, Fernández I, Holzmann N, Pan S, Krossing I, Zhou M (2021): Metal–CO bonding in mononuclear transition metal carbonyl complexes. *JACS Au* **1**(5), 623-645. DOI: 10.1021/jacsau.1c00106
- Gebhardt J, Wei W, Elsässer C (2021): Efficient modeling workflow for accurate electronic structures of hybrid perovskites. *The Journal of Physical Chemistry C* **125**(34), 18597-18603. DOI: 10.1021/acs.jpcc.1c04817
- Ghane-Motlagh R, Fammels J, Danilewsky AN, Pelz U, Woiass P (2021): Effect of surfactants on the growth and characterization of triglycine sulfate crystals. *Journal of Crystal Growth* **563**, 126081. DOI: 10.1016/j.jcrysgro.2021.126081
- Gloetz K, Barthélemy A, Krossing I (2021): A simple homoleptic gallium(I) olefin complex: mimicking transition-metal chemistry at a main-group metal?? *Angewandte Chemie* **133**(1), 210-213. DOI: 10.1002/anie.202011466
- Gujrati A, Sanner A, Khanal SR, Moldovan N, Zeng H, Pastewka L, Jacobs TD (2021): Comprehensive topography characterization of polycrystalline diamond coatings. *Surface Topography: Metrology and Properties* **9**(1), 014003. DOI: 10.1088/2051-672X/abe71f
- Guo Z, Yan S, Reiter G (2021): Formation of stacked three-dimensional polymer “single crystals”. *Macromolecules* **54**(10), 4918-4925. DOI: 10.1021/acs.macromol.1c00081
- Harris T, Heidary N, Frielingsdorf S, Rauwerdink S, Tahraoui A, Lenz O, Zebger I, Fischer A (2021): Electrografted interfaces on metal oxide electrodes for enzyme immobilization and bioelectrocatalysis. *ChemElectroChem* **8**(7), 1329-1336. DOI: 10.1002/celec.202100020
- He X, Walter M, Jiang D. (2021): Understanding superatomic Ag nanohydrides. *Small* **17**, 27, 2004808. DOI: 10.1002/smll.202004808
- Heck MA, Lüth VM, van Gessel N, Krebs M, Kohl M, Prager A, ... & Reski R (2021): Axenic in vitro cultivation of 19 peat moss (*Sphagnum* L.) species as a resource for basic biology, biotechnology, and paludiculture. *New Phytologist* **229**(2), 861-876. DOI: 10.1111/nph.16922
- Heckel J, Loescher S, Mathers RT, Walther A (2021): Chemically fueled volume phase transition of polyacid microgels. *Angewandte Chemie* **133**(13), 7193-7201. DOI: 10.1002/anie.202014417

## Publications

- Hermann M, Böttcher T, Schorpp M, Richert S, Wassy D, [Krossing I](#), [Esser B](#) (2021): Cations and Anions of Dibenzo[a,e]pentalene and Reduction of a Dibenzo[a,e]pentalenophane. *Chemistry* **27**(15), 4964. DOI: 10.1002/chem.202005131
- Hermann M, Wassy D, Kohn J, Seitz P, Betschart MU, Grimme S, [Esser B](#) (2021): Chiral Dibenzopentalene-Based Conjugated Nano hoops through Stereoselective Synthesis. *Angewandte Chemie International Edition* **60**(19), 10680-10689. DOI: 10.1002/anie.202016968
- Higham TE, Hofmann M, Modert M, Thielen M, [Speck T](#) (2021): Jumping with adhesion: landing surface incline alters impact force and body kinematics in crested geckos. *Scientific Reports* **11**(1), 1-13. DOI: 10.1038/s41598-021-02033-4
- Hone T, Mylo M, [Speck O](#), [Speck T](#), Taylor D (2021): Failure mechanisms and bending strength of *Fuchsia magellanica* var. *gracilis* stems. *Journal of the Royal Society Interface* **18**(175), 20201023. DOI: 10.1098/rsif.2020.1023
- Ikari Y, Kaihara T, Goto S, Bovenkerk M, Grenz DC, [Esser B](#), ... Takeda Y (2021): Peripherally Donor-Installed 7, 8-Diaza [5] helicenes as a Platform for Helical Luminophores. *Synthesis* **53**(09), 1584-1596. DOI: 10.1055/a-1343-5810
- Jiang N, Tansukawat ND, Gonzalez-Macia L, Ates HC, [Dincer C](#), Güder F, Tasoglu S, Yetisen AK, Ates HC (2021): Low-cost optical assays for point-of-care diagnosis in resource-limited settings. *ACS sensors* **6**(6), 2108-2124. DOI: 10.1055/a-1343-5810
- Kabay G, [Dincer C](#), Manz A (2021): Microfluidic Roadmap for Translational Nanotheranostics. *Small methods* **6**(2), 2101217. DOI: 10.1002/smt.202101217
- Kamdem Tamo A, Doench I, Walter L, Montembault A., Sudre G, David L., Morales Helguera A, Selig M, Rolaufts B, Bernstein A, Hoenders D, [Walther A](#), [Osorio-Madrado A](#) (2021): Development of bioinspired functional chitosan/cellulose nanofiber 3D hydrogel constructs by 3D printing for application in the engineering of mechanically demanding tissues. *Polymers* **13**(10), 1663. DOI: 10.3390/polym13101663
- Kanokwijitsilp T, Körner M, Prucker O, Anton A, Lübke J, [Rühe J](#) (2021): Kinetics of Photocrosslinking and Surface Attachment of Thick Polymer Films. *Macromolecules* **54**(13), 6238-6246. DOI: 10.1021/acs.macromol.1c00121
- Koch F, Thaden O, Tröndle K, [Zengerle R](#), Zimmermann S, [Koltay P](#) (2021): Open-source hybrid 3D-bioprinter for simultaneous printing of thermoplastics and hydrogels. *HardwareX* **10**, e00230. DOI: 10.1016/j.ohx.2021.e00230
- Koch S, Heizmann, PA, Kilian SK, Britton B, Holdcroft S, Breitwieser M, [Vierrath S](#) (2021): The effect of ionomer content in catalyst layers in anion-exchange membrane water electrolyzers prepared with reinforced membranes (Aemion+™). *Journal of Materials Chemistry A* **9**(28), 15744-15754. DOI: 10.1039/D1TA01861B
- Kotz F, Quick AS, Risch P, Martin T, Hoose T, Thiel M, ... [Rapp BE](#) (2021): Two-Photon Polymerization of Nanocomposites for the Fabrication of Transparent Fused Silica Glass Microstructures. *Advanced Materials* **33**(9), 2006341. DOI: 10.1002/adma.202006341
- [Krossing I](#) (2021): The first year of B. Sc. chemistry at the University of Freiburg, Germany: a report from the experimental lecture on general and inorganic chemistry. *CHIMIA International Journal for Chemistry* **75**(1-2), 9-13. DOI: 10.2533/chimia.2021.9
- Kumar C, [Speck T](#), Le Houérou V (2021): Local contact formation during sliding on soft adhesive surfaces with complex microstructuring. *Tribology International* **163**, 107180. DOI: 10.1016/j.triboint.2021.107180
- Langer M, Kelbel MC, [Speck T](#), [Müller C](#), [Speck O](#) (2021): Twist-to-bend ratios and safety factors of petioles having various geometries, sizes and shapes. *Frontiers in Plant Science* **12**, 765605-765605. DOI: 10.3389/fpls.2021.765605
- Langer M, [Speck T](#), [Speck O](#) (2021): Petiole-lamina transition zone: a functionally crucial but often overlooked leaf trait. *Plants* **10**(4), 774. DOI: 10.3390/plants10040774
- Lohner P, Zmysliá M, Thurn J, Pape JK, Gerasimaité R, Keller-Findeisen J, Groerer S, Deuringer B, Süß R, [Walther A](#), Hell SW, Lukinavičius G, [Hugel T](#), Jessen-Trefzer C (2021): Inside a Shell—Organometallic Catalysis Inside Encapsulin Nanoreactors. *Angew. Chem. Int. Ed.* **60**, 23835-23841. DOI: 10.1002/anie.202110327
- Löscher S, [Walther A](#) (2021): Multivalency pattern recognition to sort colloidal assemblies. *Small* **17**(5), 2005668. DOI: 10.1002/smll.202005668
- Ludwanowski S, Skarsetz O, Creusen G, Hoenders D, Straub P, [Walther A](#) (2021): Wavelength-Gated Adaptation of Hydrogel Properties via Photo-Dynamic Multivalency in Associative Star Polymers. *Angewandte Chemie International Edition* **60**(8), 4358-4367. DOI: 10.1002/anie.202011592

- Ludwanowski S, Skarsetz O, Creusen G, Hoenders D, Straub P, Walther A (2021): Wellenlängengesteuerte Adaption der Hydrogeleigenschaften durch Photodynamische Multivalenz in Assoziierenden Sternpolymeren. *Angewandte Chemie* **133**(8), 4404-4413. DOI: 10.1002/ange.202011592
- Luitz M, Lunzer M, Goralczyk A, Mader M, Bhagwat S, Warmbold A, Helmer D, Kotz F, Rapp BE (2021): High Resolution Patterning of an Organic–Inorganic Photoresin for the Fabrication of Platinum Microstructures. *Advanced Materials* **33**(37), 2101992. DOI: 10.1002/adma.202101992
- Mader M, Hambitzer L, Schlautmann P, Jenne S, Greiner C, Hirth F, Helmer D, Kotz-Helmer F, Rapp BE (2021): Melt-Extrusion-Based Additive Manufacturing of Transparent Fused Silica Glass. *Advanced Science* **8**(23), 2103180. DOI: 10.1002/adv.202103180
- Mader M, Rein C, Konrat E, Meermeyer SL, Lee-Thedieck C, Kotz-Helmer F, Rapp BE (2021): Fused deposition modeling of microfluidic chips in transparent polystyrene. *Micromachines* **12**(11), 1348. DOI: 10.3390/mi12111348
- Mader M, Schlatter O, Heck B, Warmbold A, Dorn A, Zappe H, Risch P, Helmer D, Kotz F, Rapp BE (2021): High-throughput injection molding of transparent fused silica glass. *Science* **372**(6538), 182-186. DOI: 10.1126/science.abf1537
- Mansell J, Reuter L, Rhea C, Kiesel A (2021): A novel network approach to capture cognition and affect: COVID-19 experiences in Canada and Germany. *Frontiers in Psychology* **12**, 2082. DOI: 10.3389/fpsyg.2021.663627
- Marquez-Bravo S, Doench I, Molina P, Bentley FE, Tamo AK, Passieux R, Lossada F, David L, Osorio-Madrado A (2021): Functional bionanocomposite fibers of chitosan filled with cellulose nanofibers obtained by gel spinning. *Polymers* **13**(10), 1563. DOI: 10.3390/polym13101563
- Martin J, Melke J, Njel C, Schökel A, Büttner J, Fischer A (2021): Electrochemical stability of platinum nanoparticles supported on N-doped hydrothermal carbon aerogels as electrocatalysts for the oxygen reduction reaction. *ChemElectroChem* **8**(24), 4835-4847. DOI: 10.1002/celec.202101162
- Martinez-Dominguez MV, Zottel A, Šamec N, Jovčevska I, Dincer C, Kahlert UD, Nickel AC (2021): Current technologies for RNA-directed liquid diagnostics. *Cancers* **13**(20), 5060. DOI: 10.3390/cancers13205060
- Masselter T, Speck O, Speck T (2021): 3D reticulated actuator inspired by plant up-righting movement through a cortical fiber network. *Biomimetics* **6**(2), 33. DOI: 10.3390/biomimetics6020033
- Mayoussi F, Doeven EH, Kick A, Goralczyk A, Thomann Y, Risch P, Guijt RM, Kotz F, Helmer D, Rapp BE (2021): Facile fabrication of micro-/nanostructured, superhydrophobic membranes with adjustable porosity by 3D printing. *Journal of Materials Chemistry A* **9**(37), 21379-21386. DOI: 10.1039/D1TA03352B
- Meder F, Armiento S, Naselli GA, Thielen M, Speck T, Mazzolai B (2021): Biohybrid generators based on living plants and artificial leaves: influence of leaf motion and real wind outdoor energy harvesting. *Bioinspiration & Biomimetics* **16**(5), 055009. DOI: 10.1088/1748-3190/ac1711
- Möller M, Höfele P, Kiesel A, Speck O (2021): Reactions of sciences to the Anthropocene—Highlighting inter- and transdisciplinary practices in biomimetics and sustainability research. *Elementa: Science of the Anthropocene* **9**(1), 035. DOI: 10.1525/elementa.2021.035
- Möller M, Höfele P, Reuter L, Tauber FJ, Grißhammer R (2021): How to assess technological developments in basic research? Enabling formative interventions regarding sustainability, ethics, and consumer issues at an early stage. *TATuP-Zeitschrift für Technikfolgenabschätzung in Theorie und Praxis* **30**(1), 56-62. DOI: 10.14512/tatup.30.1.56
- Mylo MD, Hesse L, Masselter T, Leupold J, Drozella K, Speck T, Speck O (2021): Morphology and anatomy of branch–branch junctions in *Opuntia ficus-indica* and *Cylindropuntia bigelovii*: a comparative study supported by mechanical tissue quantification. *Plants* **10**(11), 2313. DOI: 10.3390/plants10112313
- Mylo MD, Hofmann M, Delp A, Scholz R, Walther F, Speck T, Speck O (2021): Advances on the visualization of the internal structures of the European mistletoe: 3D reconstruction using microtomography. *Frontiers in Plant Science* **12**, 2085. DOI: 10.3389/fpls.2021.715711
- Netzsch P, Stroh R, Pielhofer F, Krossing J, Höpfe HA (2021): Strong Lewis and Brønsted acidic sites in the borosulfate  $Mg_3[H_2O \rightarrow B(SO_4)_3]_2$ . *Angewandte Chemie International Edition* **60**(19), 10643-10646. DOI: 10.1002/anie.202016920 10.1002/anie.202016920
- Omidvar R, Ayala YA, Brandel A, Hasenclever L, Helmstädter M, Rohrbach A, Römer W, Madl J (2021): Quantification of nanoscale forces in lectin-mediated bacterial attachment and uptake into giant liposomes. *Nanoscale* **13**(7), 4016-4028. DOI: 10.1039/d0nr07726g
- Ostendorf AK, van Gessel N, Malkowsky Y, Sabovljevic MS, Rensing SA, Roth-Nebelsick A, Reski R (2021): Polyploidization within the Funariaceae—a key principle behind speciation, sporophyte reduction and the high variance of spore diameters? *Bryophyte Diversity and Evolution* **43**(1), 164-179. DOI: 10.11646/bde.43.1.13

## Publications

- Otteny F, Perner V, Einholz C, Desmaizieres G, Schleicher E, Kolek M, Bieker P, Winter M, [Esser B](#) (2021): Bridging the gap between small molecular [pi]-interactions and their effect on phenothiazine-based redox polymers in organic batteries. *ACS Applied Energy Materials* **4**(8) 7622-7631. DOI: 10.1021/acsaem.1c00917
- Paschke S, Prediger R, Lavaux V, Eickenscheidt A, [Lienkamp K](#) (2021): Stimulus-responsive polyelectrolyte surfaces: switching surface properties from polycationic/antimicrobial to polyzwitterionic/protein-repellent. *Macromolecular Rapid Communications*, 2100051. DOI: 10.1002/marc.202100051
- Poppinga S, Schenck P, [Speck O](#), [Speck T](#), Bruchmann B, [Masselter T](#) (2021): Self-actuated paper and wood models: low-cost handcrafted biomimetic compliant systems for research and teaching. *Biomimetics* **6**(3), 42. DOI: 10.3390/biomimetics6030042
- Priester D, [Krossing I](#) (2021): Elektromobilität und synthetische Kraftstoffe. *Nachrichten aus der Chemie* **69**(9), 36-40. DOI: 10.1002/nadc.2021411
- Radtke V, Stoica D, Leito I, Camões F, [Krossing I](#), Anes B, ... & Lawrence N (2021): A unified pH scale for all solvents: part I—intention and reasoning (IUPAC Technical Report). *Pure and Applied Chemistry* **93**(9), 1049-1060. DOI: 10.1515/pac-2019-0504
- Raisch M, Maftuhin W, [Walter M](#), Sommer M (2021): A mechanochromic donor-acceptor torsional spring. *Nature communications* **12**, 4243. DOI: 10.1038/s41467-021-24501-1
- Reuter L, Fenn J, Bilo TA, Schulz M, Weyland AL, [Kiesel A](#), Thomaschke R (2021): Leisure walks modulate the cognitive and affective representation of the corona pandemic: Employing Cognitive-Affective Maps within a randomized experimental design. *Applied Psychology: Health and Well-Being* **13**(4), 952-967. DOI: 10.1111/aphw.12283
- Roumpos K, Fontaine S, [Pfohl T](#), Prucker O, [Rühe J](#), [Reiter G](#) (2021): Measurements of periodically perturbed dewetting force fields and their consequences on the symmetry of the resulting patterns. *Scientific Reports* **11**(1), 1-11. DOI: 10.1038/s41598-021-92544-x
- Scherer H, Hanske A, [Krossing I](#), Gloetz KN, Barthélemy A (2021): Ga<sup>+</sup>-catalyzed hydrosilylation? About the surprising system Ga<sup>+</sup>/HSiR<sub>3</sub>/olefin, proof of oxidation with subvalent Ga<sup>+</sup> and silylium catalysis with perfluoroalkoxyaluminate anions. *Chemical Science* (online first) / 2022, **13**, 439-453. DOI: 10.1039/D1SC05331K
- Schmidt M, [Esser B](#) (2021): Cavity-promotion by pillar[5]arenes expedites organic photoredox-catalysed reductive dehalogenations. *Chemical Communications* **57**(75), 9582-9585. DOI: 10.1039/D1CC03221F
- Schmidt M, Wassy D, Hermann M, González MT, Agrait N, Zotti LA, ... [Esser B](#), Leary E (2021): Single-molecule conductance of dibenzopentalenes: antiaromaticity and quantum interference. *Chemical Communications* **57**(6), 745-748. DOI: 10.1039/D0CC06810A
- Schmitt M, Mayländer M, Goost J, Richert S, [Krossing I](#) (2021): Chasing the Mond Cation: Synthesis and Characterization of the Homoleptic Nickel Tetracarbonyl Cation and its Tricarbonyl-Nitrosyl Analogue. *Angewandte Chemie International Edition* **60**(27), 14800-14805. DOI: 10.1002/anie.202102216
- Schmucker M, Gully TA, Schmidt A, Schmidt B, Bromberger K, Disch J, Butschke B, Burgenmeister SB, Sonnenberg K, Hasenstab-Riedel S, [Krossing I](#) (2021): Investigations toward a Non-Aqueous Hybrid Redox-Flow Battery with a Manganese-Based Anolyte and Catholyte. *Advanced Energy Materials* **11**(24), 2101261. DOI: 10.1002/aenm.202101261
- Schorpp M, Tamim R, [Krossing I](#) (2021): Oxidative addition, reduction and reductive coupling: the versatile reactivity of subvalent gallium cations. *Dalton Transactions* **50**(42), 15103-15110. DOI: 10.1039/D1DT02682H
- Sheng Y, Zhang T, Zhang S, Johnston M, Zheng X, ... [Dincer C](#), ... & Hu J (2021): A CRISPR/Cas13a-powered catalytic electrochemical biosensor for successive and highly sensitive RNA diagnostics. *Biosensors and Bioelectronics* **178**, 113027. DOI: 10.1016/j.bios.2021.113027
- Sollka L, [Lienkamp K](#) (2021): Progress in the Free and Controlled Radical Homo- and Co-Polymerization of Itaconic Acid Derivatives: Toward Functional Polymers with Controlled Molar Mass Distribution and Architecture. *Macromolecular Rapid Communications* **42**(4), 2000546. DOI: 10.1002/marc.202000546
- [Speck O](#), Langer M, Mylo MD (2021): Plant-inspired damage control—An inspiration for sustainable solutions in the Anthropocene. *The Anthropocene Review*, 20530196211018489. DOI: 10.1177/20530196211018489
- [Speck O](#), [Speck T](#) (2021): Biomimetics and Education in Europe: Challenges, Opportunities, and Variety. *Biomimetics* **6**(3), 49. DOI: 10.3390/biomimetics6030049
- [Speck O](#), [Speck T](#) (2021): Bridging the gap: from biomechanics and functional morphology of plants to biomimetic developments. *Biomimetics* **6**(4), 60. DOI: 10.3390/biomimetics6040060
- [Speck O](#), [Speck T](#) (2021): Functional morphology of plants—a key to biomimetic applications. *New Phytologist* **231**(3), 950-956. DOI: 10.1111/nph.17396

Speck T, Poppinga S, Speck O, Tauber F (2021): Bio-inspired life-like motile materials systems: changing the boundaries between living and technical systems in the Anthropocene. *The Anthropocene Review*, 20530196211039275. DOI: 10.1177/20530196211039275

Surapaneni VA, Aust T, Speck T, Thielen M (2021): Polarity in cuticular ridge development and insect attachment on leaf surfaces of *Schismatoglottis calyprata* (Araceae). *Beilstein Journal of Nanotechnology* **12**(1), 1326-1338. DOI: 10.3762/bjnano.12.98

Tahouni Y, Krüger F, Poppinga S, Wood D, Pfaff M, Rühe J, Speck T, Menges A (2021): Programming sequential motion steps in 4D-printed hygromorphs by architected mesostructure and differential hygro-responsiveness. *Bioinspiration & Biomimetics* **16**, 055002. DOI: 10.1088/1748-3190/ac0c8e

Top O, Milferstaedt SWL, van Gessel N, Hoernstein SNW, Özdemir B, Decker EL, Reski R (2021): Expression of a human cDNA in moss results in spliced mRNAs and fragmentary protein isoforms. *Communications Biology* **4**(1), 964. DOI: 10.1038/s42003-021-02486-3

Tschaikowsky M, Neumann T, Brander S, Haschke H, Rolauffs B, Balzer BN, Hugel T (2021): Hybrid fluorescence-AFM explores articular surface degeneration in early osteoarthritis across length scales. *Acta Biomaterialia* **126**, 315-325. DOI: 10.1016/j.actbio.2021.03.034

Tschaikowsky M, Selig M, Brander S, Balzer BN, Hugel T, Rolauffs B (2021): Proof-of-concept for the detection of early osteoarthritis pathology by clinically applicable endomicroscopy and quantitative AI-supported optical biopsy. *Osteoarthritis and Cartilage* **29**(2), 269-279. DOI: 10.1016/j.joca.2020.10.003

Wolff-Vorbeck S, Speck O, Speck T, Dondl P (2021): Influence of structural reinforcements on the twist-to-bend ratio of plant axes: a case study on *Carex pendula*. *Scientific Reports* **11**(1), 1-14. DOI: 10.1038/s41598-021-00569-z

## CONFERENCE PROCEEDINGS

Subhash SK, Gerach T, Sherkat N, Hillebrecht H, Woiias P, Pelz U (2021): Fabrication of  $\mu$  TEGs Based on Nano-Scale Thermoelectric Material Dispersions. In *2021 21st International Conference on Solid-State Sensors, Actuators and Microsystems (Transducers)* (pp. 471-474). IEEE.

Sherkat N, Subhash SK, Gerach T, Pelz U, Woiias P (2021): Development of manufacturing processes for vertical micro-thermoelectric generators based on printed circuit boards. DOI: 10.1109/PowerMEMS54003.2021.9658353

Kumar C, Speck T, Le Houérou V (2021): Quantitative assessment of real contact area on complex topographies and its role in attachment-detachment mechanisms. In *Proceedings of the 15<sup>th</sup> International Conference on Advances in Experimental Mechanics*.

## BOOK CHAPTERS

Friedman M, Krauthausen K, Speck T (2021): Interview with Thomas Speck: "You don't want to build an oak tree – you want to invent it." Plants as active matter. In *Active materials*, 57-78. De Gryter, Berlin. DOI: 10.1515/9783110562064-003

Tauber FJ, Masselter T, Speck T (2021): Biomimetic Soft Robotic Peristaltic Pumping System for Coolant Liquid Transport. In *Technologies for Economic and Functional Lightweight Design: Conference Proceedings 2020*, p. 173. Springer Nature. DOI: 10.1007/978-3-658-35588-3\_35

Nothdurft U, Kreil A, Kiesel A, Thomaschke R (2021): Die kognitiv-affektive Kartierung des Begriffs „Muße“. In Fludernik M, Jürgasch, T. (eds.), *Semantiken der Muße aus interdisziplinären Perspektive*, pp. 127-159. Mohr Siebeck, Tübingen.

## EDITORIAL WORK

Mazzolai B, Walker I, Speck T (eds.) (2021): *Generation GrowBots: materials, mechanisms, and biomimetic design for growing robots*. DOI: 10.3389/978-2-88971-185-7

Speck O, Speck T (eds.) (2021): Bridging the gap: from biomechanics and functional morphology of plants to biomimetic developments. *Biomimetics*.

## THESES

### HABILITATION

Poppinga, Simon (2021): *Functional principles and biomimetic potential of plant movements*. [Cumulative Habilitations Treatise, University of Freiburg, Chair of Functional Morphology & Biomimetics and Botanic Garden].

### PHD THESES

Acker, Pascal: Synthese und elektrochemische Untersuchung pi-konjugierter Redoxpolymere vom p- und n-Typ als Kathoden- und Anodenmaterialien in organischen Batterien, 2021.

Creusen, Guido: Bottom-up materials design with defined polymer and polymer-DNA structures, 2021. DOI: 10.6094/UNIFR/220833

Eisele, Lea Maren: Investigations of BF<sub>3</sub> based compounds as additives, electrolytes and as coating agent for nickel-rich cathode material, 2021. DOI: 10.6094/UNIFR/175635

Gröer, Saskia: 3D DNA origami as precise building blocks in protocellular systems, 2021. DOI: 10.6094/UNIFR/194843

Hatt, Thibaud: Electroplating approach based on self-passivated aluminium masking for metallization of silicon heterojunction solar cells, 2021.

Heckel, Jonas: Chemically fueled transient self-assembly of polymer building blocks, 2021. DOI: 10.6094/UNIFR/223560

Lossada Toro, Francisco Javier: Vitriimer-based bioinspired nanocomposites, 2021. DOI: 10.6094/UNIFR/218913

Peter, Andreas: On the anhydrous synthesis of oxymethylene dimethyl ether by the reaction of dimethoxymethane with gaseous molecular formaldehyde, 2021.

Schmucker, Maximilian; Kurz, Philipp: Chloromanganates as active materials for positive and negative electrolytes in redox flow batteries: from electrolyte synthesis to battery application, 2021. DOI: 10.6094/UNIFR/222917

Surapaneni, Venkata Amarnadh: Ontogeny and morphology of plant cuticular ridges, and their effect on insect attachment – experiments, theory and biomimetics, 2021. [PhD thesis, University of Freiburg; supervisor: Speck T, Thielen M].

### DIPLOMA, MASTER, BACHELOR AND STATE EXAMINATION THESES

Badstöber, Marie-Christin (2021): Quasistatische Charakterisierung der Querkontraktionszahl der Schalen von *Citrus limon* 'Rosso', *Citrus sinensis* 'Lane late' und *Citrus paradisi* 'Star ruby'. [Bachelor thesis, University of Freiburg; supervisors: Jentzsch M, Speck T].

Bill, Marco (2021): SiO<sub>2</sub> in mesoporösem N-dotiertem Kohlenstoff als Anodenmaterial für Li-Ionen-Batterien [supervision: Fischer, A]

Bilo, T. & Helm, J. (2021): A Further Step Towards Sustainable Development – Re-evaluating and Expanding Cognitive-Affective Mapping for Technology Acceptance Prediction. Unpublished Bachelorthesis. Freiburg: Abteilung Allgemeine Psychologie, Institut für Psychologie der Albert-Ludwigs-Universität.

Dörr, M. (2021): Eine Qualitative Analyse von Kognitiv-Affektiven Karten – Können Daten von Kognitiv-Affektiven Karten im Vergleich zu Fragebögen zusätzliche Informationen geben? Unveröff. Masterarbeit. Freiburg: Abteilung für Allgemeine Psychologie, Institut für Psychologie der Albert-Ludwigs-Universität.

Ewald, Niklas (2021): Development of spin-coated Mo doped BiVO<sub>4</sub> photoanodes for water oxidation. [supervision: Fischer, A]

Galetsa Feindt, Athina (2021): Synthesis of Mesoporous N-doped Carbons for Energy Storage Systems. [supervision: Fischer, A]

Glatz, Regina (2021): Development of a multiplexed electrochemical biosensor for on-site therapeutic drug monitoring of antibiotics, [Master thesis, University of Freiburg; supervisors: Dincer C, Urban G, Weber W].

Gros, W. J. (2021): CAMediaid: Multimethod approach to assess Cognitive-Affective Maps in mediation – A quantitative validation study. Unpublished master thesis. Freiburg: Abteilung Allgemeine Psychologie, Institut für Psychologie, Universität Freiburg.

Hirth, Linus (2021): Synthese von Ni<sub>3</sub>N auf mesoporösen N-dotierten Kohlenstoff. [supervision: Fischer, A]

Hoffmann, Tobias (2021): The effect of pore size distribution of sulfur-MPNC-composites as cathode material for Li-S-batteries. [supervision: Fischer, A]

Homburger, Jaro (2021): Ermittlung wichtiger biomechanischer Eigenschaften der federartigen Ranken von *Passiflora discophora*. [Bachelor thesis, University of Freiburg; supervisors: Thielen M, Klimm F, Speck T].

Jiang, Yuxing (2021): Soft Silver Nanowire Based Strain Gauge. [Bachelor thesis, University of Freiburg; supervisors: Schierle S, Pastewka L, Woias P].

Kaiser-Glunk, Johanna (2021): Interface design of Bismuth vanadate photoanodes. [supervision: Fischer, A]

Kardamakis, Thalia (2021): Fruit Peel Visualization of *Citrus limon* and *Citrus x latifolia* using Micro-Computed Tomography. [Bachelor thesis, University of Freiburg; supervisors: Jentzsch M, Speck T].

Kramp, Corina (2021): Vergleichende Charakterisierung eines bioinspirierten, softrobotischen Fingers, hergestellt mit verschiedenen adaptiven Fertigungsverfahren. [Bachelor thesis, University of Freiburg; supervisors: Esser F, Kappel P, Speck T].

Meyerding, L. (2021): Use of cognitive-affective maps (CAMs) to illustrate experiences with chemotherapy in women with breast cancer. A validation study. Unpublished master thesis. Freiburg: Abteilung Allgemeine Psychologie, Institut für Psychologie, Universität Freiburg.

Oechsler, Jan (2021): Carbon Supported Ni and Mo Electro Catalysts for the Hydrogen Oxidation Reaction. [supervision: Fischer, A]

Ruppert, Sebastian (2021): Funktionsmorphologie und Funktionsweise der glandulären Trichome der karnivoren Pflanze *Byblis gigantea*. [Bachelor thesis, University of Freiburg; supervisors: Pop-pinga S, Speck T].

## Awards

Sendtner, C. (2021): Kostbare Kisten: Gründe für Fehleinschätzungen der Kosten des eigenen Autos und deren Auswirkungen auf die Bewertung des ÖPNV. Unveröff. Masterarbeit. Freiburg: Abteilung Allgemeine Psychologie, Institut für Psychologie der Albert-Ludwigs-Universität.

Urban, Nadine (2021): Implementation of an optically controlled assay using optogenetic switches, [Master thesis, University of Freiburg; supervisors: Dincer C, Urban G, Weber W].

von Einem, Vicky (2021): Design and implementation of a Bluetooth low-energy front-end for a wearable system, based on a flexible capacitive sensor, monitoring knee laxity. [Master thesis, University of Freiburg; supervisors: Comella L M, Sheeja Prakash K, Reindl L, Woias P].

Westermann, Lea Katharina (2021): Kontrastmittelanalyse für hochauflösende 3D-Visualisierung der vaskulären Systeme von Monokotyledonen mittels  $\mu$ -CT. [Bachelor thesis, University of Freiburg; supervisors: Hesse L, Speck T].

## AWARDS

The publication "CRISPR-powered electrochemical microfluidic multiplexed biosensor for target amplification-free miRNA diagnostics" of the research team led by Dr. Can Dincer, microsystems engineer and member of FIT at the University of Freiburg, has been awarded the Biosensors & Bioelectronics Best Paper Award 2020/2021. (<http://news.tf.uni-freiburg.de/en/single/artikel/611/biosensors-and-bioelectronics-best-paper-award-20202021.html>)

## FIT COLLOQUIUM 2021

**8<sup>TH</sup> FIT COLLOQUIUM**  
**12.10. – 13.10.2021**  
**HYBRID EVENT****PROGRAM**

Venue: FIT, Georges-Köhler-Allee 105, Freiburg, seminar room ground floor,  
(maximal 30 persons, "first come, first served" \*) and Zoom

**TUESDAY, 12 OCTOBER 2021****Welcome by the Managing Director of FIT**

14:00 **Jürgen Rühle** "Words of welcome and status report of FIT"

**Session 1\*\*** (Chairperson: Thomas Speck)

14:30 **Charalampos Pappas** "Systems chemistry: Steps towards life-like systems"

14:45 **Naeim Ghavidelnia** (Eberl) "Bio-inspired programmable mechanical metamaterials with crack detection and sealing functionality"

15:00 **Patrick Elsässer** "PGM-free catalysts for alkaline fuel cells"

**15:15 – 16:00 Coffee break**

**Session 2\*\*** (Chairperson: Max Mylo)

16:00 **Taisiia Berestok** (Fischer) "Development of photosupercapacitors for integrated energy harvesting and storage"

16:15 **Wei Wei** (C. Elsässer) "Charging PV active perovskite materials with Li for battery applications"

16:30 **Julian Gebhardt** (C. Elsässer) "MaNiTU – Materials for sustainable tandem solar cells with extremely high conversion efficiency"

**16:45 End of first day**

**17:00 Dinner**

## WEDNESDAY 13 OCTOBER 2021

### Session 3\*\* (Chairperson: Olga Speck)

- 09:15 **Falk Tauber** (T. Speck) "Characterization of artificial Venus flytrap demonstrator combining two biological snap-trap mechanics"
- 09:30 **Max Mylo** (O. Speck) "The structural and functional connection of two biological, fibre-reinforced composites: a case study on the European mistletoe"
- 09:45 **Anna Hoppe** (Pastewka) "Simulation of plant abscission"
- 10:00 **Wafa Maftuhin** (Walter) "A mechanochromic donor-acceptor torsional spring to measure forces at the molecular level"
- 10:15 **Thorsten Hugel** "The AFM in material research and as an out of equilibrium research tool"

### 10:30 – 11:15 Coffee break

### Session 4\*\* (Chairperson: Uli Würfel)

- 11:15 **Rodrigo Delgado** (Würfel) "Integrated energy harvesting and storage devices based on organic solar cells and mesoporous carbon double-layer supercapacitors."
- 11:30 **Swathi Krishna Subhash** (Woiias) „Micro thermoelectric generators fabricated by dispensing"
- 11:45 **Negin Sherka** (Pelz) „Development of PCB-based fabrication technologies for micro-thermoelectric generators"
- 12:00 **Dennis Rusitov** (Rühe) "Tunable thermal and photochemical crosslinking of CHic-able diazo-groups containing polymers"
- 12:15 **Dan Song** (Rühe) "CHic Chemistry: Polymer microstructures through maskless photolithography and two-photon lithography"
- 12:30 **Jürgen Rühe** "Closing remarks"

### 12:45 End of second day

#### *Please note:*

\* *The current Corona rules of the University of Freiburg apply. Please arrive on time, because we have to check the **3G rules** if you are present in person. **Masks** are compulsory in the seminar room. Please note the University's documents on **data collection** and **contact tracing**, which have been sent to you by email.*

\*\* *All presentations should be given in English. Please divide your talk into 12 minutes oral presentation and 3 minutes discussion.*

## IMPRESSUM

Freiburg Center for Interactive Materials and Bioinspired Technologies (FIT)

Editor: Dr. Olga Speck

Print: Print shop of the University of Freiburg

